INDEX

MATERIALS AND METHODS **73**

SUMMARY

This work concerns cystatin B, a protein described as an antiprotease involved in Progressive Myoclonus Epilepsy of the Unverricht-Lundborg type (EPM1). In this neurodegenerative disorder, patients suffer from myoclonic jerks, tonic-clonic seizures, and progressive decline in cognition. The most common mutation described in EPM1 patients is the expansion of an unstable dodecamer in the cystatin B promoter. This sequence, repeated up to 75 times, is found in homozygosis or in heterozygosis together with an allele carrying a point mutation. Pennacchio et al [1] have shown that the knockout of the cystatin B gene generates a neurological disorder in mice, characterized by symptoms similar to those observed in EPM1 patients concluding that cystatin B protects CNS neurons against apoptosis and EPM1 is a loss of function disease. This function seems to be specific to the CNS, since in other tissues and cell types, the absence of cystatin B does not result in a pathological phenotype.

On the other hand, cystatins have been implicated in a number of diseases. A variant form of cystatin C is the major constituent of amyloid plaques in the brain of patients with hereditary cystatin C amyloid angiopathy. Increased cystatin A and B is described in the plaques of Alzheimer's and Parkinson's, and of patients suffering from senile dementia, suggesting that they are amyloid constituents. Interestingly, proteins of the cystatin family are used as models for *in vitro* studies of amyloid fiber structure and Staniforth et al.[2] have shown that cystatins form highly stable domain-swapped dimers *in vitro*.

Furthermore, Di Giaimo et al. [3] have isolated a number of cytoskeletal proteins interacting with cystatin B, none of which is a protease. Among them, the RACK-1 receptor of activated PKC, the brain beta spectrin and the neurofilament light chain form a multiprotein complex with cystatin B in the cerebellum. With a different approach, we have identified more cystatin B

partners that also interact with each other and are involved in the same cellular process, the cytoskeletal function. Altogether, our data draw cystatin B in the Ca2+-mediated cytoskeletal activity, and in particular in vesicle traffic at the membrane level. This function is at the basis of neuronal signal transmission.

By immunoprecipitation experiments, we show that the Δ68 EPM1 mutant of cystatin B does not interact with RACK-1, indicating that this mutation changes the structure of the multiprotein complex.

This work shows for the first time that cystatin B has a polymeric structure *in vivo* both in eukaryotes and in prokaryotes. The polymeric pattern consists of a dimer, oligomers, and polymers larger than 100 kDa. Mass spectrometry analysis of the polymers immunoprecipitated from a protein cell extract demonstrates that the polymers contain cystatin B only. The polymers are highly resistant to SDS and urea denaturation and boiling. They are sensitive to reducing agents and alkaline pH. Hydrogen peroxide increases the polymeric structure of the protein.

As already mentioned above, a similar pattern is observed expressing cystatin B in E. coli. Since cystatin B is an eukaryotic protein, E. coli offers a background free system to study the molecular mechanism of polymer formation. By column chromatography, we have fractionated E. coli protein extract and identified a factor that allows oligomer formation from cystatin B monomers *in vitro*. We are now characterizing the factor by mass spectrometry. Ultimately, we would like to isolate the corresponding mammalian protein for further studies.

The analysis of natural and laboratory mutants of cystatin B shows that they are polymeric. The structural organization of the polymers changes when a cysteine minus mutant is transfected into the cells. This mutant does not generate stable oligomers of intermediate molecular weight but mainly dimer and polymers larger than 100 kDa. We have also shown that the cystatin B oligomers have rather alkaline isoelectric point that makes them unstable at physiological pH.

Following 24-hour transfection in neuroblastoma cells, EPM1 and truncation mutants constructed in the laboratory generate cytoplasmic aggregates. In addition, the expression, in the same cell line, of wt cystatin B generates aggregates. In contrast, transfection of neuroblastoma cells with the cysteine minus mutant is less effective in aggregate formation. This may correlate with the absence of oligomeric cystatin B in this mutant.

We conclude that cystatin B *in vivo* has a polymeric structure, regulated by the redox microenvironment of the cell and that over-expression of the wt protein and its mutants results in the generation of toxic aggregates. The results envisage a molecular mechanism that could explain neural degeneration at least in the EPM1 patients heterozygous for both promoter and point mutations.

INTRODUCTION

1. CYSTATIN B

Cystatin B (CSTB) is a widely distributed protein found in most cell types and tissues where it may inhibit cysteine proteases of the cathepsin family [4-11]. It belongs to the cystatin super family, which includes a large number of proteins originated from an ancestral peptide [7-9].

The CSTB gene (see Appendix A) is located on human locus 21q22.3, within the Down syndrome region, has telomeric-centromeric orientation and is organized in 3 short exons and 2 introns [9], alike all genes of the cystatin super family. The wt promoter, at position –210/–174, contains 2-3 tandem copies of the polymorphic dodecamer (C_4GC_4GCG) [12]. Rarely the dodecamer is repeated 12-17 times ("premutated alleles") [13-14]. The CSTB gene has a typical "housekeeping" promoter (high GC and CpG content, Sp1 sites) without CAAT o TATA boxes [15].

1.1. THE PROTEIN

CSTB belongs to the stefin family (or type I cystatins), which is a subset of the cystatin super family [7-9]. Stefins are defined as monomeric proteins with a (molecular weight) MW of about 11 kDa, missing intramolecular disulfur bridges or glycosilation [16].

Figure 1 shows the X-ray crystal structure of recombinant human CSTB described by Stubbs et al. [17]. Structurally, CSTB consists of a five stranded β-sheet wrapped around a five turn alpha helix, with an additional C-terminal strand running on the convex side of the sheet [17].

Most of the structural studies are focused on the properties of the domains that *in vitro* interact with the proteases. They form a hydrophobic surface that

includes the motives conserved in all the inhibitory cystatins of the super family, although there are some characteristics peculiar of CSTB.

The N-terminal region misses the first 5 aminoacids, that in other cystatins are important for papain inhibition, but conserves the Gly4 [17-18]. The only cysteine in the molecule, at position 3[1], contributes to the binding of the proteases and may form a mixed disulfide bridge with an other CSTB molecule or be glutathionylated [8, 19-22].

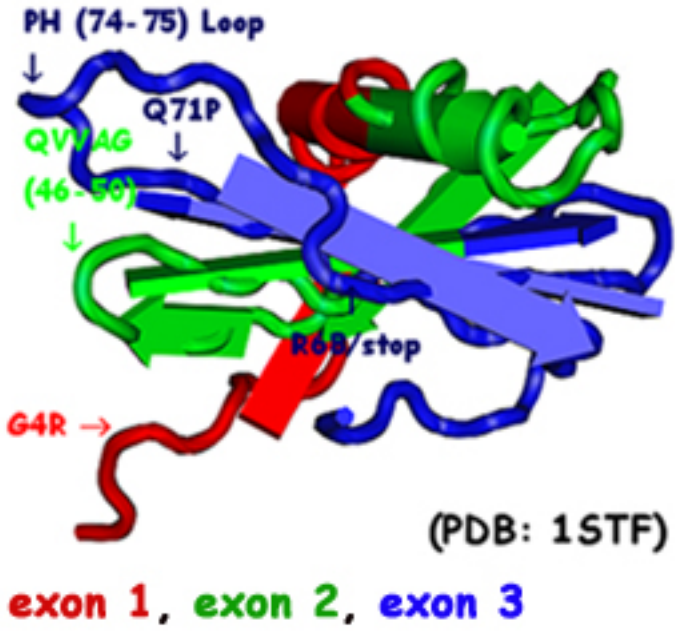

Figure 1. Crystal structure of human CSTB (PDB entry 1STF). Peptides coded by exon 1 in red, by exon 2 in green and by exon 3 in blue. The arrows indicate the position of the aminoacids conserved in the cystatin family: Gly 4, loop QXVXG (QVVAG in CSTB) between the β-strands 2 and 3 and loop PW (PH in CSTB) between β-strands 4 and 5. The position of 3 EPM1 mutants is indicated (see Table 1).

Of the two hairpin loops, loop 1 is characterized by the glutamine-X-valine-X-glycine (QXVXG) motif[2] and loop 2 by the proline- histidine (PH) sequence, which substitutes the proline-tryptophane (PW) consensus, typical of the super

[1] Most CSTB molecules contain only one Cysteineat position 3, rat and mouse CSTB contain both the conserved Cys3 and a second Cysteineat position 64 [10]

[2] QVVAG in man [25,9], in 9 mammalian cystatin B and in most of the Superfamily [10,27], QIVAG in mouse [10], QLVAG in bovine [26].

family. Single amino acid substitution experiments in loop 1 [23-24] and loop 2 [26], show that the binding between CSTB and proteases of the cysteine family is stabilized by the hydrophobicity and steric geometry of the whole interacting surface and not by few specific aminoacids. Thus, the high sequence conservation of the two loops may be due to their involvement in a different but equally critical function of cystatins [23]. The C-terminal extension of CSTB, absent in other cystatins, contributes to such interaction generating an additional hydrophobic contact region which could compensate for the absence of the first N-terminal aminoacids [26].

Cystatin, in all known cases, is a compact single-domain protein that, in agreement with the experimental results, is rather resistant to proteolytic cleavage. The N-terminal segment is essentially the only region accessible to protease attack [28].

Despite the considerable sequence similarity, CSTB shows stability and folding properties markedly different from cystatin A. In fact, while cystatin A is termostable and folds with a 2-state kinetic, CSTB is in a population of "molten globule" states under various partially unfolding conditions due to chemical, thermal or acid induced denaturation [29-33]. "Molten globules" show native-like secondary structure and compactness (globular), lack persistent tertiary interactions such as the asymmetric environment due to aromatic amino acid residues (molten) and unfold through a noncooperative process [32].

1.2. CELLULAR LOCALIZATION AND CELL SPECIFIC EXPRESSION

The subcellular localization of CSTB and cathepsin B, H, and L in Cos-1, Saos-2, L6 and neuroblastoma SHSY-5Y tissue culture cell lines has been studied by Riccio et al. [34] using confocal microscopy analysis. The authors show that, in proliferating cells, CSTB and cathepsins are concentrated in different cell

compartments. In fact, CSTB is found mainly in the nucleus of proliferating cells and both in the nucleus and in the cytoplasm of differentiated cells. Cathepsins, in either case, are essentially cytoplasmic, localized in vesicles and structures associated with the surface of the cells. These results agree with the cytoplasmic localization of CSTB and cathepsins described by Calkins et al. [35] in two cell lines derived from murine hepatoma and embryonic liver. However, these authors do not observe nuclear localization of CSTB in the following cell lines: Morris hepatoma cells, primary rat oligodendrocytes and astrocytes, and two different rat and human neuroblastoma cell lines. The distribution of Cystatin A and B in the cytoplasm of differentiated cells is diffused and most of the protein is not membrane bound, which is consistent with the absence of an N-terminal hydrophobic signal in the peptide sequence. CSTB is soluble and, although its sequence does not contain an obvious nuclear localization signal [34], the nuclear concentration of the protein in growing cells is higher than the cytoplasmic concentration. This may be due to a carrier that allows the translocation of cystatin into the nucleus or, alternatively, to the interaction of cystatin with a nuclear protein(s) or structure, which causes the retention of the anti-protease [36]. The cytoplasmic localization of cathepsin B is consistent with that found by other authors. Localization of the protein has been observed in vesicular structures, i.e., Golgi apparatus/lysosomes. It is interesting to note that Alakurtti et al. [37] have shown the presence of CSTB in the lysosomes of primary myoblasts.

CSTB has also been described in extracellular fluids and in secretory granules of rat pancreatic endocrine B-cells [38-39].

Recently, Riccio et al. [40] have analyzed the pattern of expression of CSTB, in developing and adult rat cerebellum, using double immunofluorescence microscopy with specific cell markers (Figure 2). They have shown that, in

primary glial cells, CSTB is found in progenitor and differentiated oligodendrocytes as well as in astrocytes. In the cerebellum, only oligodendrocyte progenitors express CSTB. In myelin-producing cells, CSTB synthesis is strongly down-regulated and the protein is not detectable. Astrocytes and Bergmann radial glia express CSTB at all the developmental stages analyzed, both in the cell body and in the fibers. Interestingly, terminally differentiated oligodendrocytes express CSTB *in vitro* whereas *in vivo* they do not. This observation is consistent with what has been described for differentiated cerebellar granule cells that express CSTB only *in vitro* [3]. The observed difference between CSTB expression in primary culture and cerebellar cells correlates with the reports made by Lalioti et al. [41] on EPM1 patients. In blood cells, CSTB is barely detectable whereas cultured blood and fibroblast cells from the same patients actively synthesize CSTB at a rate similar to that of normal individuals. The observed difference of CSTB expression *in vivo* and *in vitro* is consistent with the existence of a negative transcriptional control of the CSTB gene in some cell types. The down-regulation is abolished once the cells are cultivated *in vitro* [40].

Most neurons of developing and adult rat cerebellum do not express detectable amounts of CSTB, with the exception of the Purkinje cells and of some cells of the differentiated molecular layer [40]. In human cerebellum, CSTB is present in Purkinje cells and Bergmann glial fibers only [40]. A specific role of CSTB in the Purkinje cells is in agreement with the cytochemical alterations observed in EPM1 patients and in the knock-out CSTB mice [1,42].

CSTB is also found in the cortical neurons of the dentate gyrus of the hippocampus [40].

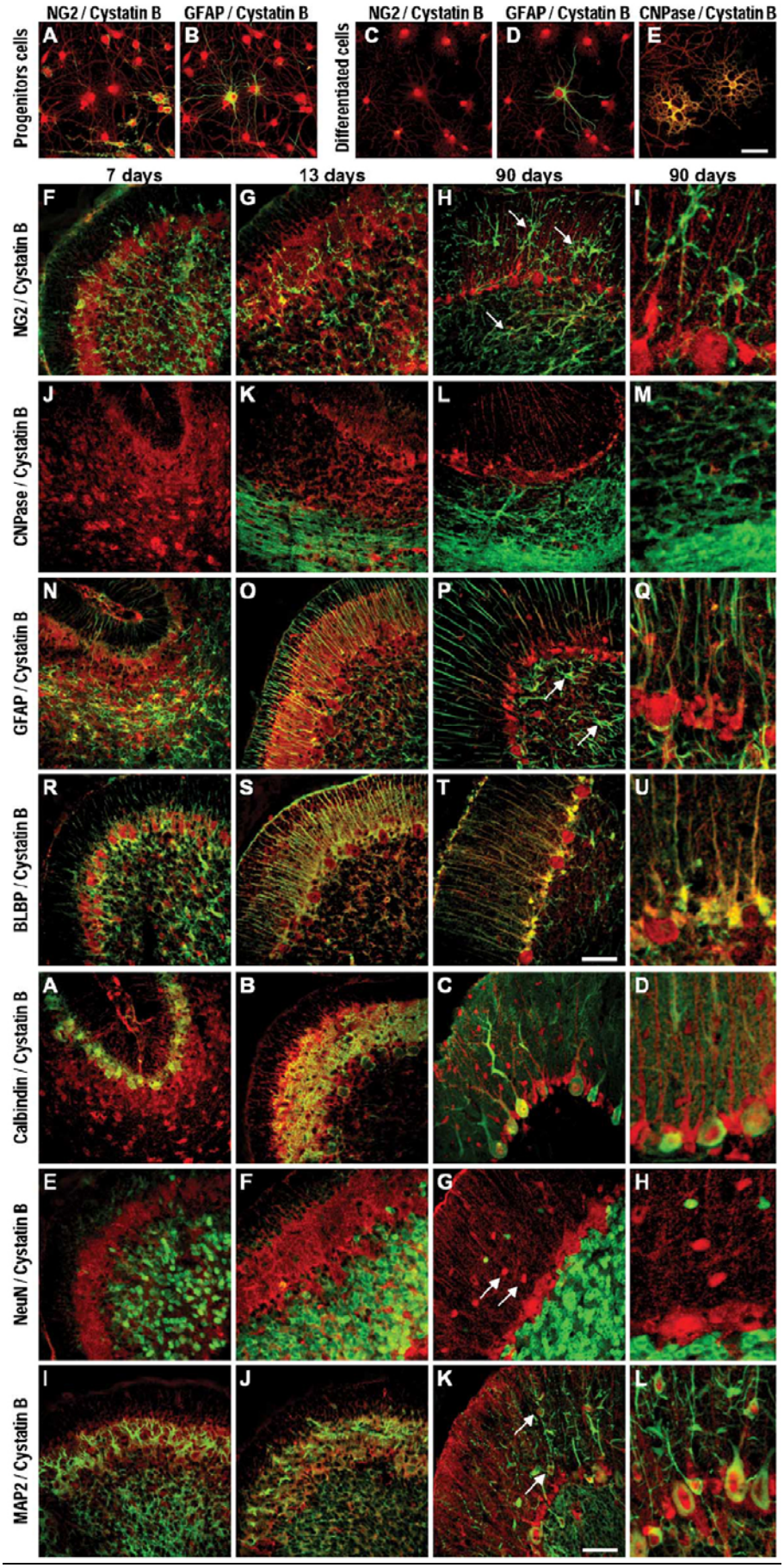
NG2 / Cystatin B
GFAP / Cystatin B
NG2 / Cystatin B
GFAP / Cystatin B
CNPase / Cystatin B
Progenitors cells
Differentiated cells
A
B
C
D
E
7 days
13 days
90 days
90 days
F
G
H
I
NG2 / Cystatin B
J
K
L
M
CNPase / Cystatin B
N
O
P
Q
GFAP / Cystatin B
R
S
T
U
BLBP / Cystatin B
A
B
C
D
Calbindin / Cystatin B
E
F
G
H
NeuN / Cystatin B
I
J
K
L
MAP2 / Cystatin B

Figure 2. Confocal analysis of CSTB expression in cells of the glial (A-U) and neuronal (A1-L1) lineage. CSTB is red; the glial and neuronal markers are green. A–E: Double immuno-fluorescence analysis of glial cell primary cultures. F–U and A1-N1: Double immunofluorescence of cryostatic sagittal sections of cerebella from 7, 13 and 90-day-old rats. Panels I, M, Q, U, D1, H1, and L1show a detail at three times magnification than in panels H, L, P, T, C1, G1, and K1, respectively. The arrows indicate: NG2+/CSTB$^-$ cells in panel H; GFAP+/CSTB+ cells in panel P; CSTB+/NeuN$^-$ cells in panel G1; CSTB+/MAP2+ cells in panel K1. Scale bar, 50 Am. Markers: NG2 stains oligodendrocyte precursor cells. GFAP is an astrocyte marker. CNPase marks terminally differentiated oligodendrocytes. BLBP is expressed in radial glia throughout the development of the CNS. Calbindin in the cerebellum is present in the cytoplasm of Purkinje cells only. NeuN neuronal marker that binds to a poorly characterized nuclear antigen present in post mitotic granule but not Purkinje cells. MAP2 neuronal marker, present in Purkinje cells and in all neurons that have a highly developed dendritic and axonal structure. From Riccio et al. [40].

2. CYSTATIN B AND DISEASE

2.1. MUTATION OF CSTB AND PROGRESSIVE MYOCLONUS EPILEPSY TYPE I

The most studied pathology characterized by mutations of the CSTB gene is Progressive Myoclonus Epilepsy of the Unverricht-Lundborg type (EPM1) [9].

EPM1 is a rare autosomal recessive disorder occurring mainly in Mediterranean and Baltic regions and in North America [43-44]. The clinical features of EPM1 are severe cortical myoclonus, typically photosensitive, tonic-clonic or clonic-tonic-clonic jerks and a neurologic deterioration that slowly leads to dementia, cerebellar ataxia and dysarthria [43,45-47]. Onset of syntoms occurs at 6-14 years of age and severity is variable both between and within families [43-45,48-49]. The benign course of the disease and the favourable response to antiepileptic drugs (i.e. valproate, piracetam, clonazepam, deazepam and zonisamide) allow patients to live to their 60s. Maybe this is the reason for EPM1 being the most common progressive myoclonus epilepsy worldwide [50-51].

The interpretation of EPM1 patients' histopathological data is confounded by the toxic effect of antiepileptic drugs (in particular phenytoin, which can be letal for EPM1 patients) and the degeneration of post-mortem specimens obtained at

late stages of the disease [42,44,50,52]. Anyway, such analyses show non specific gliosis and neuronal degeneration without intracellular inclusions in many CNS areas [44,47,49-50,52-53]. Furthermore, cerebellar hemispheres (at a high degree) and most of the basis pontis and medulla undergo atrophy and cerebellum cortex is depleted of Purkinje cells [44,48-49,52]. The phenotype described for these cells is diverse, ranging from the presence of vacuoles or swollen axons, to shrinking and apoptosis of some of the cells [44]. The varying degrees of damage observed may be due to differences in the expression and/or function of CSTB within the Purkinje cell population observed by Riccio et al. [40].

EPM1 is commonly associated with mutations in the CSTB gene (see Table 1). Most EPM1 patients carrying mutations in the CSTB gene are homozygous for the amplification of the dodecamer. The EPM1 heterozygous patients are always compound heterozygous for a dodecamer expansion and a point mutation [12,14,54-55]. Differently from other expansion diseases, EPM1 does not show anticipation [56-57].

Generally, EPM1 is associated with the loss of CSTB antiprotease activity, as a general inhibitor of proteolysis or as an inhibitor of caspases, either by direct interaction or by the inhibition of cathepsins that activate caspases. Anyway, there is no evidence of the direct interaction of cystatins either with caspases *in vitro* or *in vivo*, or with cathepsins *in vivo*. As cystatins and cathepsins are mostly localized in different cell compartments [35] it has been suggested that CSTB is involved in protecting cells against inappropriate cellular degradation by proteases that leak from lysosomes [63]. Alakurtti et al. [37] have shown that CSTB EPM1 mutants Gln71Pro and Gly4Arg prevent the association with lysosomes.

Table 1. EPM1 MUTATIONS

MUTATION	ALTERATION	HETEROZYGOSYS/HOMOZYGOSYS IN EPM1	REF.
Transversion 1510 G → C in the last nt of INTRON 1	invariant AG → AC ABNORMAL SPLICING with E2-SKIPPING	REPRESENT ~ 14% OF EPM1 ALLELES (THE MOST FREQUENT IS THE 1510G → C) NO EPM1 PATIENTS HOMOZYGOUS FOR THESE ALLELES; THEY ARE ALWAYS IN COMPOUND HETEROZYGOUS FORM: POINT MUTATION/ DODECAMER EXPANSION PROBABLY THE HOMOZYGOSYS FOR THESE MUTATIONS CAUSES A DIFFERENT PHENOTYPE	9,12, 27,54
Transition 1938 A → G at the end of INTRON 2	invariant AG → GG ABNORMAL SPLICING?		12
Transition 1612 G → A in the last nt of EXON 2	$AAG_{Lys56} \rightarrow AAA_{Lys56}$; EXON-INTRON JUNCTION ALTERATION → ABNORMAL SPLICING?		58
Transition 1973 C → T in EXON 3	$CGA_{Arg68} \rightarrow TGA_{STOP}$ PROTEIN TRUNCATION AT Lys67 (BEFORE THAN LOOP PH)		9
Deletion 1985 TC in EXON 3	FRAMESHIFT FROM Ser72 AND STOP AT CODON 75 → PROTEIN TRUNCATION AT THE NEW Ser74 (WITHIN LOOP PH)		12,55
Transversion 1983 A → C in EXON 3	$CAA_{Gln71} \rightarrow CCA_{Pro71}$		61
Transition 1612 G → A in EXON 2	$GGG_{conservedGly50} \rightarrow GAG_{Glu50}$		62
Transversion G10→ C in EXON 1	$GGG_{Gly4conservata} \rightarrow CGG_{Arg4}$	POINT MUTATION FOUND IN HETEROZYGOSYS WITH THE DODECAMER EXPANSION AND IN 1 CASE IN HOMOZYGOSYS	9,12
EXPANSION OF THE DODECAMER (C_4GC_4GCG) in PROMOTER 5'UTR	$(C_4GC_4GCG)_{2-3} \rightarrow (C_4GC_4GCG)_{30-75}$ DOWN-EXPRESSION OF THE GENE IN SOME CELL TYPES, MAY BE CAUSED BY THE SEPARATION OF PROMOTER'S REGULATORY ELEMENTS	REPRESENTS >85% OF EPM1 ALLELES IN >90% OF EPM1 PATIENTS THE DODECAMER IS EXPANDED IN BOTH ALLELES, BUT NOT NECESSARILY WITH THE SAME NUMBER OF REPETITIONS	14,54,59-60

The authors suggest a lysosome-associated physiological function for CSTB that may contribute to the molecular pathogenesis of EPM1. Of all the natural mutants described, only the substitution at position 4 may alter the catalytic site of the molecule, although the cysteine at position 3 seems to be the most relevant in terms of interaction between cystatins and cysteine proteases [10,17]. Recently, Berkovic et al. [64] and Coppola et al. [65] have described EPM1 cases in which the CSTB gene is not mutated and mutations of genes located on chromosomes others than 21 are the causative factors of the disease. The former authors [64] have studied an inbred Arab family with the clinical pattern of EPM1 and mapped the disease locus to the pericentromeric region of chromosome 12. This region currently contains known and predicted genes that have no obvious relationship to pathways involving CSTB biology. Thus, this study characterizes a novel pathway causing the EPM1 syndrome.

2.1.1. THE ANIMAL MODEL

Pennacchio et al. [66] have generated CSTB knockout mice with isogenic 129Sv and mixed 129Sv-C57BL/6 genetic background. The different genetic backgrounds produce different phenotypes. 129Sv-C57BL/6 CSTB-/- mice are not affected by myoclonus whereas the isogenic ones develop myoclonic seizures and progressive ataxia, though the EEG is not that characteristic of EPM1 [66].

All mutant mice are smaller than w/t, suggesting a negative effect on the whole body, in agreement with the ubiquitous expression of CSTB [42,66]. As in EPM1 patients, morphological and histological alterations seem to be exclusive of the CNS and cerebellum, which is the most severely affected district [42]. CSTB deficiency damages both granule and Purkinje cells and leads to cerebellar atrophy. Furthermore, several areas of the hemispheres show neuronal atrophy and gliosis [42]. Based on the data of Riccio et al. [40], the apoptosis of granule cells observed in CSTB-/- mice could be secondary to the damage of Purkinje cells.

CSTB knock out mice are used as model to unravel the etiology of EPM1 disease and the physiological function of CSTB. Lieuallen et al. [67] have identified several genes that are differentially expressed in the brain of CSTB deficient mice compared to that of wt siblings. In particular, the protease cathepsin S was over-expressed. The authors have suggested that increased levels of cathepsin S in CSTB-deficient mice may be a key factor in initiating or propagating the apoptotic cascade. Houseweart et al. [68] have investigated the possibility that cathepsins initiate or propagate proapoptotic signals through the Bid signalling pathway. They crossed CSTB-deficient mice to Bid-deficient mice, and showed that cathepsins can promote apoptosis in the absence of Bid. The same authors [69] have also crossed CSTB-deficient mice with cathepsin B, L, and S-deficient mice. The removal of cathepsin S and L from the CSTB-minus background did not rescue the EPM1-like phenotype of the CSTB-deficient mice. The removal of the cathepsin B gene allowed for a partial rescue of the phenotype. Apoptosis was markedly reduced, whereas ataxia and myoclonus remained. These results suggest that the apoptosis of cerebellar granule cells observed in CSTB deficient mice is not due to the antiprotease activity of CSTB. The authors propose that other molecules besides cathepsin B are responsible for the pathogenesis. Recently, Kopitar-Jerala et al. [70] have investigated apoptosis triggered by the treatment of thymocytes with camptothecin, staurosporin and anti-CD95 antibodies. The thymocyte cultures were obtained from CSTB-deficient and wild-type mice. The treatment with inhibitors of calpain- and papain-like cathepsins does not prevent caspase activation. Based on these results, the authors conclude that apoptosis, induced by these agents in thymocytes, is not dependent on cathepsin inhibition by CSTB.

The literature discussed so far does not univocally point to the absence of CSTB/prevalence of cathepsin(s) as the causative agent of the EPM1 disease.

On the other hand, the recent findings, concerning genes other than CSTB involved in the etiopathogenesis of the disease [64-65], suggest that the situation is more complex than envisaged so far and puts forward the existence of additional causative factors unrelated to the cystatin/cathepsin pathway in the pathogenesis of EPM1.

2.2. OVEREXPRESSION OF CYSTATINS.

Cystatin A and B and cathepsins (in particular cathepsin L and B) have been implicated in the positive/negative progression of cancer, maybe due to the unbalance between the proteases and their inhibitors [70-77] and to cystatin involvement in cell growth. In particular, CSTB has been proposed as a prognostic marker in a number of tumours. Increased levels of CSTB are often associated to a decrease of relapse risk [11,71-79]. The only exception, so far described, is colorectal cancer where high levels of extracellular cysteine proteinase inhibitors indicate a poor prognosis [72].

CSTB is also involved in the defence of tissues against invasion by viruses and parasites and plays a role in the innate immune-response to bacterial challenge [80]. Following septic injury, CSTB is upregulated together with a number of other proteins [81]. CSTB expression is upregulated in monocytes upon their differentiation into macrophages [82], in macrophages exposed to LPS [83] and in airway epithelial cells after microbial or cytokine exposure [84].

CSTB and other cystatins share an additional role independent of their inhibitory activity: they upregulate nitric oxide release from interferon-γ-activated macrophages. Macrophages contain CSTB and secrete it into the cell culture medium [85] and when exposed to LPS they up regulate its expression [83]. Upon activation, macrophages acquire antimicrobial activities involving reactive-oxygen species and reactive-nitrogen metabolites and generate

increased amounts of NO in correlation with the concentration of cystatins in the culture medium. The saturation of the cystatin inhibitory site by papain does not interfere with the CSTB enhancing activity, showing that the active site of CSTB plays no part in this important physiological response [86].

2.3. CYSTATINS AND AMYLOIDOSIS

A variant form of cystatin C is the major constituent of amyloid plaques deposited in the brain of patients with hereditary cerebral amyloid angiopathy [87]. A Leu68Gln substitution is a mutation frequently found in patients affected by the icelandic type of amyloidosis [88]. Strong implications as to the mechanism of amyloidotic aggregation [89] came with the discovery that human cystatin C [90], human cystatin A [91] and human CSTB [29] have a propensity to form inactive dimers under pre-denaturing conditions and, moreover, that the L68Q variant of cystatin C partially dimerizes under physiological conditions [89]. It is not clear whether the molecular basis of this pathology depends on the anti-protease activity of cystatin C.

The presence of cystatins in amyloid plaques of patients suffering from neurodegenerative diseases has also been described. Both cathepsins and cystatins are found in close association with senile plaques, cerebrovascular amyloid deposits, and neurofibrillary tangles in Alzheimer's disease (AD) [92-93]. Furthermore, profound changes in the lysosomal system seem to be an early event in "at-risk" neurons of AD patients. Whether or not lysosome-associated proteolytic mechanisms are causally related to the development and/or further progression of the disease [94] remains controversial. Recently, wild-type Cystatin C has been found as a component of amyloid plaques in Alzheimer’s disease [95] and a polymorphism in the cystatin C gene has been linked to late-onset Alzheimer’s disease [96-97]. Increased cystatin A and B in the senile plaques of Alzheimer's and Parkinson's, and of patients suffering from senile

dementia is a common finding and suggests that they are amyloid constituents [98]. It would be interesting to uncover the structure of these molecules in the context of the amyloid plaques and whether they exist in a polymeric form.

Increasing evidence suggests that cystatins not only have a high degree of similarity both in their amino-acid sequence and in their three-dimensional structure [99-100], but also share a common propensity to form small oligomers [101-102] and fibrils [103-105] *in vitro*. As CSTB is a simple globular protein without disulfide bonds and forms amyloid fibrils under mildly acid conditions [104], it is used as a representative model protein for studies of the mechanism of amyloid-fibril formation.

2.3.1. CSTB, A MODEL OF AMYLOID FIBRIL GENERATION *IN VITRO*

Recombinant human CSTB is a useful model system for amyloidogenesis [103,106]. Fibrillation *in vitro* is induced by the destabilization of the native state of proteins maintaining conditions that favor secondary structure formation [107]. Fibrillation of CSTB is promoted by a variety of experimental conditions (and by their combination): acidic solvents (pH3-5), high temperature (up to 65°C), presence of trifluoroethanol (TFE) (10-20%) or high ionic strength (>0.1 M NaCl) [107]. As observed for other proteins [108], within 1-3 weeks, amorphous aggregates are formed followed by the appearance of fibrillar species on the boundaries of amorphous clumps while, at later stages (1-3 months), the ordered aggregates predominate (Figure 3) [107]. This has led to the proposal that amorphous aggregates may be the source of nucleation sites for amyloid formation [109].

Local concentration of the protein and its external environment determine different morphology of deposited amyloid fibres [107]. Morphological heterogeneity is characteristic of aggregates generated by different amyloidogenic proteins [108-115].

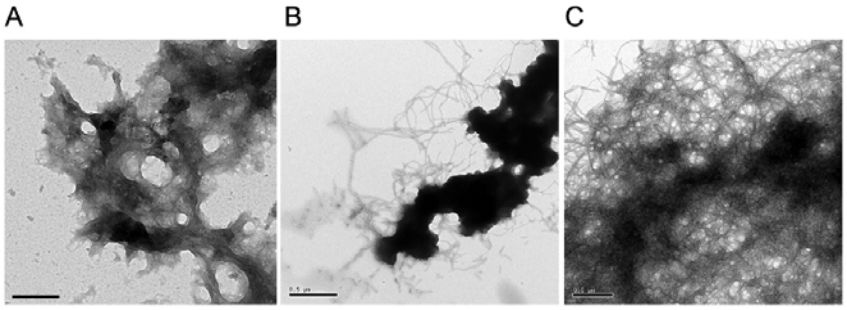

Figure 3. Amorphous aggregation. A: electron micrographs of the large amorphous aggregates occurring within an hour of triggering the reaction at pH 4.8, 10% TFE and 37°C. The scale bar represents 0.5μm. With time, small fibrillar species appear at the edges of the aggregates (B) and eventually mature fibres predominate on the EM grids (C). From Zerovnik et al. [107].

2.3.2. 3D-DOMAIN SWAPPING OF CYSTATINS *IN VITRO*

Cystatins represent a unique example of a set of proteins in which small oligomeric assemblies can be observed and isolated on the pathway to amyloid fibrils. Among cystatins, CSTB is the most suitable model for studying the kinetics and morphology of amyloid-fibrils whereas cystatin A and cystatin C are useful systems to decipher the early steps in the aggregation reaction [116]. *In vitro*, cystatins form highly stable domain-swapped dimers at physiological protein concentrations [2,102-103,117-125]. In 3D domain swapping, two (or more) subunits exchange identical structural elements or "domains" leading to the recreation of the monomeric fold in an aberrant way, from chain segments contributed by different subunits. In a protein capable of domain swapping, there must exist a flexible linker or hinge whose conformational changes allow the molecule to adopt different folds [74].

In cystatin swapped dimers loop 1 of each monomer is the hinge that opens and becomes part of a long β-ribbon running from the beginning of strand β2 to the end of strand β3. It leads to the creation of an unusually long contiguous antiparallel β-sheet formed by two copies of the β2-loop1-β3 ribbon, which cross from one domain to the other [2,120,123-125].

Sanders et al.[122] have shown that, under conditions leading to the formation of amyloid deposits, the domain-swapped dimer of chicken cystatin further oligomerizes to a tetramer, before fibrillization. In contrast with other domain swapping proteins such as CD2 [190] or RNase A [191-197], no trimeric or pentameric species are detectable, suggesting that the chicken cystatin assembly competent species is the dimer rather than the monomer. The tetramer reverts to monomers under non-reducing SDS-PAGE [122].

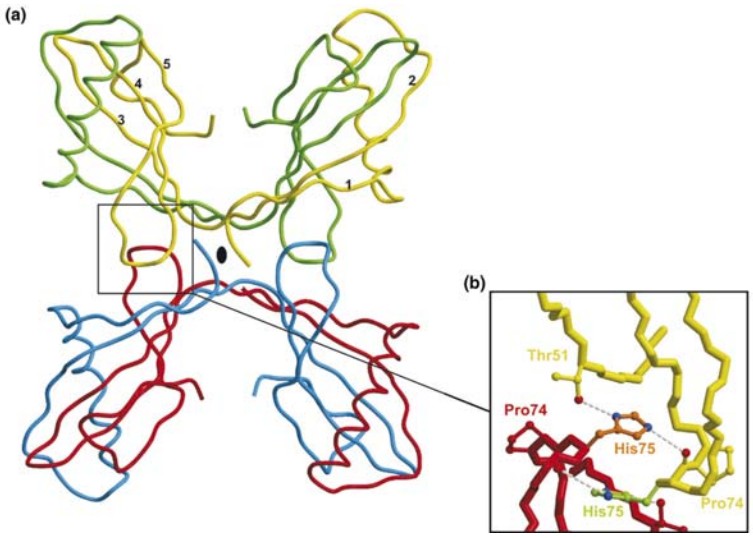

Figure 4. Crystal structure of CSTB tetramer. (a) Ribbon representation of the tetramer of CSTB. The tetramer is build of two domain-swapped dimers related by the crystallographic 2-fold axis (black ellipsoid). The upper domain-swapped dimer is composed of yellow and green chains, whereas the lower dimer is composed of red and blue chains. The upper and lower dimers are intertwined by the S72-L80 loop regions. Between the swapped domains there are linker peptides comprising residues from V47 to G50. (b) The upper dimer(yellow chain) swaps the S72–L80 loop with the lower dimer (red chain) and forms a tetramer. The hand shake is possible due to a trans/cis proline isomerization of the P74 residue. As a result, the H75 side-chains are packed together in an antiparallel arrangement. From Kokalj et al. [126]

Recently Kokalj et al. [126] determined both the crystal and NMR structures of human CSTB C3S tetrameric species (Figure 4). The crystal structure reveals that the tetramerization of CSTB, and possibly of other cystatins, is not a further domain swapping event as initially proposed by Sanders et al.[122]. In fact, the process involves a related mechanism, that the authors term “hand shaking”,

through which 3D domain-swapped dimers become entwined. The hand shaking reaction is dependent on the trans to cis isomerization of Pro74, the only proline residue that is widely conserved throughout the cystatin super family (it is the Pro of the consensus PH of loop 2). The most pronounced effect of P74 isomerization is the difference in the position of the H75 side-chain. In the monomeric and dimeric forms, it points inside its own loop 2. In contrast, in the tetrameric form, the four H75 point away from their loop 2 and are directed towards the corresponding loop 2 of the neighbouring dimer. The result is that each dimer swaps its two loops 2 with those of the other dimer generating the tetramer [126].

3. CYSTATIN B INTERACTORS

The physiological role of CSTB is unclear. The apparent contradiction between the known role of the ubiquitous CSTB antiprotease and the specificity of the district affected by EPM1 disease suggests that in the CNS it plays a specific and essential function protecting the cells against apoptosis [9, 66]. As such a specific function could be correlated to the interaction of CSTB with proteins exclusively expressed in the CNS, Di Giaimo et al. [3] have used the two hybrid system technique to isolate partners of CSTB expressed in rat cerebellum. Interestingly they did not find any proatease among the interacting proteins. The absence of proteases among the identified proteins may be explained if one takes into account the weak interaction between CSTB and cathepsin B observed in yeast and *in vitro*, and/or a fast exchange rate of the antiprotease-protease binding. Among the identified CSTB partners, several are cytoplasmic proteins involved in the regulation of cytoskeletal functions. Di Giaimo et al. [3] have characterized five of these peptides: brain β-spectrin, NF-L, RACK-1, TCrp and Mtrp. At least β-spectrin and NFL are expressed exclusively in cells of the

nervous system, mainly in neurons. The same authors have also shown that the five interactors bind CSTB in the GST pull-down assay and that the interaction occurs with the GST–CSTB exon II and GST– CSTB exon III fusion peptides [3]. Di Giaimo et al. [3] have further confirmed the interaction between CSTB and NFL, β-spectrin and RACK-1, *in vivo*, by experiments of co-immunoprecipitation of rat cerebellar protein extracts. The interaction of NF-L, β-spectrin and RACK-1 with CSTB is detectable in the cerebellum and not in the brain hemispheres, indicating the tissue specificity of the protein complex [3].

Based on these results Di Giaimo et al. [3] have hypothesized the existence of one or more possible specific roles of CSTB, mediated by its interaction with different partners either in the nucleus or in the cytoplasm. In particular, they have proposed that CSTB in the cerebellum is part of a specific complex of unknown function. The disruption of this complex in EPM1 patients may be the cause of the disease. It may be worth underlining that the region of chromosome 12 identified by Berkovic et al. [64] as the site of an EPM1 natural mutant is rich in structural and cytoskeletal genes.

In the cerebellum β-spectrin, NF-L, RACK-1 are co-expressed and co-localize with CSTB in different cells depending on the age of the animal: during development in the granule cells, and in the adult in the Purkinje cells and maybe in the Bergmann glia as well (Figure 5) [3,40]. This observation is consistent with the results of Pennacchio et al. [58] who show the loss of granule cells in the cerebellum of CSTB knock-out mice. The latter finding correlates with the marked loss of Purkinje cells revealed by autopsy of patients affected by EPM1 [44,127].

The multiprotein complex identified by Di Giaimo et al. [3] contains at least CSTB, NF-L, β-spectrin and RACK-1, but may also contain further peptides, which may not interact directly with CSTB. The size of the five proteins interacting with CSTB varies from approximately 30 to more than 200 kDa and

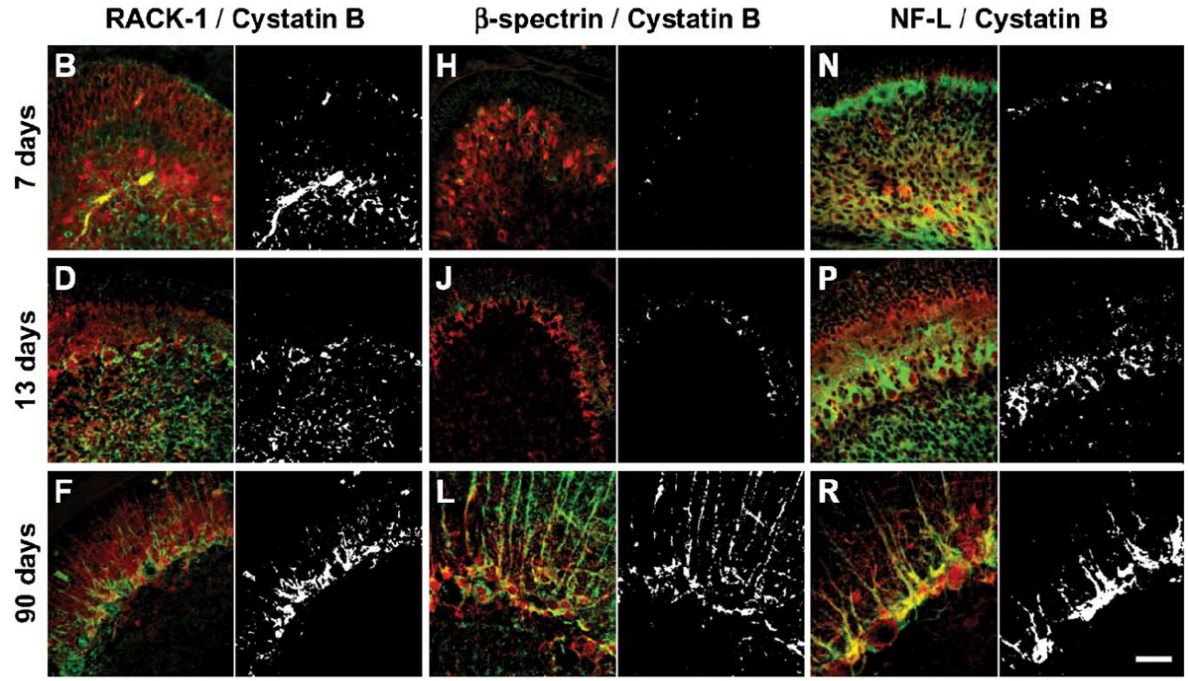

Figure 5. Double immunofluorescence analysis of cryostatic sagittal sections of cerebellum from 7, 13 and 90-day-old rats. CSTB is red. RACK-1 (B, D, F), β-spectrin (H, J, L), and NFL (N, P, R) are green. On the right of each image, the co-localization of the signals is shown in white. Scale bar, 50 Am. From Riccio et al. [40].

CSTB is a small protein of approximately 12 kDa. It seems therefore unlikely that all these proteins interact directly with CSTB at once, unless CSTB is in a dimeric or polymeric form [3]. However, RACK-1, NF-L and β-spectrin have multiple interaction domains and may interact in different sites with one another as well as with CSTB.

The RACK-1 receptor (Receptor for Activated C-Kinase 1) is a scaffolding protein of 36 kDa and belongs to the family of WD40 repeat proteins [128]. Its seven WD40 protein interaction domains make RACK1 especially versatile. In fact, it specifically binds several proteins and can simultaneously contact more than one protein. For this reason RACK1 is involved in a variety of signalling pathways. The receptor's main function is to translocate to the cell membrane some of the activated isoforms of PKC [129]. The three C-terminal WD

domains of RACK1 interact with several kinase (different from PKCs) and phosphatase proteins [130-133].In conditions that promote cell spreading and adhesion, RACK1 directly and specifically interacts with the cytoplasmic domains of IGF-1R [134-135] and integrin-β [136], being thus implicated in their signalling pathways and in the contacts between plasma membrane and cytoskeleton [137]. It is abundant during cell proliferation and differentiation [138-139] and it is induced during angiogenesis, including that of tumours [140]. In the CNS RACK1 is involved in the neurite outgrowth in retinal ganglion cells [141] and Yaka et al. [142] have demonstrated that, in the CA1 hippocampal region, RACK1 decreases NMDA receptor activity binding the NR2B subunit of the NMDA receptor and the protein-tyrosine kinase Fyn that phosphorilates the NR2B subunit.

NF-L (Neurofilament Light chain) is the 68 kDa subunit of the structural core of neurofilaments, the most abundant intermediate filaments (IF) in neurons of the central and peripheral nervous systems. NF-L conforms to a tripartite structure consisting of a highly conserved a-helical rod domain flanked by variable non-a-helical N- and C-terminal domains (“head” and “tail”, respectively), responsible for specific functions [143-145]. In neurons, NFL plays important roles in the growth, maintenance and regeneration of large myelinated axons [146]. Furthermore, it is involved in neuronal differentiation including migration, neurite outgrowth, target recognition, and synaptogenesis [147]. In mammalian neurons, NF-L may target the functions of protein phosphatase-1 in membranes and cytoskeleton [148]. In the dendrites and growth cones of cultured hippocampal neurons, NF-L directly interacts with the NR1a subunit of NMDA receptor [149]. NF-L mutations are correlated to Charcot-Marie-Tooth disease type 2, a severe hereditary motor and sensory neuropathy [150-154]. Furthermore, its down-expression is associated with ageing [155-156] and

neurodegenerative diseases, i.e. Alzheimer's and Parkinson's diseases and amyotrophic lateral sclerosis (ALS) [157-163]. Parkinson's disease and ALS are characterized by neurofilamentous accumulations (Lewy bodies and spheroids, respectively) and anomalies in NFL expression, distribution and/or phosphorylation. The cytoplasmic accumulations may be toxic or represent a residual regenerative activity or an aspecific response to axonal or neuronal damage.

β-spectrin (about 240 kDa) is one of the two subunits of spectrin, a giant, extended and flexible molecule in which two antiparallel elongated α-β heterodimers are associated head-to-head to generate a tetrameric filament of about 200 nm [164-168]. All spectrin subunits share the same structural organization. The central portion of the molecule contains 17-30 repeats, the "spectrin repeats" that characterize the family and are organized in three α-helices (A, B, C) connected by two β-turns [164, 166, 169-170]. The N- and C-terminal regions are highly variable and comprise protein-protein interaction domains [168]. The modular structure is probably at the basis of the implication of spectrins in a variety of physiological processes. In fact, it combines numerous protein-protein interaction domains in several different isoforms, differentially expressed and localized according to organs, developmental stages, cell populations or sub-populations and cell compartments [168, 171]. Spectrin is the major component of the membrane skeleton. It associates to the cell membrane directly, interacting with membrane proteins, or indirectly, binding membrane attachment proteins such as ankyrins and protein 4.1. Spectrin also binds Ca2+ and calmodulin, which regulate its binding to the membrane [198]. Spectrins crosslink actin filaments into an isotropic meshwork underlying cellular shape and asymmetry, membrane stability and deformability, as well as the formation of membrane subdomains [167, 172-176]. Spectrins are

localized in most cell compartments and may play a role in membrane protein sorting, vesicle trafficking and formation/maintenance of nucleus shape [177-182]. In neurons, spectrin is implicated in neurite outgrowth and in the topographical organization of groups of receptors or of cytoplasmic multiprotein complexes, in specialized domains [182-185].

β-spectrin interacts with the rod domain of NFL [186]. The binding requires at least an other protein, still unknown, that connects the two proteins and modulates their association [187]. *In vitro* a single β-spectrin molecule can bind up to 60 NFL molecules [188].

Rodriguez et al. [189] have shown that β-spectrin interacts with RACK1 as well. In this case, the interaction is direct and independent from the binding between RACK1 and PKCβ.

RESULTS

1. INTERACTION OF CYSTATIN B WITH CYTOPLASMIC PROTEINS

1.1. CSTB INTERACTORS

Cell proteins are compartmentalized and can interact only if they are in the same sub-cellular district. The analysis of protein interactions with purified proteins, in *in vitro* systems, indicates the possibility of their interaction but does not guarantee that the binding takes place *in vivo*. In order to confirm and expand the analysis of CSTB interactors initiated by Di Giaimo et al. [3] with the two hybrid and the GST-pull down techniques, we have analysed the proteins that interact with CSTB, directly or indirectly, in a (neuronal) mammalian cell line. We have chosen the 293T cells as model system because they have an expression phenotype surprisingly similar to early differentiating neurons and to well defined cell lines of the neuronal lineage (PC12 and Ntera-2 cells) [199]. These cells are easy to colture and, in contrast with other neuronal cell lines, easy to transfect. As commercial anti-CSTB abs are not efficient in immunoprecipitation experiments, we have immunoprecipitated HA-CSTB from 293T cells transfected with the pRK7-HA-CSTB vector. The immunoprecipitated proteins were separated by 2D-PAGE (Figure 6).

The gel contains spots of a MW ranging from 12 to more than 200 kDa. The isoelectric point is within pH 3 to 10. This suggests that, in agreement with Di Giaimo et al. [3], CSTB interacts with many proteins generating different multiprotein complexes. The indicated spots were analysed by mass spectrometry. They correspond to proteins involved in vesicle traffic, cytoskeletal modelling and calcium metabolism, i.e. annexin A2 and 11,

neuronal copine and calreticulin and to cytosolic proteins, i.e. glyceraldehyde-3-phosphate dehydrogenase (GAPDH), enolase and trioso-phosphate isomerase. The intense spot at the bottom of the gel with a pI of about 7.5 is HA-CSTB. The nature of the CSTB partners points to a cytoskeletal function. Furthermore, our results suggest a role of CSTB in Ca2+ signalling at the membrane level. It is worth to underline that Ca2+ signalling is essential in neuronal signal transmission.

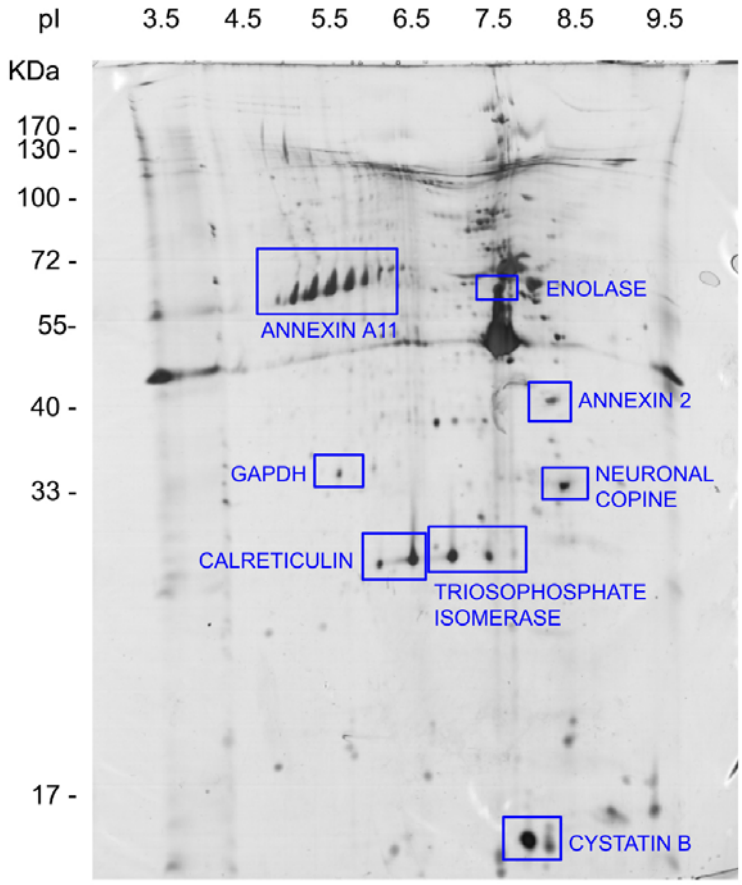

Figure 6. 2D gel electrophoresis of CSTB interactors. Immunoprecipitate with anti HA(F-7) abs from 293T cell protein extract. The indicated spots, stained with silver, were analysed by mass spectrometry and the corresponding proteins were identified.

1.2. INTERACTION OF CSTB AND EPM1 MUTANTS WITH RACK1, NFL AND β-SPECTRIN

If the alteration of the multiprotein complex described by Di Giaimo et al. [3] plays a role in EPM1 etiology, it is possible that one or more of the EPM1 mutants fail to interact with the CSTB partners. Our working hypothesis is that a stable mutant, when over-expressed, acts as a negative dominant. In order to analyse the binding of CSTB and its mutants *in vivo*, we have chosen a cell line where RACK1, NFL and β-spectrin are expressed. The western blot analysis of a 293T cell extract stained with anti-CSTB, anti-RACK1, anti-NFL and anti-β spectrin abs, shows that the four proteins are detectable in these cells (Figure 7A). Panels B-D show the results of the imunoprecipitation of protein extracts from 293T cells transfected with wt, G4R, Δ68 CSTB (lanes 1-3) and non transfected cells. The abs used for the immunoprecipitation were anti-β spectrin (B), anti-NFL (C) and anti-RACK1 (D). The immunoprecipitated proteins were separated on SDS-PAGE and the western blots were stained with anti-HA abs. Panels B and C show that the WT and G4R immunoprecipitates have a very similar pattern of bands, mainly in the regions corresponding to the MW of CSTB monomer and dimer. Fainter bands of higher MW are also detectable. The Δ68 deletion mutant, which is missing 30 amino acids at the C-terminus, shows faster running bands, both in the low and high MW range. These results show that NFL and β-spectrin interact with wt CSTB and EPM1 mutants, indicating that neither the catalytic site nor the C-terminus of CSTB are involved in this interaction. Panel D analyses the interaction of RACK1 with CSTB. The banding pattern is similar for the WT and G4R samples, indicating interaction between the proteins. In contrast, RACK1 does not immunoprecipitate Δ68 CSTB as the only detectable band corresponds to IgM. We conclude that

RACK1 interacts with the C-terminus of CSTB. This result is very interesting as we have used a CSTB mutant derived from EPM1 patients.

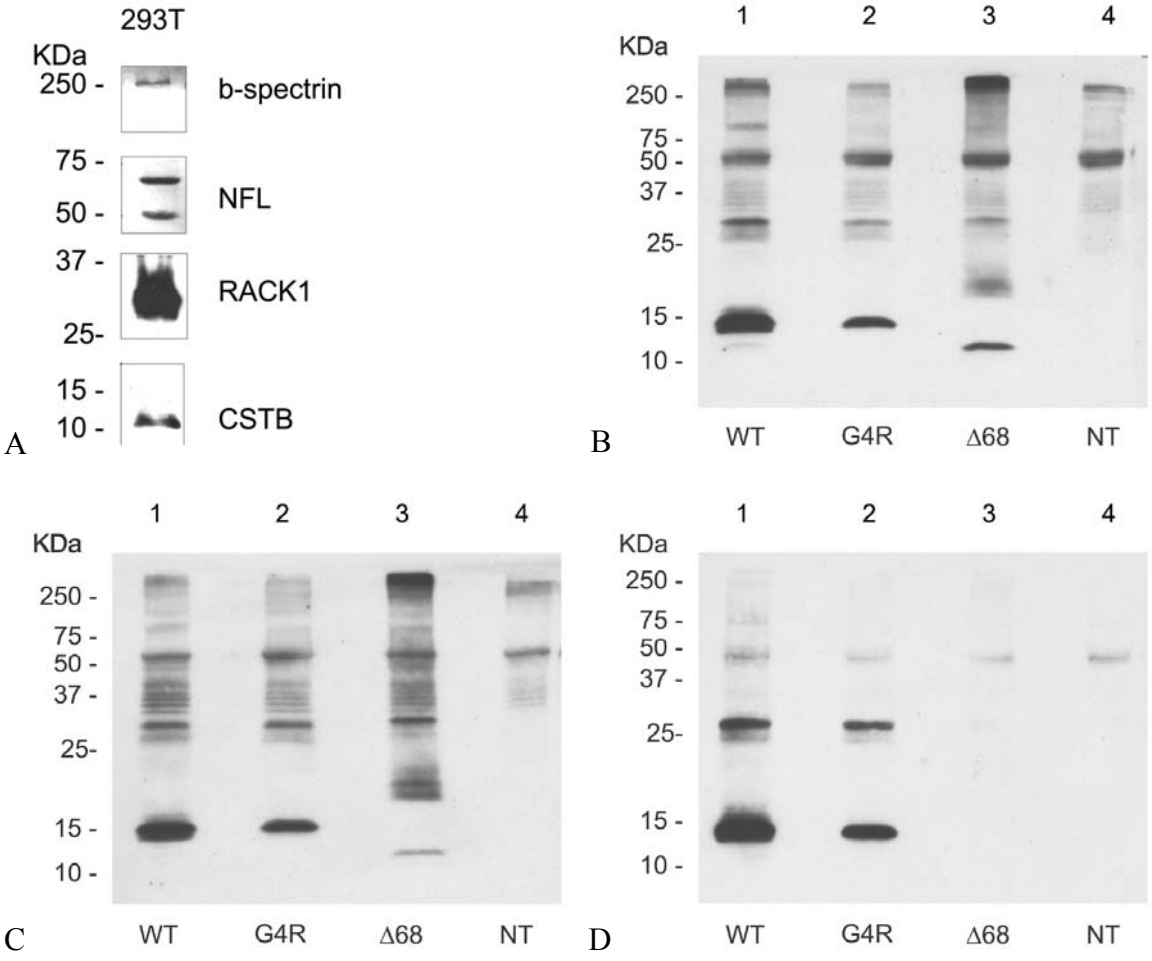

Figure 7. Western blot of immunoprecipitated CSTB and EPM1 mutants. A: Protein extracts from 293T cells stained as indicated. B-D: Immunoprecipitation of protein extracts from 293T cells, transfected and non transfected (NT) as indicated.

2. CYSTATIN B IS POLYMERIC *IN VIVO*

2.1. CELLULAR CSTB HAS A POLYMERIC STRUCTURE

The western blots in figure 7 show, in addition to monomeric CSTB, bands of MW higher than expected, corresponding to the position of dimers and larger components. Thus, we have decided to examine the structural organization of endogenous CSTB in a series of cell lines (293T, SAOS, HeLa and SKNBE cells). Figure 8 shows a western blot analysis of protein extracts from cells lyzed under different conditions and electrophoresed in absence or presence of 50 mM DTT. The expected MW for CSTB is approximately 12 kDa. In the absence of DTT, a complex pattern of bands ranging between 10 and 250 kDa is present in all lysates with a similar distribution. The reducing condition increases the intensity of the 12 kDa band although some of the polymers are still detectable. It should be noticed that the CSTB pattern is similar in all samples, independent of the lysis conditions.

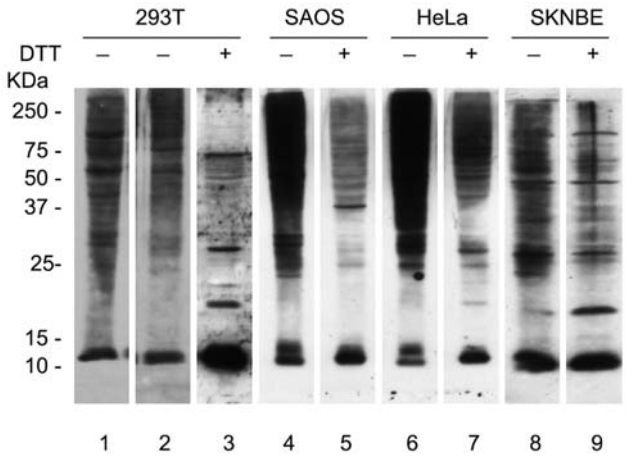

Figure8. Western blot analysis of CSTB in human cell lines. SDS-PAGE of protein extracts lyzed under non denaturing conditions (buffer 1: lanes 1 and 3), denaturing conditions (buffer 2 containing 1%SDS: lane2) or lyzed directly in protein loading buffer (lanes 4-9). Staining with anti-CSTB abs.

To make sure that the high MW components were real and not due to antibody background, we have checked the antibody specificity by preabsorption experiments. Figure 9A shows that preabsorption of the anti-CSTB abs with human CSTB, synthesised in E. coli, erases the endogenous signal. The same is true in B, were the 293T cells were transfected with rat HA-CSTB and preabsorption was carried out with rat HA-CSTB synthesised in E. coli. The results of these experiments show that CSTB, *in vivo*, has a polymeric structure which is resistant to SDS denaturation (Figure 8: lanes 2, 4-9) and partially sensitive to DTT treatment (Figure 8: lanes 3, 5, 7, 9). The observed SDS resistance suggests the existence of covalent bonds responsible for the high MW structures which may represent either co- or homo-polymers.

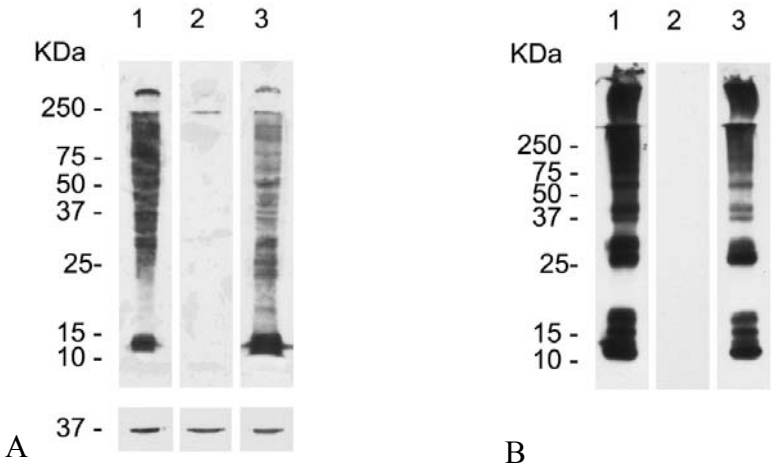

Figure 9. Abs specificity. SDS-PAGE and western blot analysis. A: Protein extract from cells lyzed in buffer 1. Staining with anti-CSTB abs: untreated (lane 1), preabsorbed with E. coli protein extract expressing human CSTB (lane 2) or E. coli protein extract (lane 3). Lower panel: staining with anti-GAPDH abs. B: Protein extract from 293T cells transfected with the pRK7-HA vector containing rat CSTB cDNA lyzed in buffer 2. Staining with anti-HA(F-7) abs: untreated (lane 1), preabsorbed with E. coli protein extract expressing rat HA-CSTB (lane 2) or E. coli protein extract (lane 3).

A treatment with 8 M urea does not denature CSTB polymers (Figure 10), although a few bands, in the intermediate MW region of the gel, are no longer detectable. We conclude that the polymeric structure of CSTB is resistant to denaturation in 1% SDS and 8 M urea, and partially resistant to reducing agents.

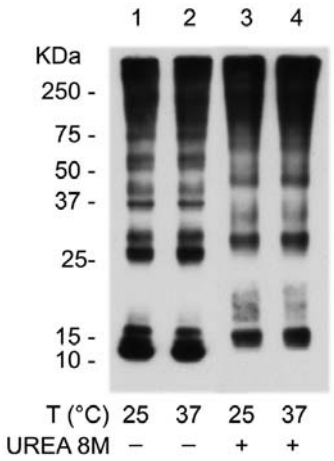

Figure 10. SDS-PAGE and western blot analysis of the same protein extracts as in figure 9B incubated 1 Hr as indicated. No reducing agents added. Staining with anti-HA(F-7) abs.

We have analysed native CSTB by size fractionation on a Superdex 75 column (Figure 11). The MW range for optimal separation with this column is 3-70 kDa. Fractions 17-18 contain the excluded peak of the column and from fraction 19 onward the separation starts (see material and methods). The size distribution of proteins stained with Poinceau red shows the expected separation of the MW in fractions 19-30 (panel A). Immunostaining of the filters with anti-CSTB abs shows that low MW components, mainly monomers, are in fractions 21-30 (panel B). Fractions 27-30 correspond to the approximate MW of CSTB monomer, dimer and trimer suggesting that a small amount of CSTB is not bound to other proteins. Monomeric CSTB in fractions 21-26 is probably released from its interaction with cellular proteins of increasing MW upon SDS boiling and SDS PAGE. In fact, native CSTB interacts with a number of proteins that increase its size on fractionation (Di Giaimo et al., 2002; Figures

6-7). Polymeric CSTB is detectable in fractions 17-20 that include the excluded peak and its position may indicate again interaction with other proteins. The separation between low and high molecular mass components shows that polymerization of CSTB is not an artefact due to SDS or self-assembly.

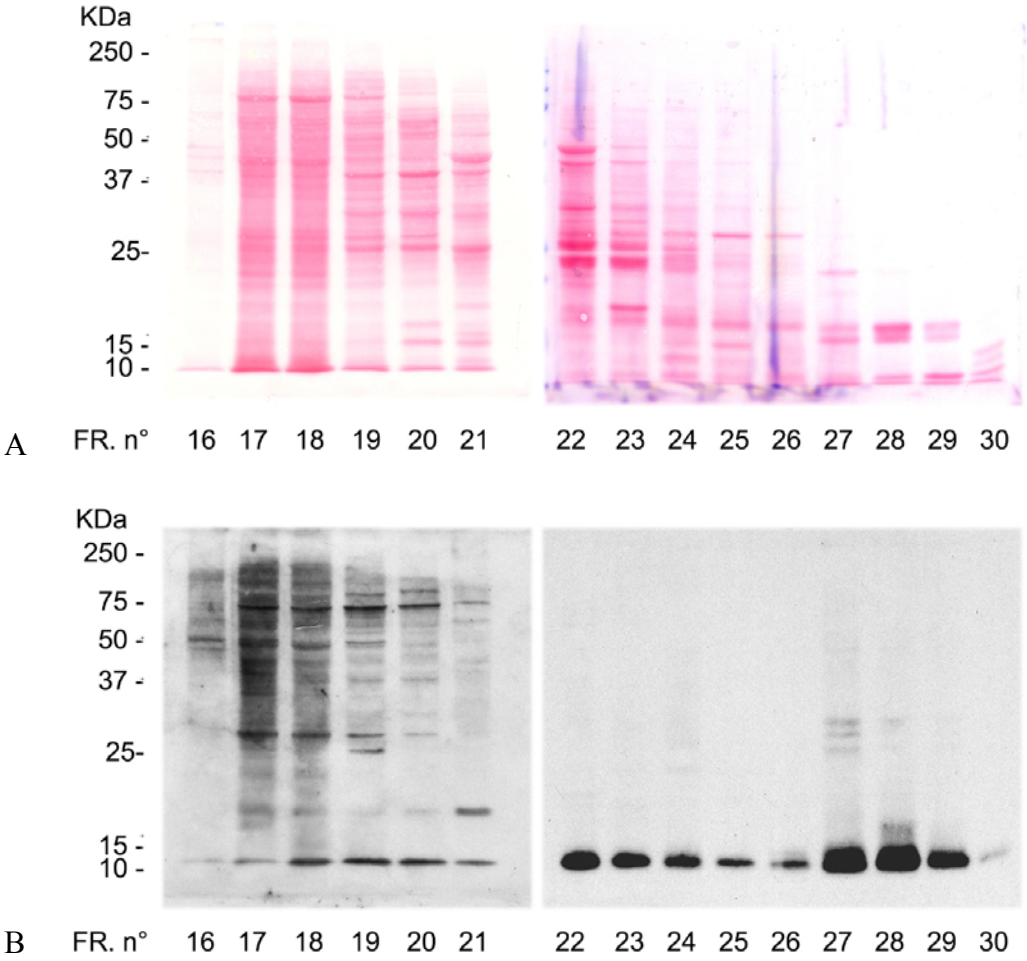

Figure 11. SDS-free size exclusion chromatography of CSTB from a native protein extract of 293T cells analysed on a Tricorn Superdex®75 column: Fractions from the column loaded on SDS Laemmli gel without reducing agents and analysed by western blot. A: Staining with Poinceau red. B: Staining with anti-CSTB abs.

2.2. CSTB FORMS HOMOPOLYMERS

To clarify the nature of the SDS resistant proteins, the CSTB polymers were analysed by in gel digestion and mass spectrometry, following lysis in buffer 2 (Figure 12). Protein extracts from human 293T cells, transfected with the rat HA-CSTB construct, were immunoprecipitated with anti-HA abs, and electrophoresed on SDS-PAGE. The bands indicated in A were analysed and the experimental results were compared to the theoretical molecular mass values (panel B). Bands 1, 2, 3 migrate at the position of endogenous and transfected monomers. Bands 4 and 5 migrate as homo- and hetero-trimers and band 6 as a pentamer. Protein modifications are not detectable although monomer, dimer and trimer migrate in multiple bands within the range of approximately 2 kDa. We envisage two possible reasons for this: 1. The N-terminal region of the protein (fragment 1-24) was not identified by mass spectrometric analysis, therefore the presence of modifications within the first 24 aminoacids can not be excluded. 2. The structure of the protein is unstable and shows conformational differences [2]. The identity between the experimental and theoretical molecular mass values confirms that the bands contain CSTB only, and that their position in the denaturing gel is not due to the interaction with other proteins. As we have transfected human 293T cells with rat CSTB and the rat and human sequences are different, we can distinguish the endogenous human from the transfected rat molecules (panel B and Figure 16). Accordingly, the peptide analysis shows the presence of a mixture between human and rat CSTB. Both species are present in polymeric and monomeric forms. The presence of heteropolymers is explained by the interaction between endogenous and transfected CSTB. The presence of the human CSTB monomer may reflect the formation and partial denaturation of heteropolymeric CSTB following boiling. We conclude that SDS resistant CSTB polymers are not due to covalent interaction with proteins different from itself and that CSTB forms highly stable homopolymeric structures.

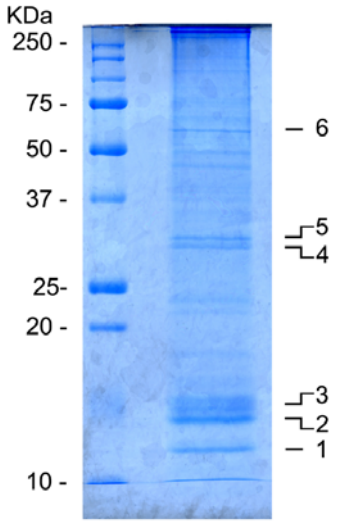

A

B

BAND 1

MM (Exp)	PEPTIDE	MM (Th)
732,4	25-30 H	732,4
636,5	35-39 H	636,4
550,5	40-44 H	550,3
1325,9	45-56 H	1325,7
1421,9	57-68 H	1421,7
2457,6	69-89 H	2457,3
923,5	92-98 H	923,4

BAND 2

MM (Exp)	PEPTIDE	MM (Th)
733,0	39-44 R	732,8
655,0	49-53 R	654,8
592,9	54-58 R	592,7
1223,6	60-70 R	1223,4
775,0	71-77 R	774,8
683,9	78-82 R	683,8
2444,1	83-101R	2443,7
924,3	106-112 R	924,0

BAND 3

MM (Exp)	PEPTIDE	MM (Th)
733,0	39-44 R	732,8
655,0	49-53 R	654,8
592,9	54-58 R	592,7
1223,6	60-70 R	1223,4
775,0	71-77 R	774,8
683,9	78-82 R	683,8
924,3	106-112 R	924,0

BAND 4

MM (Exp)	PEPTIDE	MM (Th)
733,0	39-44 R	732,8
655,0	49-53 R	654,8
1223,6	60-70 R	1223,4
775,0	71-77 R	774,8
683,9	78-82 R	683,8
924,3	106-112 R	924,0
732,4	25-30 H	732,4
1325,9	45-56 H	1325,7
1421,9	57-68 H	1421,7
2457,6	69-89 H	2457,3

BAND 5

MM (Exp)	PEPTIDE	MM (Th)
733,0	39-44 R	732,8
655,0	49-53 R	654,8
1223,6	60-70 R	1223,4
775,0	71-77 R	774,8
683,9	78-82 R	683,8
732,4	25-30 H	732,4
1325,9	45-56 H	1325,7
1421,9	57-68 H	1421,7
2457,6	69-89 H	2457,3

BAND6

MM (Exp)	PEPTIDE	MM (Th)
733,0	39-44 R	732,8
655,0	49-53 R	654,8
1223,6	60-70 R	1223,4
683,9	78-82 R	683,8
924,3	106-112 R	924,0
732,4	25-30 H	732,4
1421,9	57-68 H	1421,7
2457,6	69-89 H	2457,3

Figure 12. Mass spectrometry analysis of CSTB polymers. A: Immunoprecipitation with anti HA(F-7) abs from the same protein extract as in figure 9B. No reducing agents added to the sample. Gel stained with colloidal brilliant blue G (Sigma). Numbers on the right indicate the analysed bands. B: Mass spectrometry analysis. The position of each peptide within the CSTB sequence is shown. H refers to human and R to rat CSTB.

2.3. CSTB POLYMERS ARE SENSITIVE TO THE REDOX ENVIRONMENT

Figure 13 analyses the properties of polymers in relation to a treatment with reducing agents. The effect of increasing pH on the structure is shown in panel A where polymers are barely detectable at pH 9.8. Glutathione at a concentration 2.5-20 mM decreases but does not eliminate the high MW CSTB bands (panel B). The effect of these treatments suggests that CSTB polymers are somewhat resistant to denaturation and that a combination of reducing and denaturing conditions are necessary to depolymerise most of the protein.

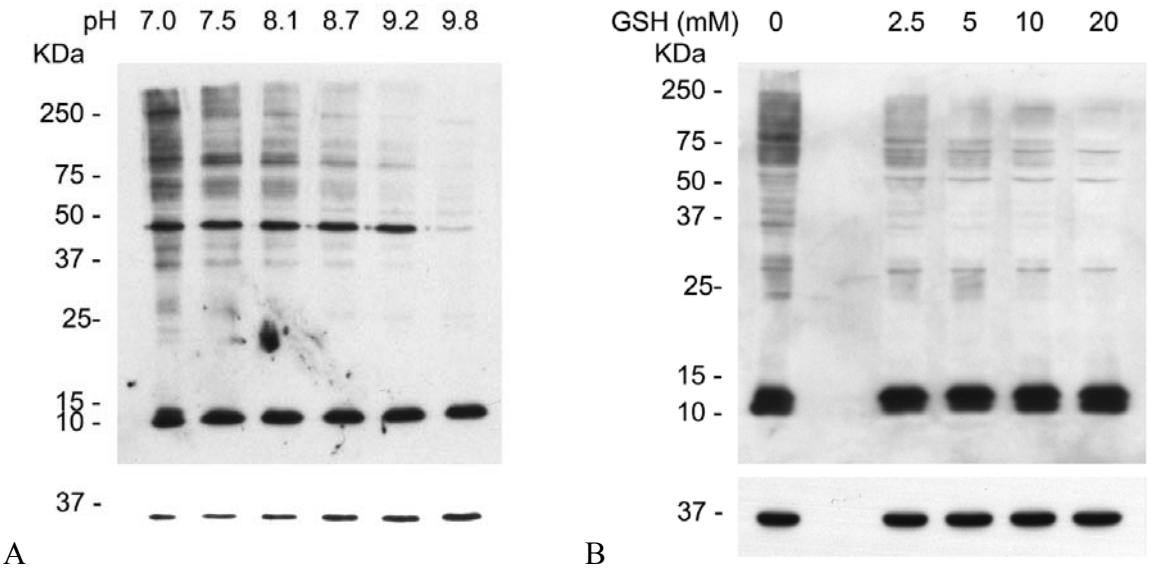

A B

Figure 13. Effect of pH and GSH on CSTB polymers from the same protein extract as in figure 11. No reducing agents added to the samples. Staining with anti-CSTB abs. Lower panels: staining with anti-GAPDH abs. A: pH curve as indicated. B: Samples treated with increasing concentrations of GSH as indicated.

Figure 14 shows the effect of H_2O_2 addition to a protein extract from 293T cells. As the concentration of H_2O_2 increases, first we observe an increase of the dimer band, followed by the trimer that becomes the dominant species starting from 1 M H_2O_2 (B-D). This result suggests that, under oxydising conditions, the trimeric structure of CSTB is very stable. Under reducing conditions (D) monomers are released from the high MW components up to a concentration of 0.8 M H_2O_2. The sample treated with 1.0 M H_2O_2 shows considerable resistance to denaturation of the trimer and of some higher MW components suggesting the existence of irreversible hyperoxydated species, carrying sulphonylated, carbonylated or nitrated residues [200-201].

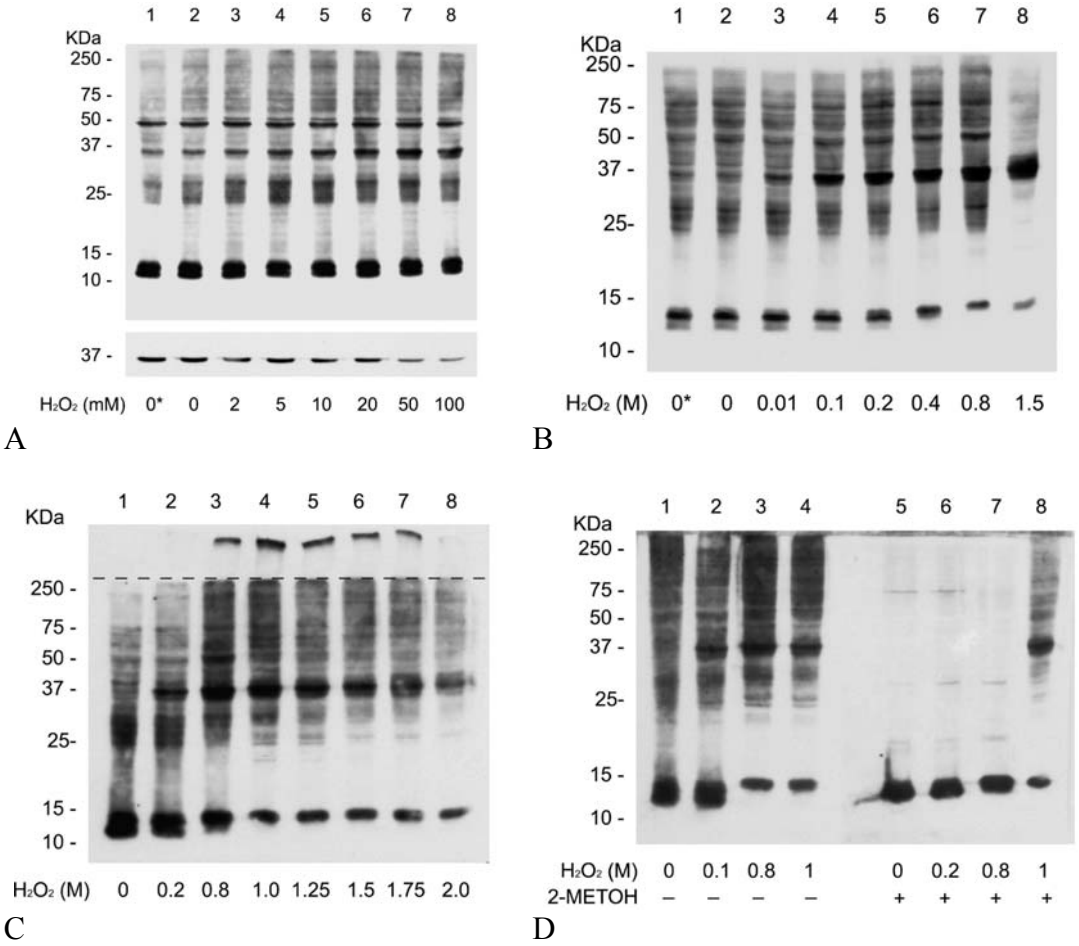

Figure 14. Effect of H2O2 on CSTB polymers from the same protein extract as in figure 11. Samples treated 10 min at RT with increasing concentrations of H_2O_2 as indicated, 0* non incubated sample. Staining with anti-CSTB abs. Lower panel in A: staining with anti-GAPDH abs. In C, the dotted line indicates the position of the stacking region of the gel. A-C: No reducing agents added to the samples. D: Lanes 1-4: minus reducing agents, lanes 5-8: plus reducing agents.

3. CYSTATIN B MUTANTS ARE POLYMERIC

3.1. THE CYSTEINE MINUS MUTANTS

The reactive thiol groups fulfil a sensory and regulatory role on proteins, in response to a defined redox environment. A highly conserved residue of CSTB is the cysteine at position 3. Most CSTB, including the human molecule, contain only this cysteine, while rodent CSTB has an additional cysteine at position 64.

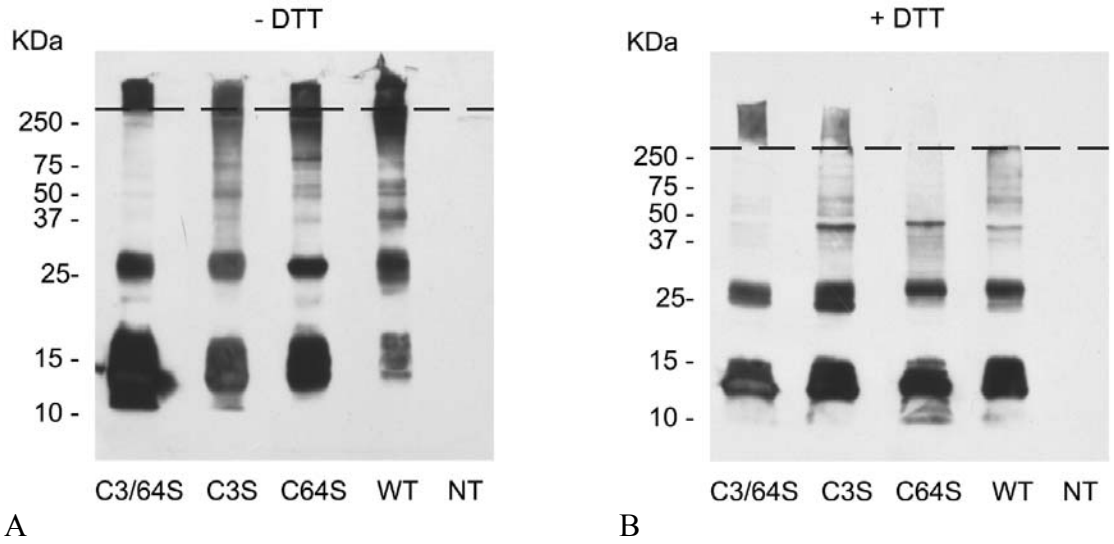

Figure 15. Transfection of CSTB mutants in 293T cells lyzed in buffer 2. Immunoprecipitation with anti-HA(F-7) abs of protein extracts from 293T cells transfected with wt and mutant constructs indicated under the lanes. NT refers to non-transfected cells. SDS polyacrylamide gels run minus (A) and plus (B) 200 mM DTT. Staining with anti-HA(Y11) abs. The dotted line indicates the position of the stacking region of the gel.

Since both human and rat cells contain polymeric CSTB, disulphur bonds can not be responsible for their formation. However the phylogenetic conservation of Cys3 and the sensitivity of the high MW species to the redox environment suggest that at least one cysteine is important. Thus, we have analysed the structure of single and double cysteine substitution mutants of rat CSTB. The immunoprecipitates from protein extracts of cells transfected with these constructs are in figure 15. The banding pattern of the single substitution mutants is similar to that of the wt protein suggesting that the two cysteines present in the rat molecule are interchangeable. In contrast, the ΔCys mutant shows mainly monomers and dimers in addition to high MW polymers stacked in the high portion of the gel. The middle MW components are not detectable. The addition of 200 mM DTT (B) to C3S, C64S and wt CSTB decreases the amount of protein in the stacking gel and releases components migrating in the middle MW range. The ΔCys mutant does not respond to DTT addition. We can conclude that disulphur bonds are not necessary to form dimers, and that neither

the phylogenetically conserved Cys3 nor Cys64 are necessary for the formation of high MW species. However, reactive thiol groups seem to be important to stabilize the intermediate MW species which are clearly visible and stable when at least one cysteine is present in the sequence. Cystatin dimers generated *in vitro* by domain swapping have been described by Staniforth et al. [2] as the initial step to the formation of amyloid fibers. It is possible that the dimer that we observe *in vivo* has a similar origin implicating hydrophobic interactions. However, the existence of different types of covalent bonds can not be excluded.

3.2. THE DISEASE MUTANTS

We have analysed the structural organization of a number of CSTB mutants including those isolated from EPM1 patients (Figure 16). The following natural mutants were constructed: G4R, Q71P, Δ68 and Δtc. Laboratory mutants were constructed using the cystatin sequence alignments published by [202]: Δ64 (stop codon at position 64), ΔE1(deletion of exon 1 encoding aminoacids 1-22), the substitution mutants V59Q and T87K. The latter substitutions are derived from the cystatin C mutants I66Q and I102K described by Staniforth et al [2]. I66Q is the chicken equivalent of human L68Q, from patients affected by the Icelandic type of amyloidosis [203]. Staniforth et al [2] have shown that the I66Q mutant forms essentially dimers while the I102K generates monomers only.
All CSTB mutants generate high MW structures (Figure 17A). Differences in the banding patterns are mainly due to the different MW of the constructs. In agreement with the previous experiments, the addition of 200 mM DTT is not sufficient to depolymerize CSTB completely (panel B). Both carboxyl- and amino-terminus deletion mutants seem to polymerize very efficiently. In contrast to the results obtained by Staniforth et al. [2] *in vitro*, the V59Q and T87K generate monomers and high MW components, suggesting that there is a difference between the *in vivo* and *in vitro* process of polymerization. We

conclude that none of the mutations analysed interferes with the process of polymerization of CSTB *in vivo*.

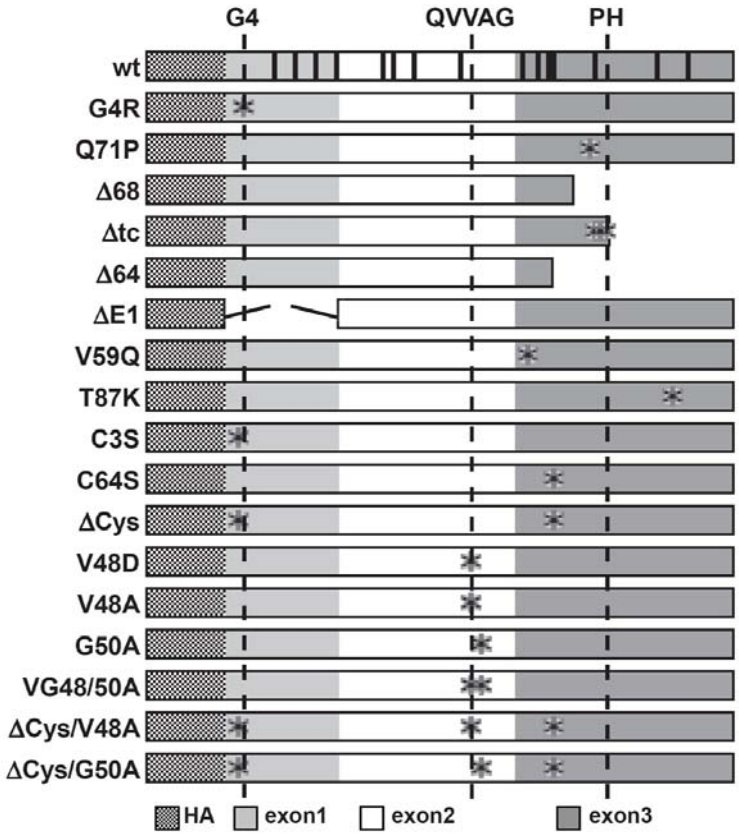

Figure 16. Structure of wt and mutant rat CSTB constructs. The vertical lines in the wt scheme indicate the position of amino acids which differ between rat and man. The asterisks indicate the position of the amino acid substitutions in the mutants. The dotted lines indicate the position of the phylogenetically conserved motives shown above.

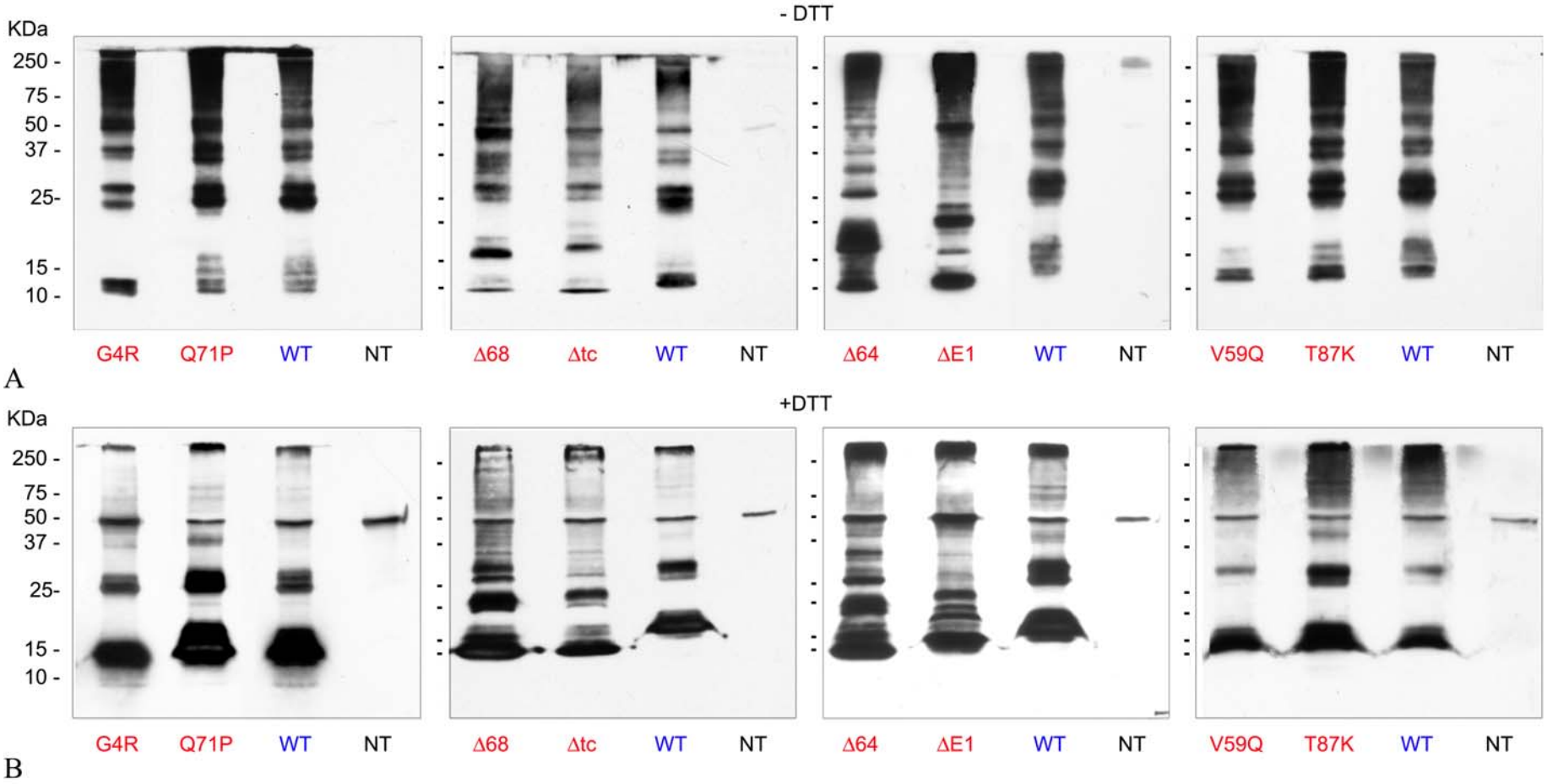

Figure 17. Transfection of CSTB mutants in 293T cells lyzed in buffer 2. Immunoprecipitation with anti-HA(F-7) abs of protein extracts from 293T cells transfected with wt and mutant constructs indicated under the lanes. NT refers to non-transfected cells. SDS-PAGE run minus (A) and plus (B) 200 mM DTT. Staining with anti-HA(Y11) abs.

3.3. THE LOOP 1 MUTANTS

According to Staniforth et al [2], aminoacid substitutions in the QVVAG loop of cystatins do not allow polymerization of the molecule. We have generated single and double substitution mutants of this region to see whether *in vivo* polymerization requires the integrity of loop I. The mutant V48D corresponds to the chicken mutant V55D of Staniforth et al [2]. We have also generated additional mutations at the most highly conserved sites of the QVVAG loop: V48A, G50A and VG48/50A. The substitutions at aminoacid positions 48 and 50 were also inserted in the cysteine minus constructs (ΔCys/V48A and ΔCys/G50A). The distribution of the CSTB bands in all mutants is similar to that of the wt protein with the exception of the cysteine minus constructs that show monomers, dimers and bands larger than 250 kDa as dominant species, while the intermediate forms are barely detectable (Figure 18).

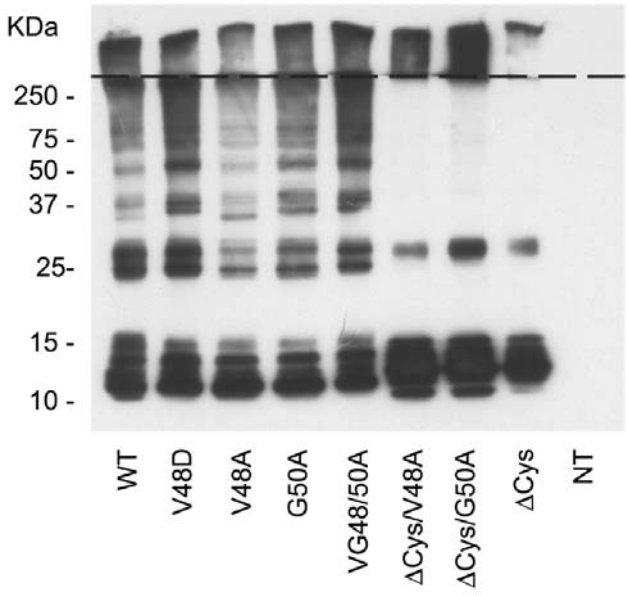

Figure 18. Western blot analysis of protein extracts from 293T cells transfected with single and multiple substitution mutants of loop 1. Cells lyzed in buffer 2. No reducing agents added to the samples. Staining with anti-HA(F-7) abs. The dotted indicates the position of the stacking region of the gel.

We conclude that aminoacid substitutions in loop I do not alter the polymerizing capacity of CSTB *in vivo*, irrespective of the presence/absence of cysteines in the molecule. These results are in contrast with those obtained by Staniforth et al [2] *in vitro*. This difference may be due to the presence of chaperon or other proteins involved in the *in vivo* polymerization [204].

4. MOLECULAR MECHANISM OF CYSTATIN B POLYMERIZATION

4.1. CSTB POLYMERS IN PROKARYOTIC CELLS

The experiments described so far show that eukaryotic cells polymerize CSTB and that the polymeric structure is sensitive to reducing and oxydising agents. It is possible that 1) the redox environment regulates the reaction and 2) the reaction is mediated by a factor, possibly an enzyme. While expressing wt CSTB in E. coli, we have observed that the protein has a polymeric structure undistinguishable from that found in the mammalian 293T cells. Figure 19A shows the SDS−PAGE of protein extracts from E. coli cells transformed (lanes 1, 3) and 293T cells transfected (lanes 2, 4) with expression vectors empty or plus wt CSTB cDNA. Panel B shows the SDS-PAGE of wt and mutant HA-CSTB constructs expressed in E. coli. The banding pattern observed in the wt protein is also present in all the mutants with the exception of the proteins in which both cysteines were substituted by either alanine or serine. The pattern of the latter mutants differs from the others mainly for the paucity of bands in the middle MW range, between approximately 25 and 250 kDa. Interestingly, this pattern is the same as that observed in transfected 293T cells (Figure 17). We can conclude that the polymerizing activity found in 293T cells is present also in the E. coli prokaryotic system.

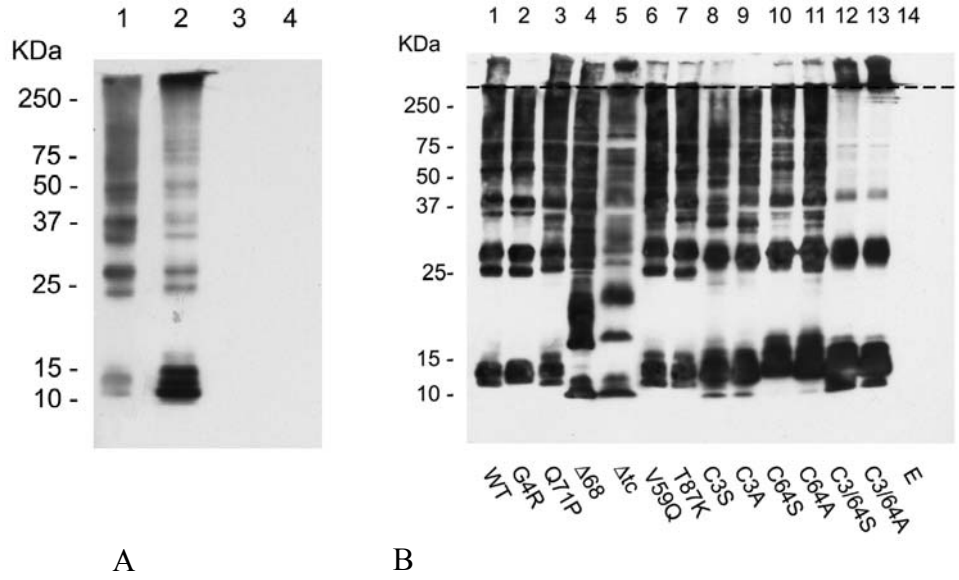

Figure 19. Expression of CSTB. Western blot analysis of total protein extracts. The staining was with anti−HA abs, no DTT added. A. protein extracts from 293T cells transfected (lane 1) and non transfected (lane 3) and E. coli cells transformed (lane 2) and non transformed with the HA-CSTB expression vectors. B. Protein extracts from E. coli cells transformed with wt and mutant HA-CSTB vectors, and with the empty vector (E).

Figure 20 shows the western blot of a 2D-PAGE of HA-CSTB immunoprecipitated from an E. coli protein extract. The anti-HA immunoblot allows the identification of a variety of spots (panel A). According with the results obtained with mammalian cells, the polymers are resistant to urea and reducing agents. Interestingly the polymeric species have a pI different from that of the monomeric protein which is represented by a number of spots with pIs ranging between 5-6. This is different from what we have seen in 293T cells, where the pI of the monomer is approximately 7. The dimer, of approximately 25 kDa, has a pI >9.5, which is the limit of the strip. The larger species are characterized by pIs decreasing gradually towards neutrality up to a MW of approximately 250 kDa. These latter components migrate at a position corresponding to that of the monomers, with a slightly acidic pI. This experiment suggests a radical change of structure in the transition from monomer to dimer, involving the exposure of residues with a positive charge

and the burying of negative residues. Furthermore, the results indicate the existence of two structurally defined populations of polymers of different MW. The oligomers ranging between 25 and 100/200 kDa and the >250 kDa polymers. The presence of oligomers characterized by alkaline pI strongly suggests a high degree of structural instability at the physiological pH of the cells.

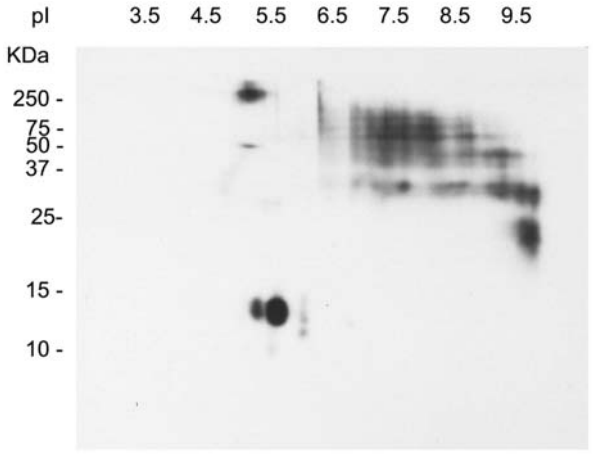

Figure 20. 2D-PAGE of E. coli CSTB immunoprecipitated with anti HA(F-7) abs. Staining with anti-HA(Y11) abs.

4.2. A CSTB POLYMERIZING FACTOR

The results described above suggest that the mechanism of CSTB polymerization is the same in prokaryotes and eukaryotes, implying the existence of a conserved factor(s) responsible for the process. This may be useful, since, contrary to mammalian cells, E. coli does not express endogenous CSTB, offering a background free system to study CSTB polymerization. Thus, we have sought the putative polymerizing factor (PF) in the E. coli protein extract with the following experiments.

4.2.1. THE POLYMERIZATION ASSAY

The HA-CSTB monomer was purified by electroelution from E. coli cells transformed with the pET16b-HA-CSTB expression vector. A polymerization assay was carried out by mixing HA-CSTB monomers with 10 μg of E. coli protein extract from cells transformed with the empty vector. The samples were analysed by SDS−PAGE and western blot (Figure 21, lane 3). A similar experiment was carried out using the protein extract from human 293T cells (lane 2). Lane 1 contains the untreated monomer that shows a weak band in the position of the dimer and two very faint higher MW species. The addition of the protein extract from both E. coli and 293T cells drastically decreases the amount of monomeric CSTB and shows a strong polymeric pattern with components up to 90−100 kDa. Once again, the two patterns obtained with prokaryotic and eukaryotic protein extracts are indistinguishable.

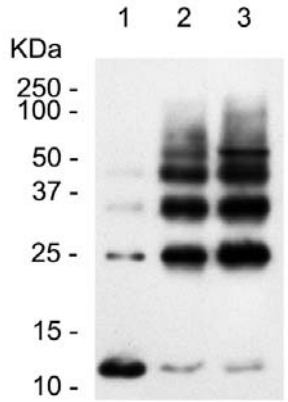

Figure 21. Polymerization assay. HA-CSTB monomer untreated (lane 1) and incubated with 1 mg/ml of protein extract from 293T (lane 2) and E. coli cells (lane 3) lysed in buffer 1. Western blot analysis with anti HA(F-7) abs. No reducing agents added.

In order to determine the amount of total E. coli protein extract necessary to polymerize CSTB, equal amounts of monomer were incubated with increasing concentrations of protein extract (Figure 22 lanes 3-7). The untreated monomer is in lane 1 and the protein extract alone is in lane 2. The intensity of the

polymeric bands increases with the increase of the protein extract and 50 μg/ml of protein extract is sufficient to obtain an easily detectable polymerization. This concentration of protein or its equivalent was used in all the following experiments.

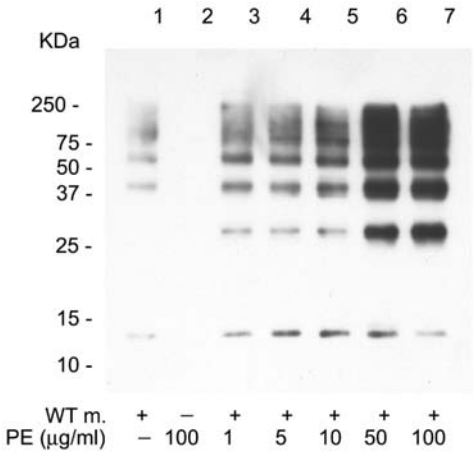

Figure 22. Polymerization assay. HA-CSTB monomer untreated (lane 1) and incubated with increasing concentrations of protein extract from E. coli cells lysed in buffer 1. Western blot analysis with anti HA(F-7) abs. No reducing agents added.

4.2.2. CHARACTERIZATION OF CSTB POLYMERIZING FACTOR BY COLUMN CHROMATOGRAPHY.

The following experiments show that PF can be further characterized by fractionating total E. coli protein extract by column chromatography. 2 mg total E. coli cell extract from cells transformed with the empty pET16b-HA expression vector, were fractionated on a Tricorn Superdex®200 (Amersham) column (Figure 23). 30 samples containing 0.5 ml fractions were collected. Fractions 9-22 contain the excluded volume. Fractions 23-34 represent the size fractionation volume ranging between approximately 10 and 100 kDa. We have mixed the HA-CSTB monomers with 5ul (approximately 0.5 μg protein) of each column fraction. As expected, the fractions from the excluded peak induce polymerization without a defined pattern. This may be due

to the interaction of PF with other E. coli proteins and to the lack of fractionation in this region. Fractions 23−34 show a weaker polymerizing activity in the initial and final samples of the column, while the middle fractions show a stronger activity, suggesting a peak shape in the region of 40−80 kDa. The polymerization assay was repeated with fractions 23−34 utilizing monomers obtained from 4 different CSTB mutants.

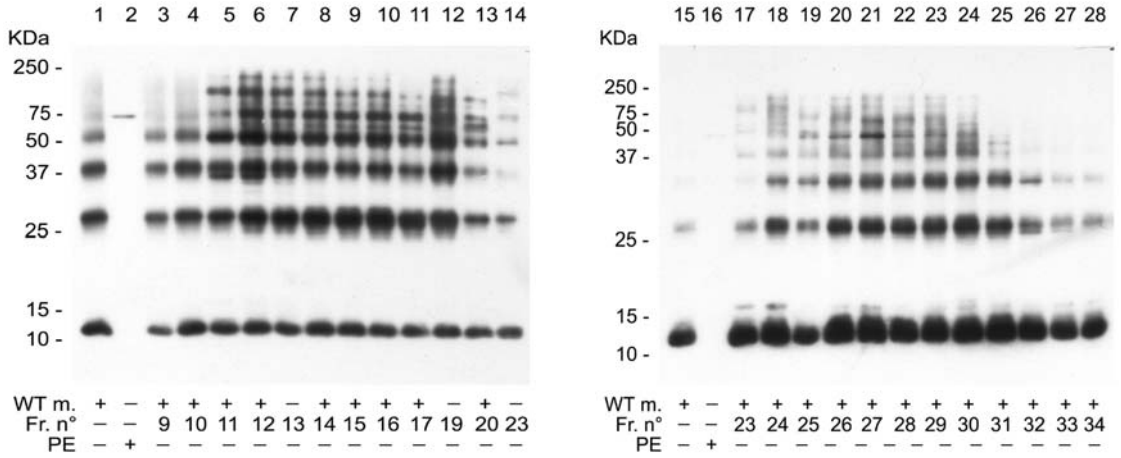

Figure 23. Polymerization assay of wt HA−CSTB monomers added to the protein extract fractions of a superdex 200 column. No DTT added. Western blot analysis and staining as in figure 22.

Figure 24 shows the fractionation assay on the same column as in figure 23 using monomers from the G4R EPM1 natural mutant (A). Again, the polymerizing activity is present in fractions 24−30. B shows that DTT addition depolymerizes CSTB although some resistant high MW species remain.

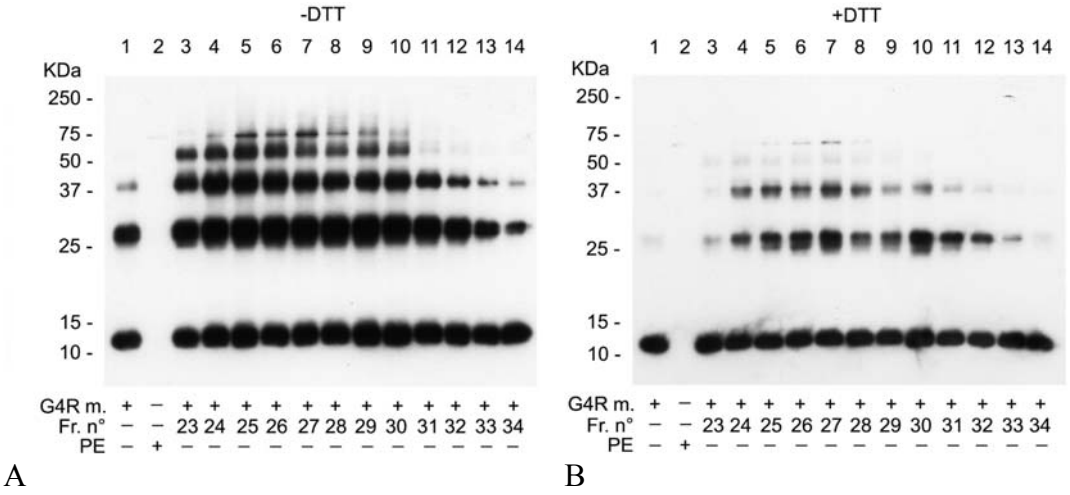

Figure 24. Polymerization assay of G4R HA−CSTB monomers added to the protein extract fractions of a superdex 200 column. Western blot analysis and staining as in figure 22. A: minus DTT, B: plus 50 mM DTT.

Figure 25 represents a similar experiment carried out with monomers obtained from the Δ68 EPM1 natural mutant. Polymerization occurs in the same fractions and with a very similar distribution (A) as in figure 23. B shows that the addition of DTT depolymerizes the protein, releasing a large amount of monomers and dimers.

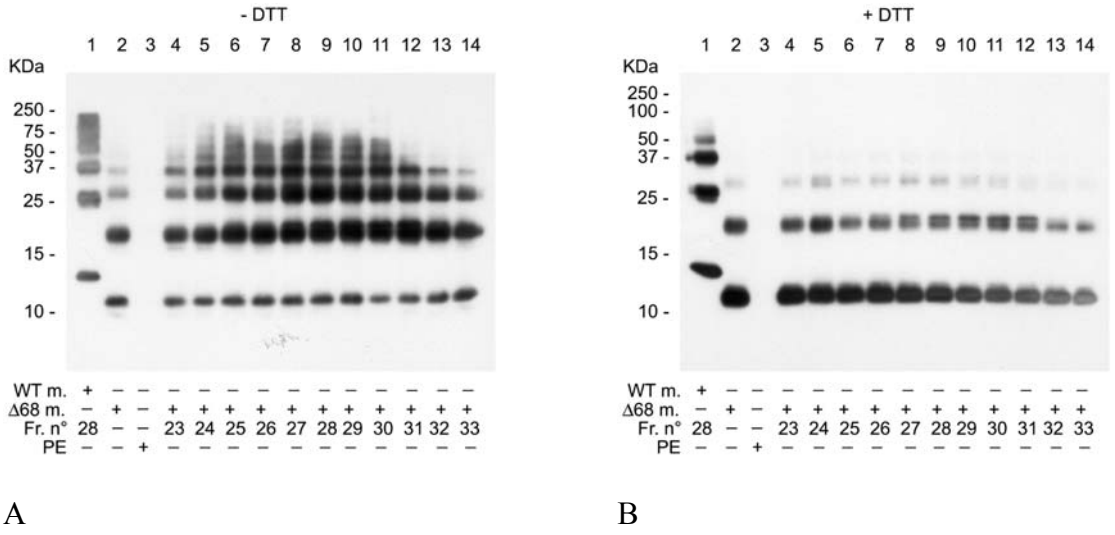

Figure 25. Polymerization assay of Δ68 HA−CSTB monomers added to the protein extract fractions of a superdex 200 column. Western blot analysis and staining as in figure 22. A: minus DTT, B: plus 50 mM DTT.

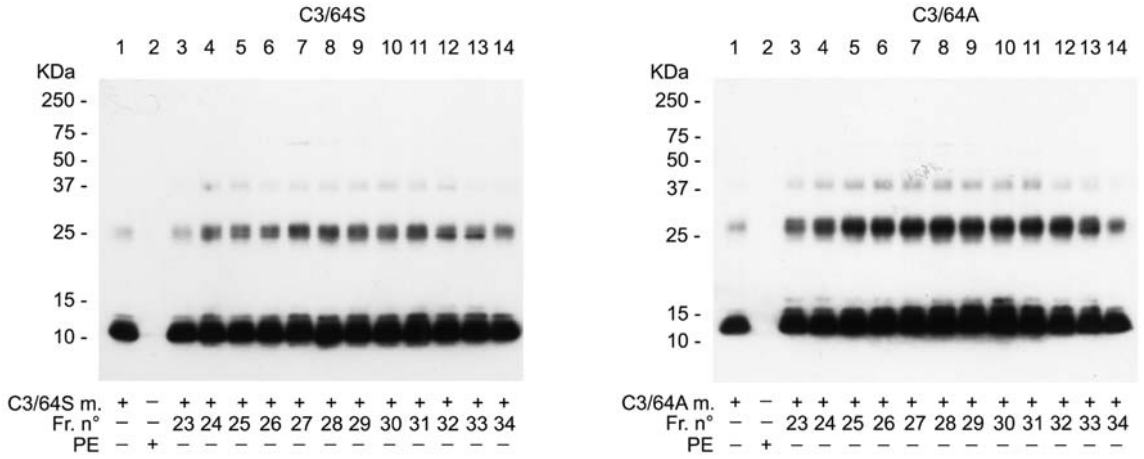

A B

Figure 26. Polymerization assay of cysteine minus HA−CSTB monomers added to the protein extract fractions of a superdex 200 column. Western blot analysis and staining as in figure 22. No DTT added. A: C3/64A. B: C3/64S.

The most interesting result is in figure 26, where monomers isolated from the cysteine minus mutant were used for the assay. These monomers are not polymerized by any of the gradient fractions. This is true whether the cysteines are substituted by serine (A) or alanine (B). Polymerization occurs also with monomers that contain only one cysteine either in position 3 or 64 (not shown), suggesting that one cysteine is necessary and sufficient to allow polymer formation. Fractions 24−31 of the Superdex 200 column were pooled and loaded onto a monoQ ion exchange column (Amersham) (Figure 27). The elution was on a 0−1M NaCl gradient, in 20mM TRIS pH7.9. The polymerization assay was carried out only with wt monomers, as described above. The beginning and the end of the gradient are in fractions 8 and 54. Polymerizing activity is evident in fractions 24−30. To check the MW of the polymerizing activity obtained from the mono Q column, we have loaded fractions 24, 26, 27, 28, 29 and 30 separately on a Tricorn Superdex® 75 column. (Amersham).

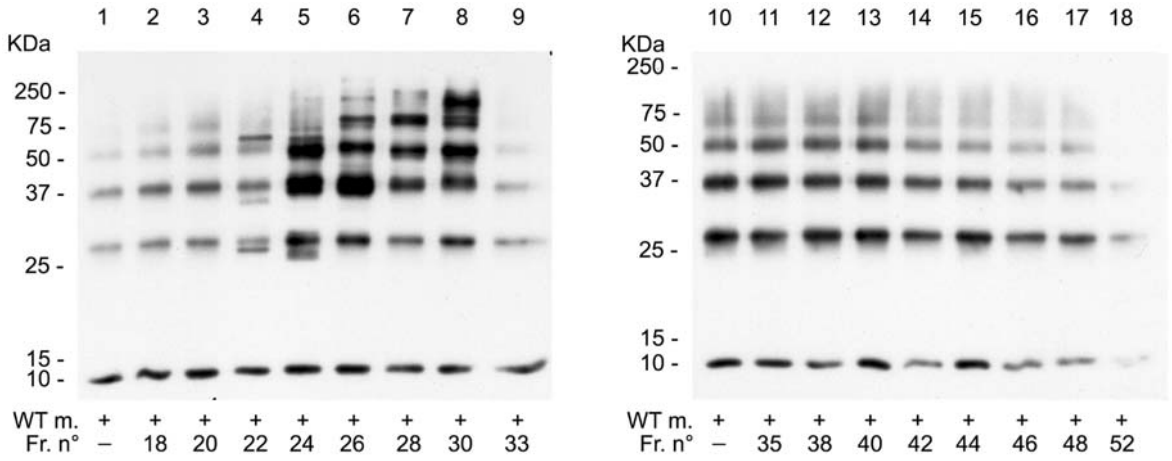

Figure 27. Polymerization assay of wt HA−CSTB monomers added to the protein extract fractions of a monoQ column. Western blot analysis and staining as in figure 22. No DTT added.

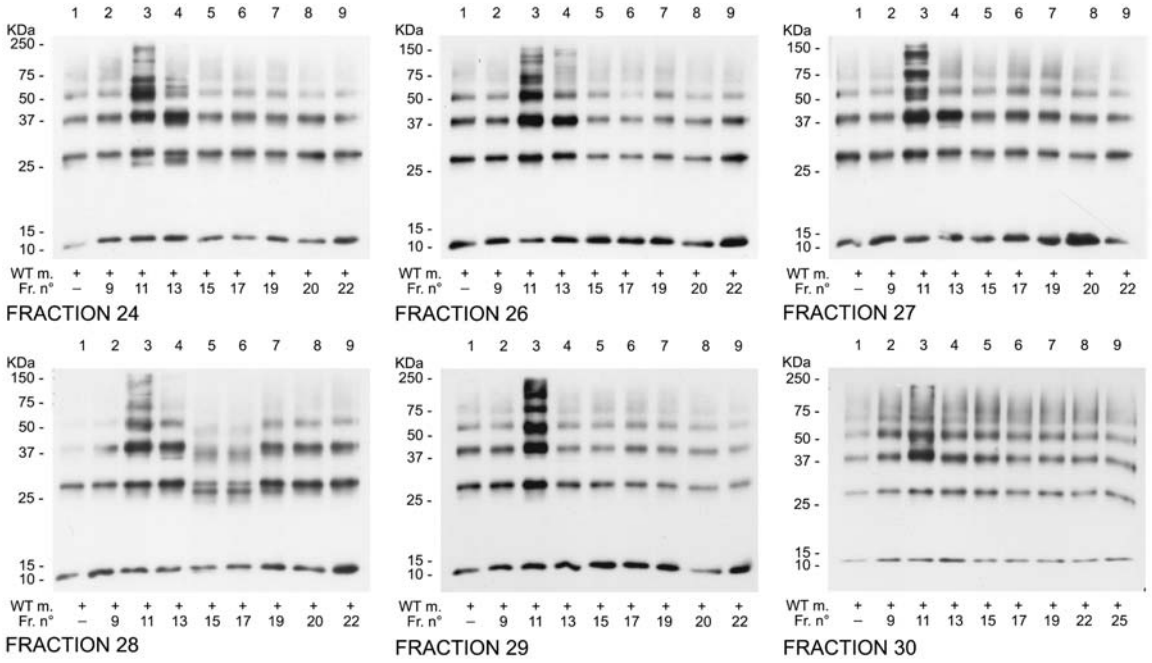

Figure 28. Polymerization assay of wt HA−CSTB monomers added to the protein extract fractions of a superdex 75 column, as indicated. No DTT added. Western blot analysis and staining as in figure 22.

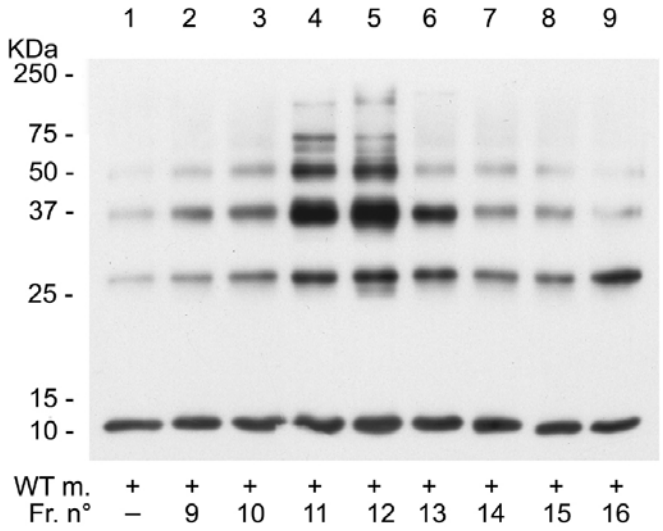

Figure 29. Polymerization assay of wt HA−CSTB monomers added to the protein extract fraction 26 of a superdex 75 column, as indicated. No DTT added. Western blot analysis and staining as in figure 22.

The analyses of fraction 24-30 are shown in figure 28. Fraction 11 of the superdex 75 column contains the highest activity in all samples tested. Fraction 26 was analysed in detail (Figure 29). The highest polymerizing activity observed in fractions 11/12 suggests that PF has a MW ranging between 50 and 70 kDa. .

These data show that E. coli protein extract contains a protein of approximately 70 kDa MW that triggers the polymerization of CSTB monomers by monomer addition. We think that this protein may be a redox related enzyme, possibly a modifier of the thiol group of cysteine. In fact, the cysteine minus mutant does not polymerize, while wt and mutant proteins, containing this aminoacid residue, polymerize. It is interesting to notice that the polymerizing activity that we describe refers to the generation of oligomers, while we do not see species larger than 100 kDa.

5. EXPRESSION OF CYSTATIN B AND ITS MUTANTS IN SKNBE CELLS

5.1. CSTB GENERATES AGGREGATES *IN VIVO*

Since 293T cells tend to form foci during growth and are detached from the plate surface by the fixation procedure, we have chosen SKNBE neuroblastoma cells for the microscopic analysis. The *in vivo* phenotype induced by expression of rat CSTB and its mutants in SKNBE cells was analysed by immunofluorescence confocal microscopy (Figure 30). The distribution of the wt protein is similar in transfected and non-transfected SKNBE cells. The localization of the protein is mainly nuclear [34], although in transfected cells the protein is clearly detectable also in the cytoplasm. Following 24 Hr transfection, the localization of the substitution mutants is similar to that of wt rat CSTB. In contrast, the carboxy- and amino-terminus deletion mutants show a different distribution: the staining with anti-HA abs is barely detectable in the nuclear compartment and is strong in the cytoplasm (Figure 31). Furthermore, the signal is concentrated in randomly distributed aggregates of variable size and number, similar to the cytoplasmic inclusion bodies described by Rajan et al. [205]. In some cases, the aggregates are numerous and small (Δ68), in other cases we see larger aggregates which may result from the confluence of small ones (Δ64 and ΔE1). In agreement with the nuclear presence of the endogenous protein, the same cells are stained by the anti-CSTB abs both in the nucleus and in the cytoplasm, and aggregated forms are also detected.

Figure 30. Expression of CSTB. Confocal microscopy analysis of SKNBE cells transfected 24 hr with CSTB wt and aminoacid substitution mutants as indicated. Staining with anti-CSTB and anti-HA Abs. Co-localization is shown. Bar: 5 μm.

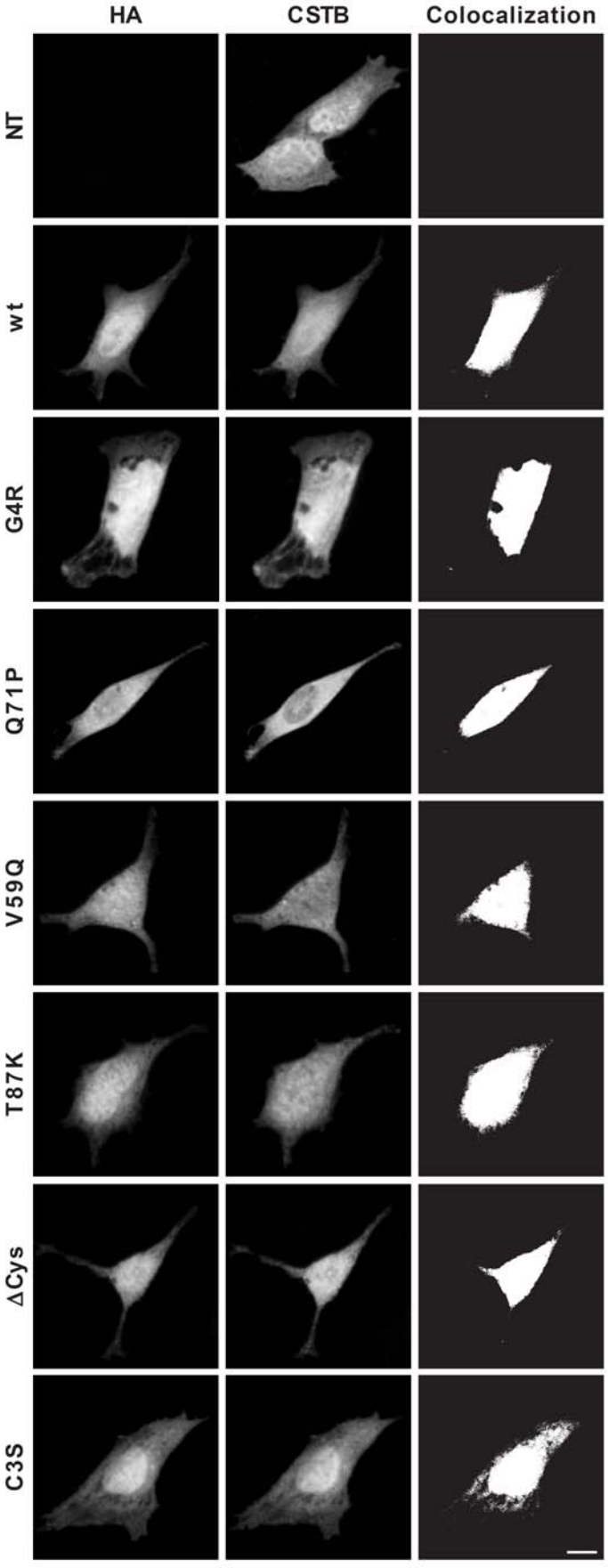
HA
CSTB
Colocalization
NT
wt
G4R
Q71P
V59Q
T87K
ΔCys
C3S

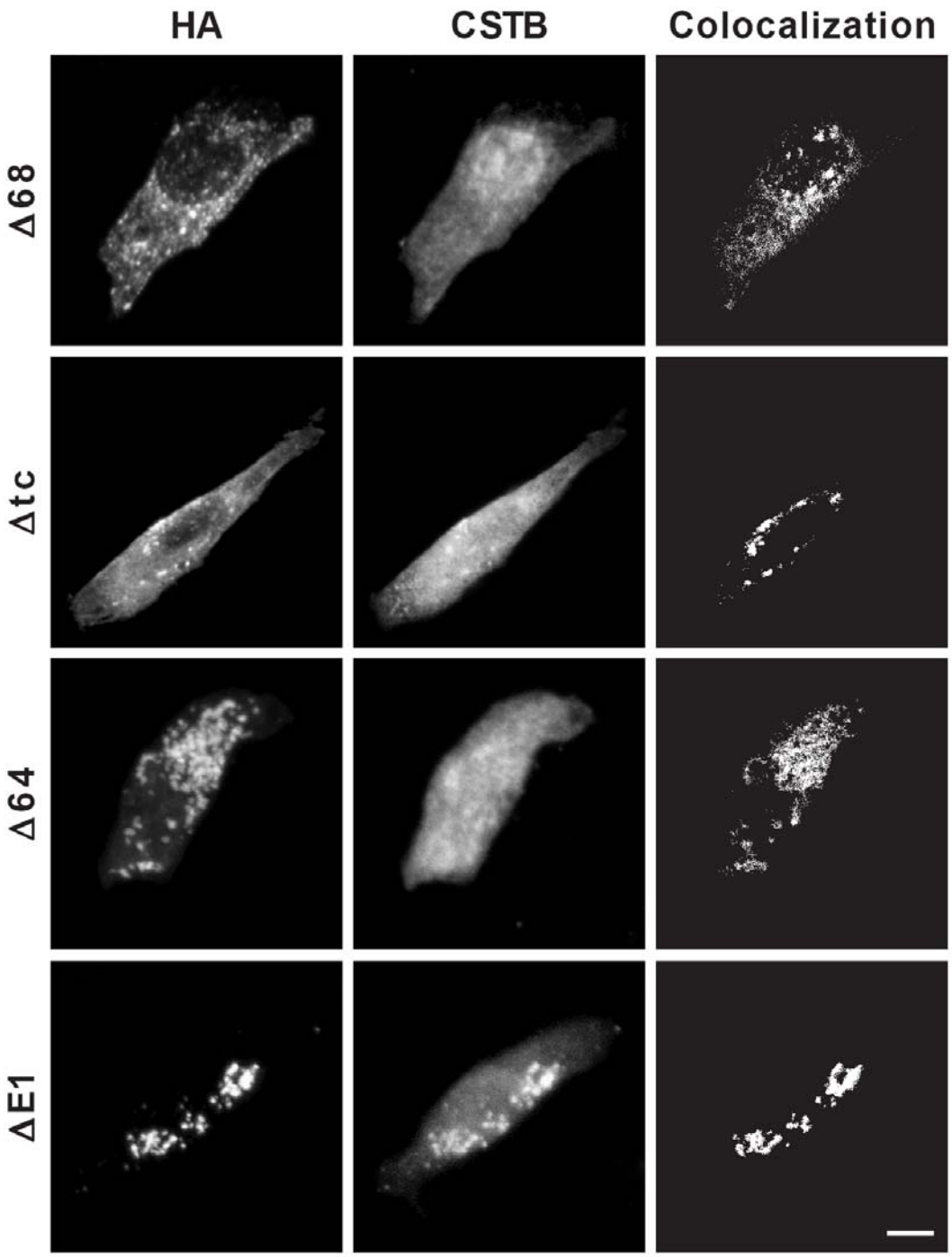

Figure 31. Expression of CSTB. Confocal microscopy analysis of SKNBE cells transfected 24 hr with deletion mutants of CSTB as indicated. Confocal microscopy analysis as in figure30. Bar: 5 μm.

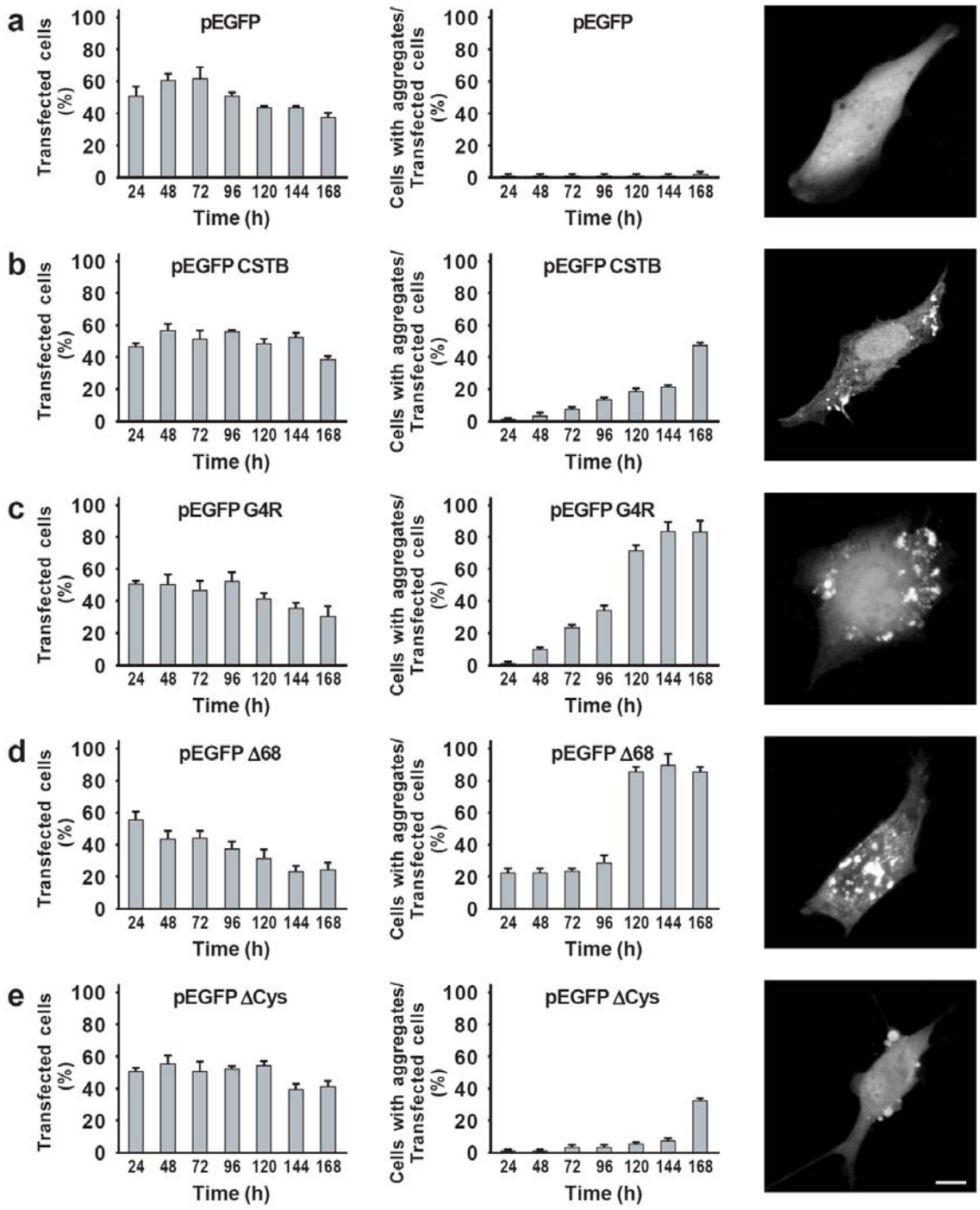

Figure 32. Time course of transfection of SKNBE cells with pEGFP fusion constructs of wt and mutants CSTB. The percentage of transfected cells shown in the histogram on the left is compared with the percentage of cells containing CSTB aggregates on the right. The latter value is calculated as the ratio of aggregate containing over transfected cells. Fluorescent aggregates generated by the CSTB fusion proteins are shown on the right of the histograms. The transfected constructs are indicated over each histogram. Bar: 5 μm.

We have carried out a time course of transfection up to 7 days in order to study the rate of aggregate formation throughout this period (Figure 32). The ΔCys mutant, that seemed to modify the polymerization properties of CSTB, and two natural EPM1 mutants were chosen for this experiment. The proportion of transfected cells is relatively constant up to 7 days when, in most samples, a slight decrease becomes visible. The exception is the Δ68 mutant that shows a decline of the transfected cell number. The green fluorescent protein (EGFP) alone, up to 7 days after transfection, does not produce detectable aggregates (panel A). The wt CSTB fusion construct starts generating aggregates 48 Hr after transfection and the number of positive cells increases gradually for 7 days, when approximately 50% of the transfected cells contain CSTB inclusions (panel B). The G4R mutant shows a steeply growing curve where, from day 5 to 7, 70-90 % of the transfected cells contain aggregates (panel C). After 24 Hr transfection, the Δ68 fusion generates aggregates already in 20% of the cells (panel D) and, at day 5, almost 100% of the cells contain aggregates. The time coincides with the decrease of transfected cell number due to death .

The ΔCys fusion does not produce detectable aggregates until day 7, when approximately 30% of the transfected cells are affected (Figure 15E). This result is interesting as we have seen that the transfected ΔCys mutant does not show detectable oligomers, altering the polymerization pattern of CSTB (Fig. 15). The observation is also in good agreement with figure 29, where the ΔCys mutants do not oligomerize on addition of the fractionated protein extract from E. coli.

DISCUSSION

1. INTERACTION OF CYSTATIN B WITH CYTOPLASMIC PROTEINS

Di Giaimo et al. [3] have shown that, in rat cerebellum, CSTB interacts with a number of cytosolic proteins involved in the cytoskeletal function. Two of them, NFL and β-spectrin, are exclusive of the nervous system and the authors have suggested that the binding of CSTB with CNS-specific proteins can be at the basis of the CNS-specific phenotype associated with EPM1.

We have obtained comparable results analysing CSTB interactions in the 293T human cell line, confirming the binding of the protein with RACK1, NFL and β-spectrin. We have extended the list of the CSTB-binding proteins through a 2D-PAGE analysis and found another CNS-specific partner, neuronal copine. Neuronal copine belongs to the copine family of proteins which, upon Ca2+ activation, bind phospholipid membranes through the action of two C2 domains in the N-terminal region of the protein. Their C-terminal domain interacts with a number of intracellular target proteins [206-207]. Thus, copines are thought to mediate the Ca2+-dependent association of target proteins with phospholipides, regulating their intracellular localization and activity and being involved in growth control, cell cycle, apoptosis and cytoskeletal organization. Tomsing et al [207] have shown that copines bind preferentially coiled-coil domains of target proteins, among which there are β-actin and the CSTB partner brain β-spectrin [206-207]. Nakayama et al [208] have suggested that neuronal copine may have a role as a Ca2+ sensor in postsynaptic events, in contrast to the known role of other “double C2 domain-containing proteins” such as synaptotagmin I, in presynaptic events. Interestingly, CSTB interacts also with

the double C2 domain-containing protein synaptotagmin II [Rossella Di Giaimo and Marialuisa Melli, unpublished]. It is possible to propose that CSTB, by interacting with all these partners, is also involved in pre- and post-synaptic events.
The involvement of CSTB in vesicle traffic, cytoskeletal modelling and calcium metabolism is further implicated by its interaction with annexin A2 11 and A8 that we have observed both in the yeast two hybrid system and by 2D-gel. Annexins are characterized by a conserved membrane-binding domain Ca2+-regulated and a N-terminal domain of protein interaction, unique for a given member of the family. They can associate with negatively charged phospholipids in a Ca2+-dependent and reversible manner. This property links annexins to Ca2+ signalling and membrane-related events [209-210]. In particular, annexin A2 is implicated in the organization of membrane lipids at sites of actin cytoskeleton attachment [211-212]. Annexin A2 is also involved in Ca2+-regulated exocytosis and endocytosis [211-212]; this may correlate with the isolation by the two hybrid system of a number of proteins involved in vesicle traffic and cytoskeletal modelling (clathrin light chain, α−tubulin and the microtubule-binding proteins dynactin subunit p25 and kinesin which is involved in anterograde axonal transport of synaptic vesicles) [Rossella Di Giaimo and Marialuisa Melli, unpublished]. Annexin A2 is also implicated in the regulation of the Ca2+ channels in the sarcoplasmic reticulum [209-210]. Interestingly we have found another protein associated with ER Ca2+-regulated function, calreticulin, which is the major Ca2+ binding protein in ER lumen, where it is involved in protein glucosylation through the calnexin/calreticulin cycle [213-214]. While annexin A2 has a nuclear export signal in its N-terminal domain and may be involved in RNA nuclear export [209-210], annexin A11 has been detected as a nuclear protein that translocates from the nucleoplasm to the nuclear envelope in cells at prophase [215-216]. It is worth noting that CSTB is mainly localized in the nucleus, although its

function in this compartment has never been investigated. The main localization of annexin A11 is at the midbody, where it probably functions in the terminal phase of cytokinesis, in the trafficking, or insertion and fusion of the new membrane that is known to be required for abscission [217]. Rossella Di Giaimo and Marialuisa Melli (unpublished) have isolated another protein essential for cytokinesis, the actin binding protein prophilin. Although actin has never been individuated as a CSTB interactor, both sets of data (immunoprecipitation and two-hybrid experiments) define proteins that interact with actin, including thymosin beta−10, which regulates actin polymerization [Rossella Di Giaimo and Marialuisa Melli, unpublished].

With the two different approaches used in our laboratory, the two-hybrid system and the immunoprecipitation analysis, we have identified both direct- and indirect-CSTB interactors. It is interesting that many of the CSTB partners interact with each other and are involved in the same cellular process, the cytoskeletal function. Altogether, our data seem to draw CSTB in the Ca2+-mediated cytoskeletal activity, and in particular in vesicle traffic at the membrane level. This function is at the basis of neuronal signal transmission. Interestingly, our immunoprecipitation experiments with the EPM1 mutants of CSTB suggest that its cytoskeletal function could be altered in EPM1. In fact the absence of interaction between the Δ68 mutant and RACK1 indicates that this mutation changes the structure of the multiprotein complex.

In conclusion, these experiments show that CSTB binds many different proteins, some of which very large. As CSTB entails 100 aminoacids only, it seems very reasonable that the interaction with the partners is mediated by CSTB polymers.

2. CYSTATIN B IS POLYMERIC *IN VIVO*

So far, CSTB has been described as a protein that, *in vivo*, is monomeric and , *in vitro,* is prone to amyloid fiber formation [105]. Cystatins have been associated

with amyloidosis, in particular, the L68Q variant of cystatin C is the cause of a hereditary amyloid angiopathy and is a major constituent of the plaques found in the brain of the patients. Another common finding is the presence of cystatin A and B in the senile plaques of the Alzheimer and Parkinson diseases, and of senile dementia patients. Our results show that CSTB *in vivo* has a polymeric structure very resistant to denaturation and its over-expression generates cellular aggregates. Manning and Colòn [218] have described a number of proteins characterized by high kinetic stability and resistance to SDS denaturation, that require boiling for any change in structure. Interestingly, some of these proteins are polymeric and reach in β-sheets. We find that the polymeric structure of CSTB is resistant to 20 min boiling in 1% SDS and this is confirmed by the very similar distribution pattern of polymers from cells lyzed plus and minus 1% SDS. According to Manning and Colòn [218] the specific stabilizing characteristics of SDS resistant proteins are the presence in the structure of disulfide bonds, oligomeric interfaces and bound metals. These features are also present in CSTB polymers that seem to bind cupper as well [Rossella Di Giaimo, Elena Cipollini, Marialuisa Melli, unpublished]. The resistance of the polymers to 8 M urea confirms their exceptional stability. This recalls the resistance to SDS and 8M urea of oligomers from amyloid plaques of Alzheimer disease patients, described by Walsh et al. [219].

In order to find out whether the polymerization of CSTB is artifactual, due to the presence of the highly charged SDS molecule, we have analysed the MW of the native protein by SDS-free size fractionation on column chromatography [220-221]. In a native extract, the fractionation of a protein that interacts with partners of different MW may not reflect precisely the size of the protein itself. The low MW components may fractionate in the high MW region of the column. In fact, the already mentioned predominance of monomers in the linear part of the column and the presence of polymers of variable size in the high MW fractions,

can be explained by the interaction of monomeric and polymeric CSTB with other proteins. The bias toward monomers, in the light region of the column, could also be due to higher sensitivity to boiling in 1% SDS of the intermediate MW, as compared to the larger components. Alternatively, some of the monomers/dimers are complexed with proteins that increase the size of CSTB. However, the result of this experiment shows clearly that polymeric CSTB from a native protein extract of 293T cells fractionates in the high MW region of the column, and is separate from monomers and dimers. This result confirms the existence in 293T cells of CSTB monomers and polymers as real components, which are independent of the method of cell lysis. The mass spectrometry analysis confirms the homopolymeric nature of the high MW species as well as the absence of gross modifications in the molecule.

pH has been used by several authors to alter the conformation of SDS and urea resistant prion and amyloid proteins [222-223]. Accordingly, CSTB polymers are unfolded either by increasing the pH or by increasing the concentration of GSH, a reducing agent that acts like DTT or β-METOH. Consistent with this result, oxidation by addition of increasing concentration of H_2O_2 triggers the polymerization of CSTB. During this reaction the trimer seems to become particularly stable and, at the concentration of 1M H_2O_2, polymers and trimers are quite resistant to the reducing activity of β-METOH. We can conclude that the CSTB polymers are physiological and show features similar to those of β-amyloid structures. These characteristics are typical of proteins regulated by the redox microenvironment [200].

3. CYSTATIN B MUTANTS ARE POLYMERIC

Since polymeric CSTB may be related to its cytoskeletal function and the truncation mutant associated with EPM1 alters the multiprotein complex, we

have decided to analyse a number of natural and laboratory mutants of CSTB in relation to their polymerization properties. Our results show that none of the mutants, that we have constructed, inhibits the capacity of CSTB to generate polymers. However, this does not exclude the existence of differences between the structure and stability of the wt and mutant polymers. A different organization of the polymers is shown by the cysteine minus mutants. The presence of at least one cysteine is sufficient to generate the wt polymeric pattern and this is in agreement with the presence of only one cysteine at position 3 in the great majority of the species, including man. The strong decrease of the oligomers, observed in the absence of cysteines, is interesting and in agreement with our results on the effect of redox on CSTB structure. Clearly the cysteine is not required to obtain dimers and high MW polymers but is crucial to stabilize and perhaps regulate the intermediate MW species.

Several authors have shown that amyloid fibers *in vitro* are generated by an initial event of domain swapping [123-224]. Staniforth et al. [2] have demonstrated that, in cystatins, this event occurs by a rearrangement of loop 1 and that amyloid fibers grow by dimeric addition. This is not true for cellular CSTB, where polymers grow by monomer addition, and are insensitive to amminoacid substitutions in loop 1. We can conclude that in the two cases polymerization occurs differently. The presence, *in vivo,* of chaperon-like and/or redox response proteins may be very important to this process [200,204].

4. MOLECULAR MECHANISM OF CYSTATIN B POLYMERIZATION

Under physiological conditions native CSTB monomer does not self assemble and the denatured monomer shows a modest polymerization, in agreement with the denaturing conditions and prolonged times required for *in vitro* fibrillation of

CSTB [107]. However, the monomer oligomerizes within minutes when incubated with a cell protein extract (eukaryotic or prokaryotic) or a cellular fraction containing proteins of about 50-70 kDa (and ionic strength corresponding to 150-550 mM NaCl). Furthermore, eukaryotes and prokaryotes generate undistinguishable CSTB polymers both *in vivo* and in the polymerization assay. Altogether these data point to the existence of a polymerizing factor(s), highly conserved in evolution, that can olygomerize CSTB when it contains a cysteine, but that is not sufficient to generate molecular species larger than 100 kDa. It is possible that these species require the presence of other factor(s) or an energy source that are lost during the lysis of the cells. It is interesting to notice that CSTB interacts with the heat shock proteins 70, 73, 86, 90, and ERP99 [Rossella Di Giaimo and Marialuisa Melli, unpublished], which could play a role in its polymerization. Chaperone activities, in fact, are conserved in evolution, may function alone or with other chaperones and usually require ATP or GTP [225]. The lack of oligomerization *in vivo* and *in vitro* of the cysteine minus mutants, suggests that a cysteine is necessary for the recognition of CSTB by the oligomerizing factor. A single cysteine can function as a sensor being the target of various modifications i.e. nitrosilation, sulfonation, sulfenilation, glutathionylation, cysteinyl−glycylation and homocysteinylation. These modifications can generate binding surfaces that allow structural changes [200]. Structural changes certainly occur during the transition from monomer to oligomers. This is shown by the migration properties of the oligomers in the 2D gel of figure 20. The gradual change of the isoelectric point could be consistent with a different modification of the SH residue of cysteine, resulting in structural change. The instability of the oligomers contrasts with the high stability of the largest polymers, characterized by a slightly acidic pI and acidic pH favours polymerization. The instability of

the oligomers correlates with the widely accepted notion that they are responsible for amyloid fiber formation.

5. EXPRESSION OF CYSTATIN B AND ITS MUTANTS IN SKNBE CELLS

Amyloid-like proteins in yeast are described as physiological proteins through which individuals can be preadapted to selective niches . In mammals they are usually associated with pathologies. Amyloid formation involves the generation of soluble oligomers as a result of relatively non specific interactions and/or specific structural transitions such as domain swapping. These precursors acquire a distinct morphology and become protofibrils that later assemble into mature fibrils. It is generally accepted that amyloid formation is triggered by a nucleation event that occurs stochastically and may occur more frequently at high concentration of the protein [226-229]. Given the characteristics of polymeric CSTB, we have analysed the effect of its over-expression in neuroblastoma cells. The appearance of cellular aggregates is almost immediate in cells transfected with the deletion mutants, and takes longer time with the wt and the G4R substitution mutant. All mutants tested generate aggregates except the cysteine minus constructs. In the latter case, it is not clear whether aggregate formation is slowed down or actually not present. Only a small proportion of cells are affected after 7 days of transfection, when the cells are over-confluent and start to die. Interestingly, the ΔCys mutant does not show a detectable amount of intermediate MW oligomers and a growing body of evidence suggests that oligomers are the toxic species that give rise to amyloid diseases [219,229-230].

6. CONCLUSIONS

This work makes the following points.

1. The nature of the possible partners of CSTB suggests a cytoskeletal function involved in neural transmission.
2. The existence of a physiological polymeric protein with amyloid-like properties in mammalian cells. Berson et al. [231] have shown that the Pmel 17 melanocyte protein polymerizes into amyloid-like fibrils during the process of melanosome biogenesis. Prions with positive functions for the cell have been widely studied in yeast. E. coli and Salmonella form amyloid-like extracellular fibrils orchestrated by two different operons [232]. In synthesis we may say that fibril formation is an evolutionary conserved mechanism for creating biologically active quaternary structures. The unique properties of amyloid structures have been exploited by several species for specific purposes [233]. We think that also polymeric CSTB belongs to this category of proteins, being functional because of its amyloid-like properties.
3. The results envisage a molecular mechanism that could explain neural degeneration at least in the EPM1 patients heterozygous for both promoter and point mutations. In fact we find that the natural mutants are stable proteins that within 24 Hr already generate amyloid aggregates in neuroblastoma cells. This strongly suggests that, when these alleles are present, the same happens in the CNS of patients. A similar suggestion as been made by Ceru et al. [234] on the basis of the aggregation propensity of the G4R EPM1 mutant. In this context, it is interesting to notice that many prion diseases lack cerebral plaques that stain with amyloid specific dyes [229]. This could be also true for EPM1, where cerebral aggregates were not described.

MATERIALS AND METHODS

1. PLASMIDS

1.1. EUKARYOTIC EXPRESSION VECTORS

1.1.1.pRK7-HA

Wt and mutant CSTB sequences were inserted in the pRK7 vector containing one copy of the HA tag sequence (pRK7-HA) upstream from the Bam HI site (nt 921-959). The fusion protein expression is under the control of the CMV promoter (nt 60-598). SV40 polyadenylation signal (nt 1028-1158) downstream of the multiple cloning site (MCS) directs proper processing of the 3' end of the fusion protein mRNA. The ampicillin resistance gene (nt 2733-3593) allows propagation and selection in E. coli. The plasmid backbone also provides a pUC origin of replication (nt 3738- 4411) for propagation in E. coli and a f1 origin (nt 1941- 2269) for single stranded DNA production.

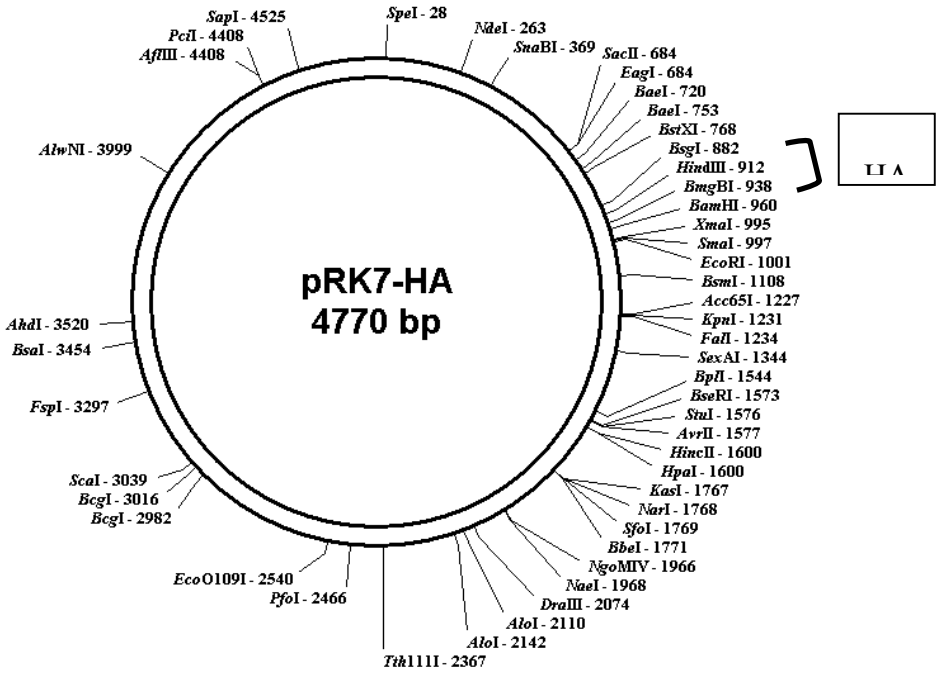

Poly-linker sequence of pRK7-HA vector:

```
                HindIII                       BmgBI
 901 ACCTCGGTTC TAAGCTTACC ATGGCCTACC CCTACGACGT GCCCGACTAC

                                                 XmaI
                                                 SmaI
             BamHI                               AvaI
 951 GCCTCCCTCG GATCCGCTCT TTATCTTCTT CTGTGGGGGC GATCCCCGGG

     EcoRI  ClaI   SfiI                           PsiI
1001 GAATTCAATC GATGGCCGCC ATGGCCCAAC TTGTTTATTG CAGCTTATAA

1051 TGGTTACAAA TAAAGCAATA GCATCACAAA TTTCACAAAT AAAGCATTTT

           BsmI
1101 TTTCACTGCA TTCTAGTTGT GGTTTGTCCA AACTCATCAA TGTATCTTAT

              ClaI
1151 CATGTCTGGA TCGATCGGGA ATTAATTCGG CGCAGCACCA TGGCCTGAAA
```

aaa HA tag sequence

1.1.2. pEGFP-C1

For the cell count experiments, wt and mutant CSTB sequences were inserted in the pEGFP-C1 vector (BD Biosciences Clontech).

The MCS in pEGFPC1 is between the EGFP coding sequences and the SV40 poly A. Genes cloned into the MCS are expressed as fusions to the C-terminus of EGFP. SV40 polyadenylation signals downstream of the EGFP gene direct proper processing of the 3' end of the EGFP mRNA. The vector backbone also contains a SV40 origin for replication in mammalian cells expressing the SV40 T-antigen. A neomycin resistance cassette (Neor), consisting of the SV40 early promoter, the neomycin/kanamycin resistance gene of Tn5, and polyadenylation signals from the Herpes simplex virus thymidine kinase (HSV TK) gene, allows stably transfected eukaryotic cells to be selected using G418. A bacterial promoter upstream of this cassette expresses kanamycin resistance in E. coli. The pEGFP-C1 backbone also provides a pUC origin of replication for propagation in E. coli and a f1 origin for single stranded DNA production.

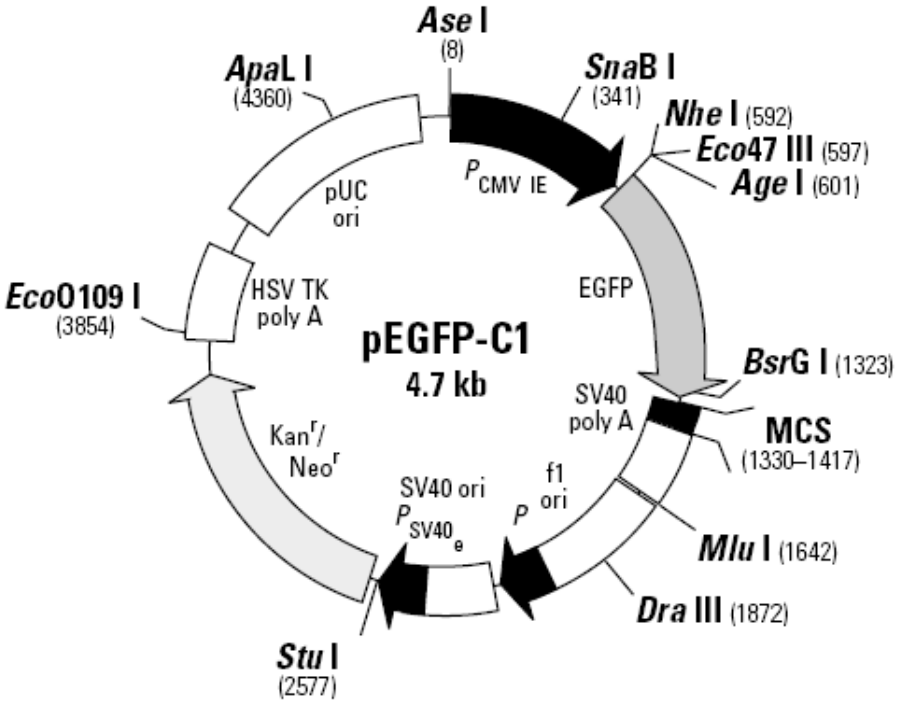

Poly-linker sequence of pEGFP-C1 vector:

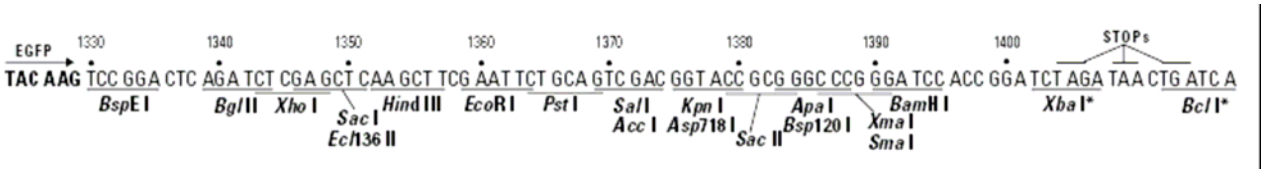

(*) The Xba I and Bcl I sites are methylated.

1.2. PROKARYOTIC EXPRESSION VECTOR

1.2.1. pET16b

Wt and mutant CSTB sequences were inserted in the pET16b-HA vector, generated from the pET16b vector (Novagen) as described in paragraph 2.4.

The pET-16b vector (Cat. No. 69662-3) carries an N-terminal His•Tag® sequence followed by a Factor Xa site upstream of three cloning sites. The target gene is cloned under the control of the T7*lac* promoter, which allows to induce

the expression of the target gene by addition of IPTG to the bacterial culture. The vector codes for the selective marker for ampicillin resistance.

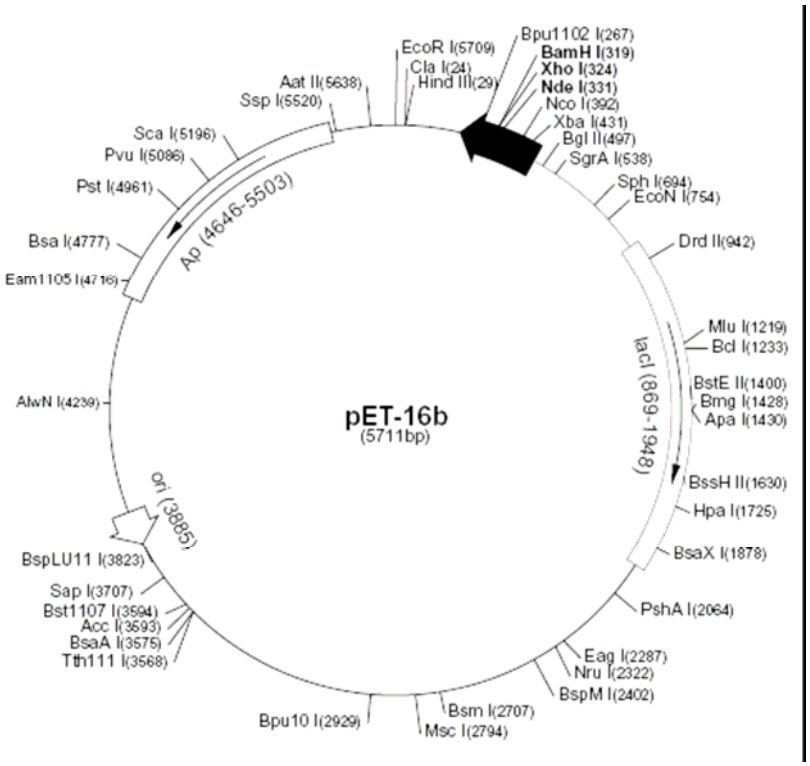

pET-16b cloning/expression region:

1.2.2. pET11a-HUMAN C3S CSTB

pET11a-human C3S CSTB vector was a kind present from Eva Zerovnik.

2. PREPARATION OF PLASMIDIC CONSTRUCTS

2.1. pRK7-HA-CSTB WT

PCR AMPLIFICATION

Wt rat CSTB sequence was cloned in the pRK7-HA between the Bam HI and Eco RI sites.

The restriction sites Bam HI and Eco RI were inserted at the 5' and 3'-terminus of CSTB cDNA, respectively, by PCR amplification using the 5'BamH1 cstb terminal primer and the 3' EcoRI cstb terminal primer (see Table 2).

The PCR reaction was:

50 ng template DNA
1X DNAZyme buffer with 1.5 mM Mg2+ (Finzyme)
0.2 mM dNTPs
0.2 μM 5'primer
0,2 μM 3'primer
3 U DNAZyme Taq (Finzyme)
H_2O to a final volume of 200 μl

The thermal cycler was programmed as follows:

1 time: 95°C for 5 min
30 times: 95°C for 5 min
65°C for 40 sec
72°C for 1 min
1 time: 72°C for 10 min

DNA AGAROSE GEL

At the end of the reaction, the PCR product was checked on a DNA 2% agarose gel.

The gel was run in TAE 1X buffer supplemented with 5 μg/ml Etidium bromide.

- for 2% agarose gel, add 2g agarose powder to 100 ml TAE 1X + 5 μg/ml EtBr buffer,
- heat the mixture up to boiling
- pour the mixture on the apposite horizontal plate (BioRAD 6,5x10 cm) and let it cool for at least 30 min
- transfer the gel in the horizontal electrophoresis cell containing the TAE 1X + 5 μg/ml EtBr buffer
- add the DNA loading buffer (1x final concentration) to the samples and load on the gel
- run the gel at 70/80 V for at least 1 h.

ORGANIC SOLVENT EXTRACTION AND ETHANOL PRECIPITATION OF DNA

The PCR product was purified by organic solvent extraction, adding 1 volume of phenol saturated with Tris pH 8-chloroform 50:50. Residual phenol was removed by two extractions with equal volumes of chloroform. The water phase was recovered and precipitated in 0.3 M NH4-acetate pH 5,3 and 3 volumes of 100% ethanol, incubated at least 45 min at –20°C and centrifuged 20 min at 17000 g. The pellet was washed in 70% ethanol and dried in a vacuum fuge. A small aliquot of water phase was used for the quantification of DNA on an agarose gel.

RESTRICTION DIGESTION

The amplified cDNA and the pRK7-HA vector were digested with the Bam HI and Eco RI enzymes as follows:

2 μg DNA
1X Multicore buffer (Promega)
0.1 μg/μl BSA
10 U BamHI (Promega)

10 U EcoRI (Promega)

Incubation at 37°C for 4 hr.

The digested vector and the cDNA were purified by gel filtration using a *Chromaspin 1000* and a *Chromaspin 100* (Clontech), respectively.

LIGATION

The plasmid and the insert were ligated in a 1:3 ratio according to the following protocol:

pRK7-HA-CSTB cDNA
1X T4 ligase buffer with 1mM ATP (New England Biolabs)
400 U T4 ligase (New England Biolabs)
in a final volume of 10 μl

Incubation at room temperature (RT) for 4 hr.

The ligation product (pRK7-HA-CSTB) was precipitated in 0.3 M NH4-acetate pH 5,3 and 3 volumes of 100% ethanol as described above.

E.COLI ELECTROPORATION

pRK7-HA-CSTB was used to transform E. coli electrocompetent cells by electroporationwith the . E. coli cells used had a transformation efficiency of 10^8-10^{10} transformants/DNA μg. The electroporation was performed with the Gene-Pulser (Bio-RAD) electroporator and 0,2 cm cuvettes (Bio-RAD), pre-cooled at –20°C. Electric pulse was –2.5 KV.

- unfrost, on ice, the electrocompetent cells
- mix a 30 μl aliquot of cells with 100 ng ligation product pellet
- transfer the mixture in a cuvette

- immediately after transformation, transfer cells in 960 µl of SOC medium in a 15 ml polyropilene tube and incubate 1 hr at 37°C, 250 rpm
- plate aliquots of cells (10, 50, 100, 200 and 600 µl) on selective medium (LB + 0.02 g/ml Agar + 100µg/ml Ampicillin)
- incubate overnight (ON) at 37°C.

PCR-COLONY SCREENING

The recombinants were analysed by PCR-colony screening, according to the following protocol:

Each E. coli colony was diluted in 30 µl H2O and lysed by boiling at 100°C, 10 min. A few cells from each colony were plated on selective medium (LB + 0.02 g/ml Agar + 100µg/ml Ampicillin).

2 µl colony dilution
1X DNAZyme buffer with 1.5 mM Mg2+ (Finzyme)
0.2 mM dNTPs
0.5 µM 5'BamH1 cstb terminal primer
0.5 µM 3'EcoRI cstb terminal primer
0.2U Taq DNAZyme (Finzyme)
H_2O to a final volume of 20 µl

The termocycler was programmed as described above.

The recombinant frequency was checked on a DNA 2% agarose gel.

The construct was checked by sequencing with the Big Dye®Terminator v1.1 Cycle Sequencing kit (Applied Biosystem), according to manufacturer's instructions.

The positive recombinants were grown in 1 ml of LB+100µg/ml Ampicillin, ON at 37°C, 250 rpm. Cells were pelletted at 4000 rpm 10 min, suspended in LB+15% Glycerol medium and stored at –80°C.

2.2. pRK7-HA-MUTANT CSTB: SITE DIRECTED MUTAGENESIS

CSTB mutants were inserted in pRK7-HA between the Bam HI and Eco RI sites. All constructs were checked by sequencing.

2.2.1. 5' AND 3' TERMINAL MUTANTS

For the C3S and ΔE1mutants, the restriction site Bam HI and the 5' terminal mutations were inserted by PCR amplification using specific 5'primers and the Eco RI site using the 3'EcoRI cstb terminal primer (see Table 2).
For the Δ64, Δ68, Δtc and T87K mutants, the restriction site Eco RI and the 3' terminal mutations were inserted by PCR amplification using specific 3'primers and the Bam HI site using the 5'BamH1 cstb terminal primer (see Table 2).

The PCR reaction was as described in section 2.1 and PCR cycles were:

1 time: 95°C for 5 min
10 times: 95°C for 5 min
72°C for 1 min 40 sec
20 times: 95°C for 5 min
69°C for 40 sec
72°C for 1 min

1 time: 72°C for 10 min

The cloning of CSTB mutants in pRK7-HA was as described for the cloning of the wt protein in the same vector.

2.2.2. pRK7-HA-CSTB G4R

pRK7-HA-CSTB vector was digested with Bss HII restriction enzyme as follows:

8 μg pRK7-HA-CSTB wt
1X H buffer (Promega)
0.1 μg/μl BSA
50 U BssHII (Promega)

Incubation at 37°C for 4 hr.

The digested vector was precipitated in 0.3 M NH4-acetate pH 5,3 and 3 volumes of 100% ethanol, as described above and digested with BamH1 restriction enzyme as follows:

8 μg pRK7-HA-CSTB wt
1X buffer E (Promega)
0.1 μg/μl BSA
50 U BamHI (Promega)

Incubation at 37°C for 4 hr.

The digested vector was purified by gel filtration using a *Chromaspin 1000* (Clontech).

The two complementary sequences 5'BamH1 cstb G4R BssHII and 3'BamH1 cstb G4R BssHII were annealed in 0.2 M Na-acetate by denaturation at 70-100°C for 3 min and renaturation by slow cooling. The double strand oligo was then inserted directly into the BamHI-BssHII sites of the pRK7-HA-CSTB vector. The vector: insert ratio in the ligation reaction was 1:400.

2.2.3. INTERNAL SINGLE SUBSTITUTION MUTANTS

The Q71P, V59Q, C64S, V48D, V48A and G50A mutations were inserted by three PCR amplifications:

PCR1: amplification to insert the Bam HI site and the internal mutation using the 5' BamH1 cstb terminal primer and the 3' primer with the specific mutation;
PCR2: amplification to insert the internal mutation and the Eco RI site using the 5' primer with the specific mutation and the 3'EcoRI cstb terminal primer;
PCR3: amplification to generate the whole cstb mutant sequence using the 5' BamH1 cstb terminal primer and the 3'EcoRI cstb terminal primer to amplify a mix of the products of PCR1 and 2 which is used as template cDNA.
The PCR cycles were as described in section 2.2.1.
The cloning was according to the protocol described for the cloning of the wt protein in the same vector.

2.2.4. DOUBLE SUBSTITUTION MUTANTS

CSTB C3/64S double substitution mutant was generated by PCR amplification of the single mutant C64S with the 5' BamH1 cstb C3S and 3'EcoRI cstb terminal primers as described in section 2.2.1.
CSTB VG48/50A double substitution mutant was generated by PCR amplification from the single mutant V48A according to the protocol described in section 2.2.3.

2.3. pEGFP-C1-CSTB CONSTRUCTS

Wt and mutant sequences were inserted between the Xho I and Eco RI sites of the pEGFP-C1 vector (BD Biosciences Clontech).
Xho I and Eco RI sites were inserted by PCR amplification using pRK7-HA CSTB wt or mutated as DNA template and specific terminal primers (in bold letters in Table 1). PCR reaction and cloning protocols were as described in section 2.2.1.

2.4. pET16b-HA

The pET16b-HA vector was generated from the pET16b vector (Novagen).

pET16b vector was separately digested with NcoI (Promega) and Bam HI restriction enzymes, as described in section 2.2.2. The His tag, Factor Xa and polylinker sequences were removed running the digested plasmid on a DNA 1% agarose gel, excising the vector fragment from the gel and recovering it using the QIAquick®Gel Extraction Kit (Qiagen).

The two complementary sequences 5'Nco1-HA-polylinker and 3' Nco1-HA-polylinker were annealed in 0.2 M Na-acetate by denaturation at 70-100°C for 3 min and renaturation by slow cooling. The double strand oligo was then inserted directly into the NcoI-BamHI sites of the pET16b vector. The vector: insert ratio in the ligation reaction was 1:400.

The pET16b-HA vector obtained contains the HA tag sequence between NcoI and Bam HI sites and a new MCS. The frame between the HA tag and Bam HI site sequences is the same as in pRK7-HA, allowing the use of the same 5' BamH1 cstb(wt or mutated) terminal primers (see table 1).

```
          Nco1          HA tag                          BamH1 KpnI  SmaI  XhoI
5'   TACCATGGCCTACCCCTACGACGTGCCCGACTACGCCTCCCTCGGATCCGGTACCCGGGCTCGAGCC   3'
```

2.5. pET16b-HA-CSTB CONSTRUCTS

Wt and mutant sequences were inserted between the Bam HI and Xho I sites of the pET16b-HA vector.

Xho I and Bam HI sites were inserted by PCR amplification using pRK7-HA CSTB wt or mutated as DNA template and specific terminal primers (in italic

letters in Table 2). PCR reaction and cloning protocols were as described in section 2.2.1.

The C3A mutant was generated and cloned as described in section 2.2.1., the C64A as described in section 2.2.3.and the C3/64A double substitution mutant as described in section 2.2.3.

Table 2.

primers	sequence
5’ BamH1 cstb terminal primer	TATGGATCCATGATGTGTGGCGCGC
3’ EcoRI cstb terminal primer	CCGGAATTCTCAGAAGTAGGTTAGCTC
5’ cstbQ71P	GGGTGTTTCCACCCCTCCCTC
3’ cstbQ71P	GAGGGAGGGGTGGAAACACCC
3’ EcoRI cstb Δ68	ATAGAATTCTCACAAGTGCACACATTTTTC
3’ EcoRI cstb Δtc	TAGGAATTCTCATGAGGGAGGTTCAAACA
3’ EcoRI cstb Δ64	TCAAGAATTCTCATTTTTCTTCGCCGACATCAAC
5’ BamH1 cstb ΔE1	TATGGATCCTAGTGAAGTCTCAACTTGAAG
5’ cstb V59Q	CCAACTTCTTCATCAAGGTTGATCAGGGCGAAGAAAAATGTGTGC
3’ cstb V59Q	GCACACATTTTTCTTCGCCCTGATCAACCTTGATGAAGAAGTTGGG
3’ EcoRI cstb T87K	CCGGAATTCTCAGAAGTAGGTTAGCTCATCGTGCTTTTCTTTGTCCTTCTGGTAAGAGG
5’ BamH1 cstb C3S	CTATGGATCCATGATGTCTGGCGCGCC
5’ cstb C64S	CGGCGAAGAAAAATCTGTGCACTTGAGGGTGTTTGAACCCC
3’ cstb C64S	GGGGTTCAAACACCCTCAAGTGCACAGATTTTTCTTCGCCG
5’ cstbV48D	CCTTCAGGAGACAGGTAGACGCCGGCACCAACTTCTTCATCAAGG
3’ cstbV48D	CCTTGATGAAGAAGTTCCTGCCGGCGTCTACCTGTCTCCTGAAGG
5’ cstbV48A	CCTTCAGGAGACAGGTAGCGGCCGGCACCAACTTCTTC
3’ cstbV48A	GAAGAAGTTGGTGCCGGCCGCTACCTGTCTCCTGAAGG
5’ cstbG50A	GGAGACAGGTAGTGGCCGCCACCAACTTCTTCATCAAGG
3’ cstbG50A	CCTTGATGAAGAAGTTGGTGGCGGCCACTACCTGTCTCC
5’ BamH1 cstb G4R BssHII	GATCCATGATGTGTCG
3’ BamH1 cstb G4R BssHII	CGCGCGACACATCATG
5’ cstbVG48/50A	GGAGACAGGTAGCGGCCGCCACCAACTTCTTCATCAAGG
3’ cstbVG48/50A	CCTTGATGAAGAAGTTGGTGGCGGCCGCTACCTGTCTCC
5’ XhoI cstb terminal primer	**TATCTCGAGGAATGATGTGTGGCGCGC**
5’ XhoI cstb G4R	**TATCTCGAGGAATGATGTGTCGCGCGCCATCCG**
5’ XhoI cstbC3S	**TATCTCGAGGAATGATGTCTGGCGCGCC**
5’Nco1-HA-polylinker	CATGGCCTACCCCTACGACGTGCCCGACTACGCCTCCCTCGGATCCGGTACCCGGGCTC GAGCC
3’ Nco1-HA-polylinker	GATCGGCTCGAGCCCGGGTACCGGATCCGAGGGAGGCGTAGTCGGGCACGTCGTAGGG GTAGGC
3’XhoI CSTB terminal primer	*CGATTCTCGAGTCAGAAGTAGGTTAGCTCATCG*
5’ BamH1 CSTB C3A	*CTATGGATCCATGATGGCTGGCGCGCC*
5’ BamH1 CSTB G4R	*TATGGATCCATGATGTGTCGCGCGCCATCCG*
5’ CSTB C64A	*CGGCGAAGAAAAAGCTGTGCACTTGAGGGTGTTTGAACCCC*
3’ CSTB C64A	*GGGGTTCAAACACCCTCAAGTGCACAGCTTTTTCTTCGCCG*
3’ XhoI CSTB Δ68	*CGATTCTCGAGTCACAAGTGCACACATTTTTC*
3’ XhoI CSTB ΔTC	*CGATTCTCGAGTCATGAGGGAGGTTCAAACA*
3’ XhoI CSTB Δ64	*CGATTCTCGAGTCATTTTTCTTCGCCGACATCAAC*

2.6. PLASMID DNA PURIFICATION

Plasmid DNA was purified using the QIAGEN Plasmid Maxi Kit and QIAprep Miniprep Kit (Qiagen), according to manifacturer's instructions.

Bacteria cell coltures for maxipreps were in Terrific Broth medium, for minipreps were in LB.

3. EXPRESSION OF CYSTATIN B IN EUKARYOTIC COLTURE CELLS

3.1. CELL COLTURE

Cells were grown in DMEM medium supplemented with 10% Fetal Bovine Serum (FBS), glutamine, penicillin/streptomycin and Na-pyruvate at 37°C in 5% CO_2. Cells were diluted 1:3 every 2 days.

3.2. CELL TRANSFECTION

3.2.1. TRANSFECTION OF SKNBE CELLS USING LIPOFECTAMINE PLUS

SKNBE cells were transfected with Lipofectamine Plus (GIBCO), according to manufacturer's instructions.

3.2.2. TRANSFECTION OF 293T CELLS USING PEI

31000 293T cells/cm^2were plated 16 hours before transfection. Cells were transfected with 5 μg/ml plasmid (pDNA) and 165 μM PolyEthylenImine (PEI) (Sigma-Aldrich) as follows.

Transfection Solution Volumes (TS vol) were 4 ml for 10 cm petri dishes and 11 ml for 175 cm2 flasks.

- Add 150 mM NaCl (sterile) to pDNA to a final volume of 1/20 TS vol, vortex 1 min and let the mixture to equilibrate at RT for 15 min
- Add 150 mM NaCl (sterile) to PEI to a final volume of 1/20 TS vol, vortex 1 min and let the mixture to equilibrate at RT for 15 min. Use 0.33 µl 100 mM PEI/µg pDNA)
- Remove colture medium from the cells and add DMEM, incubate at 37°C in 5% CO_2 until transfection
- Add equilibrated PEI to equilibrated pDNA, vortex 1 min and let the mixture to equilibrate at RT for 30-35 min
- Prepare the Transfection solution adding 9/10 TS vol of DMEM to the pDNA + PEI mixture
- Transfect cells removing the DMEM and adding the Transfection solution, incubate at 37°C in 5% CO_2 for 3 hr
- Remove the Transfection solution from the cells and add fresh colture medium. Grow the cells at 37°C in 5% CO_2 for 16 hr before harvesting.

3.3. CELL LYSIS

Cells were harvested by scraping in the colture medium, pelletted centrifuging 5 min at 1000 rpm, RT. The pellet was thoroughly washed in 1X PBS and pelletted as described above. Lysis was carried out under three different conditions.

3.3.1. CELL LYSIS IN BUFFER 1 (NON DENATURING CONDITIONS AND SONICATION)

Cells were lyzed in 1X PBS containing 20% Glycerol, 0.4 mM EDTA, 1 mM DTT, 0.5% NP40, anti-protease and anti-phosphatase cocktail (Sigma).

The samples were sonicated, on ice, 5 times for 5sec at 15% amplitude using the Sonifier®Cell Disruptor (Branson) with a 3mm microtip. The samples were then centrifuged at 13200 rpm, 4°C, and 30 min. The supernatants were collected, aliquoted and stored at –80°C. Protein concentration was determined using the Bio-Rad Protein Assay, according to manufacturer's instructions.

3.3.2. CELL LYSIS IN BUFFER 2 (DENATURING CONDITIONS AND SONICATION)

Cells were lyzed in 1X PBS containing 1% SDS. The samples were boiled 10 min and diluted 10 times in PBS, containing anti-protease and anti-phosphatase cocktail (Sigma), to a final concentration of 0.1% SDS. Diluted samples were sonicated as described in section 3.3.1.

3.3.3. CELL LYSIS IN PROTEIN LOADING BUFFER (DENATURING CONDITIONS)

Cells were lyzed in 1X Protein Sample Buffer and the samples were boiled 10 min.

4. EXPRESSION OF CYSTATIN B IN PROKARYOTIC CELLS

Wt and mutant HA-CSTB was expressed in E.coli BL21 as follows.

- The day before induction, inoculate a single colony of E.coli BL21, transformed with the prokaryotic expression vector of interest, in 20 ml 2XYT medium + 100μg/ml Ampicillin and incubate at 37°C, 240 rpm, ON.

- The following day dilute the bacteria 1:100 in 40 ml 2XYT medium + 100μg/ml Ampicillin, incubate at 37°C, 240 rpm, for about 2 hr
- When the colture's OD_{550} is 0.5, add 0.4 mM IPTG (isopropyl-beta-D-thiogalactopyranoside) and incubate at 37°C, 240 rpm, 3 hr
- Harvest the cells centrifuging at 6000 g, 10 min, remove the colture medium
- Wash the bacteria pellet with 1XPBS and lyze cells with buffer 1 or 2 as described in sections 3.3.1. and 3.3.2.

5. IMMUNOPRECIPITATION (IP) EXPERIMENTS.

5.1. IP OF DENATURED PROTEIN EXTRACTS

5.1.1. IP FOR WESTERN BLOT ANALYSYS

Protein extracts from 293T cells, non transfected or transfected with pRK7-HA-CSTB wt and mutated, lyzed in buffer 2 (see section 3.3.2.) were immunoprecipitated with mouse anti-HA (F-7) abs according to the following protocol.

Preclearing of the protein extract:

~ 800 μg protein extract
20 μl 50% Protein A-Sepharose™CL-48 (Amersham Biosciences) 1XPBS
1X anti-protease cocktail (Sigma),
1X anti-phosphatase cocktail (Sigma)

Gently mix for 3 Hr at 4°C.

Centrifuge at 1000 rpm, 4°C and 5 min.

Immunoprecipitation:

Transfer the supernatant in a clean eppendorf and add 2 μg abs. Gently mix at 4°C, ON.

IP-resin interaction:

Add to the IP mixture 20 µl 50% Protein A-Sepharose^{TM}CL-48 (Amersham Biosciences) 1XPBS.

Gently mix for 2 Hr at 4°C.

Purification of the immunoprecipitated proteins:

Load the IP on a Bio-Spin disposable chromatography column (BioRAD) and thoroughly wash it with cold 1XPBS.

The immunoprecipitates are eluted in 0.1 M glycine. The acidic pH of the glycine is immediately neutralized with 3M TRIS pH 9.

¼ of each IP was loaded on SDS-PAGE and analysed by western blot as described in section 6.

5.1.2. IP FOR MASS SPECTROMETRY ANALYSIS

30 mg protein extract from 293T cells transfected with pRK7-HA-CSTB wt, lyzed in buffer 2 (see section 3.3.2.) was immunoprecipitated with 40 µg mouse anti-HA (F-7) abs and 350 µl 50% Protein A-Sepharose^{TM}CL-48 (Amersham Biosciences) 1XPBS as described in section 5.1.

5.2. IP OF NATIVE PROTEIN EXTRACTS

5.2.1. IP OF 293T CELL PROTEIN EXTRACT FOR SDS-PAGE

1.2 mg protein extracts from 293T cells, non transfected or transfected with pRK7-HA-CSTB wt and mutated, lyzed in buffer 1 (see section 3.3.1.) were immunoprecipitated with 20 µl 50% Protein A-Sepharose^{TM}CL-48 (Amersham Biosciences) 1XPBS and 3.2 µg mouse anti-RACK1 (BD Biosciences), 12 µg

goat anti-NFL (Santa Cruz) and 6 μg goat anti-brain spectrin βI (C-19) (Santa Cruz) plus 6 μg goat anti-brain spectrin βI (N-19) (Santa Cruz) abs as described in section 5.1. For the IP with anti-RACK1 abs, Anti-mouse IgM (μ-chain specific) Agarose (Sigma) was used. Elution was in 30 μl of 2X2D-gel buffer.

5.2.2. IP OF 293T CELL PROTEIN EXTRACT FOR 2D-PAGE

15 mg protein extract from 293T cells transfected with pRK7-HA-CSTB wt, lyzed in buffer 1 (see section 3.3.1.) was immunoprecipitated with 17 μg mouse anti-HA (F-7) abs and 100 μl 50% Protein A-Sepharose^{TM}CL-48 (Amersham Biosciences) 1XPBS as described in section 5.1. Elution was in 100 μl of 2X2D-gel buffer.

5.2.3. IP OF E. COLI PROTEIN EXTRACT FOR 2D-PAGE

1.6 mg protein extract from E. coli transformed with pET16b-HA-CSTB wt, lyzed in buffer 1 (see section 3.3.1.) was immunoprecipitated with 3.2 μg mouse anti-HA (F-7) abs and 24 μl 50% Protein A-Sepharose^{TM}CL-48 (Amersham Biosciences) 1XPBS as described in section 5.1. Elution was in 30 μl of 2X2D-gel buffer.

6. PROTEIN EXTRACT ANALYSIS

6.1. SDS-POLYACRYLAMIDE GEL ELECTROPHORESIS (SDS-PAGE)

Most of the SDS-PAGEs were carried out in 12% polyacrylamide gels. Gels for β-spectrin and NFL were 6% polyacrylamide. All samples were boiled 20 min in Protein Loading Buffer before loading on the gel.

Electrophoresis was carried out in vertical electrophoretic cells *Mini-PROTEAN II* (BioRAD), or *Mini-PROTEAN III* (BioRAD), applying 24 mA/gel.

6.2. 2D-SDS-PAGE

6.2.1. FIRST DIMENSION: ISOELECTRIC FOCUSING (IEF)

IPG STRIP pH 3-10, 7 CM

Sample preparation:

15 µl IP from E. coli protein extract (see section 5.2.3)
4 µl Bromophenol Blue 0.1 %
1.25 µl Ampholine pH 3.5-9.5 (Pharmacia Biotech, n. 80-1127-15)
105 µl IPG Rehydration solution

- Load sample in the strip holder, put the strip (Immobiline DryStrip pH3-10, 7 cm, GE Healtcare Europe) paying attention that gel side is in contact with the sample solution and cover the strip with Dry Strip Cover Fluid (GE Healtcare Europe).
- Put the holder on the IPG Isoelectric Focusing Unit and set the following program:

Rehydration for 10-12 h at 20°C
120 µA/strip at 20°C
S1: 500 V for 1 hr
S2: 1000 V for 1 hr
S3: gradient voltage from 1000 V to 8000 V in 3 hr
S4: 8000 V for 1 h
S5: 50 V until stop

At the end of the IEF experiment the value of Vh was > 8000

IPG STRIP pH 3-10, 13 CM

Sample preparation:

100 µl IP from 293T cell protein extract (see section 5.2.2)

6 µl Bromophenol Blue 0.1 %
1.6 µl Ampholine pH 3.5-9.5 (Pharmacia Biotech, n. 80-1127-15)
143 µl IPG Rehydration solution

- Load sample in the strip holder, put the strip Immobiline DryStrip pH3-10, 13 cm, GE Healtcare Europe) paying attention that gel side is in contact with the sample solution and cover the strip with Dry Strip Cover Fluid (GE Healtcare Europe).
- Put the holder on the IPG Isoelectric Focusing Unit and set the following program:

Rehydration for 10-12 h at 20°C
120 µA/strip at 20°C
S1: 500 V for 2 hr
S2: 1000 V for 2 hr
S3: gradient voltage from 1000 V to 8000 V in 6 hr
S4: 8000 V for 2 h
S5: 50 V until stop

At the end of the IEF experiment the value of Vh was > 16000

6.2.2. SECOND DIMENSION: SDS-PAGE

- Put the strip in the reduction solution for 10 min (agitation).
- Put the strip in the alkylation solution for 10 min (agitation).
- Load the strip on the surface of a SDS-polyacrylamide separating gel and cover the strip with an agarose solution containing Bromophenol Blue.
- Load the protein marker using a sample application piece.

For the 7 cm strips the separating gel was 15% polyacrilamide and the electrophoresis was carried out in vertical electrophoretic cells *Mini-PROTEAN II* (BioRAD), applying 30 mA .

For the 13 cm strips, the separating gel was 12% polyacrylamide and the electrophoresis was carried out in a vertical 18 cm electrophoretic cell, applying 24 mA/gel constant, 180V.

6.3. TRANSFER OF PROTEINS FROM SDS-POLYACRILAMIDE GEL TO NITROCELLULOSE FILTER

Proteins were transferred from polyacrylamide gel to nitrocellulose filter (OSMOMIC) using the *Mini Trans-Blot* (Bio Rad).

Proteins from 6% polyacrylamide gel were transferred using the Transfer buffer with SDS at 30mA constant, 50V, 2W for 14-16 hr.

Proteins from 12% polyacrylamide gel were transferred using the Transfer buffer without SDS at 120V constant, 340mA, 2W for 2 hr.

Proteins from 15% polyacrylamide gel were transferred using the Transfer buffer without SDS at 120V constant, 340mA, 2W for 3 hr.

Transfer was confirmed staining the nitrocellulose filter with Ponceau S as follows.

- Incubate the membrane in Ponceau Red Solution, 5min
- Remove the staining solution and wash the filter with deionized H_2O until protein bands are visible

6.4. IMMUNOLOGICAL DETECTION OF PROTEINS IMMOBILIZED ON NITROCELLULOSE FILTERS (WESTERN BLOT)

After Ponceau S staining the filters were used for immunodetection with specific antibodies as follows.

- Wash the membrane with 1XPBS-0.1%Tween 20 (PBS-T), 5 min
- Block aspecific sites incubating the membrane in 5% fat free dry milk PBS-T, at RT for 1-3 hr
- Incubate the membrane with the primary abs diluted in 5% fat free dry milk PBS-T, 4°C, ON
- Wash the filter with 3 % fat free dry milk PBS-T, 5-10-5 min
- Incubate the membrane with the secondary abs diluted in 5% fat free dry milk PBS-T, RT, 1 hr
- Wash the filter with 3 % fat free dry milk PBS-T, 5-15-5 min
- Wash the filter with PBS, 4 times 5 min
- Detect immunoreactive proteins with ECL plus (GE Healthcare Europe) according to manufacturer's instruction. Filters were exposed to autoradiographic X-OMAT AR Film (Kodak).

For immunodetection with anti-CSTB abs all steps until wash after the secondary abs incubation were in 5% fat free dry milk PBS and Tween 20 was never added.

	PRIMARY ABS		SECONDARY ABS HRP CONJUGATED	
		Dilution		Dilution
CSTB	Rabbit anti-cystatin b (Biogenesis)	1:300	Goat anti-rabbit IgG (Santa Cruz)	ALL 1:2500
RACK1	Mouse anti-RACK1 (BD Biosciences)	1:1500	Goat anti-mouse IgG (Santa Cruz)	
NF-L	Goat anti-NFL (Santa Cruz)	1:300	Donkey anti-goat IgG (Santa Cruz)	
β-spectrin	Goat anti-brain spectrin βI (C-19) (Santa Cruz)	1:300	Donkey anti-goat IgG (Santa Cruz)	
	Goat anti-brain spectrin βI (N-19) (Santa Cruz)	1:300	Donkey anti-goat IgG (Santa Cruz)	
HA	Mouse anti HA (F-7) (Santa Cruz)	1:2000	Goat anti-mouse IgG (Santa Cruz)	
HA	Rabbi anti HA (Y11) (Santa Cruz)	1:600	Goat anti-rabbit IgG (Santa Cruz)	
GAPDH[a]	Mouse anti-GAPDH (MAB374) (Chemicon)	1.1000	Goat anti-mouse IgG (Santa Cruz)	

a. In the second immunoblot

6.5. SILVER STAINING OF POLYACRILAMIDE GEL

- Fix the proteins in the gel with MetOH 50%, Glacial acetic acid 12%RT, ON
- Rinse the gel with EtOH 50%, 3X15 min
- Sensitise the gel with Thiosulfate solution, 60 sec
- Wash the gel with milliQ H2O2, 3X20 sec
- Stain the gel with cold Silver solution, 15 min
- Wash the gel with milliQ H2O2, 2X20 sec
- Develop the staining with Developing solution until the desired intensity is achieved (usually not more than 2-5 min)
- Stop the developing reaction with the stop solution for at least 5 min
- Wash the gel with milliQ H2O2, 4X5 min
- Store the gel at 4°C in milliQ H2O2

6.6. BRILLIANT BLUE G STAINING OF POLYACRILAMIDE GEL

- Fix the proteins in the gel with EtOH 40%, Glacial acetic acid 10%RT, ON
- Wash the gel with milliQ H2O2, 3X15 min

- Incubate the gel with 1X Colloidal brilliant blue G (Sigma), MetOH 34% RT, 3 days
- Wash the gel with milliQ H2O2
- Store the gel at 4°C in milliQ H2O2

7. PROTEIN IDENTIFICATION BY MASS SPECTROMETRY

MS analysis was performed in collaboration with Fabrizio Dal Piaz at Salerno University.

The bands were excised from the polyacrylamide gel, reduced, alkylated using iodoacetamide, and digested by trypsin. The resulting fragments were extracted and analysed by LC/MS on a Q-Tof Premier instrument (Waters, Corporation, Milford, MA-USA) coupled with a Waters 1065 HPLC apparatus (Waters Corporation). Peptides separation was carried out on a Proteus C18 (100x1 mm) column (Phenomenex, Foster City, CA-USA) using a linear gradient from 5% to 60% of 1% Formic Acid, 0.05% TFA in CH_3CN over 50 min (flow 50 µl/min). Mass spectra were acquired over a *m/z* range from 400 to 2000.

The resulting fragments were extracted, purified using C18 ZipTip (Millipore) and measured by MALDI-TOF mass spectrometry on a Biflex instrument (Bruker, Bremen).

8. PRE-ABSORPTION EXPERIMENTS

24 µg/ml Anti-CSTB abs were mixed with 9.5 mg/ml protein extract from BL21 cells expressing or non-expressing human CSTB, lyzed in buffer 1 (see section 3.3.1.).

0.28 μg/ml Anti HA(F-7) abs were mixed with 9.5 mg/ml protein extract from BL21 cells expressing or non-expressing rat HA-CSTB, lyzed in buffer 1 (see section 3.3.1.).

Following 1Hr incubation at RT the abs-protein extract mixtures were centrifuged 10 min at 17000g.

The supernatants were collected and used for immuno-staining of the western blots.

9. REDOX EXPERIMENTS.

60 μg protein extract from 293T cells lyzed in buffer 1 (see section 3.3.1.) were used for each redox experiment. The reactions were stopped by addition of protein loading buffer with or without 50 mM β–METOH, as indicated.

pH CURVE

Protein extract from 293T cells lyzed in was incubated 5 min on ice, in 100 mM Tris HCl or 50mM Na carbonate/bicarbonate buffers at the indicated pH.

GSH CURVE

Protein extract was incubated 10 min at RT, in 100 mM Tris pH 7.5 with GSH at the indicated concentrations.

H_2O_2 CURVE

Protein extract was incubated 10 min at RT, in H_2O_2 at the indicated concentrations.

10. SDS-FREE SIZE EXCLUSION CHROMATOGRAPHY (SEC) OF 293T PROTEIN EXTRACT

Chromatography experiments were carried out in collaboration with Francesca Sparla and Paolo Trost at Bologna University (see also section 13).

Approximately 400 µg protein extract from 293T cells lyzed in buffer 1 (see section 3.3.1.) were loaded on Tricorn Superdex®75 PC 3.2/30 (Amersham) equilibrated with 50 mM Tris pH 7.5 and run at a flow rate of 0.1 ml/min. 50 µl fractions were collected. Calibration curve and graphic of the fraction OD against volume of elution are shown below.

Tricorn Superdex®75 PC 3.2/30 Calibration curve:

	ml	ml	
Bovine serum albumine		1.03	67000
Ovalbumin		1.12	43000
Chimotrypsinogen		1.27	25000
Ribonuclease A		1.43	13700

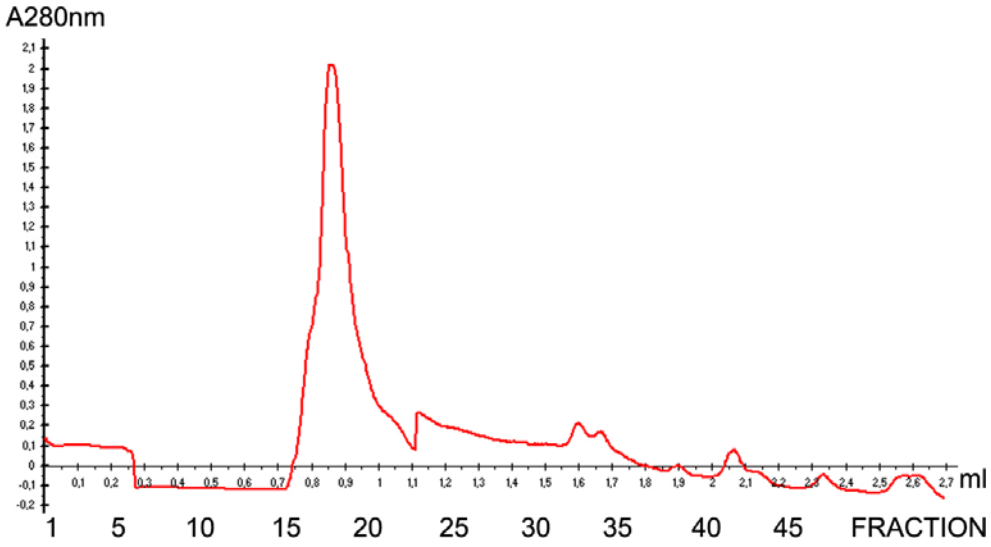

Fractions were analysed by western blot as described in section 6.

11. PURIFICATION OF CYSTATIN B MONOMER

11.1. PREPARATIVE SDS-PAGE

0.3 mg protein extract from E. coli transformed with pET16b-HA-CSTB wt or mutant, lyzed in buffer 1 (see section 3.3.1.) was loaded on preparative 15% SDS gels in the presence of 50 mM DTT. For each monomer 2 preparative gels were prepared.

The gel was stained with Coomassie Blue R250 (Fluka) as follows:

- Fix and stain the proteins in the gel with Coomassie Blue R250 solution, RT, ON
- Destain with Destaining solution until the desired intensity is achieved
- Excise the CSTB monomer band from the gel and store it at –20°C

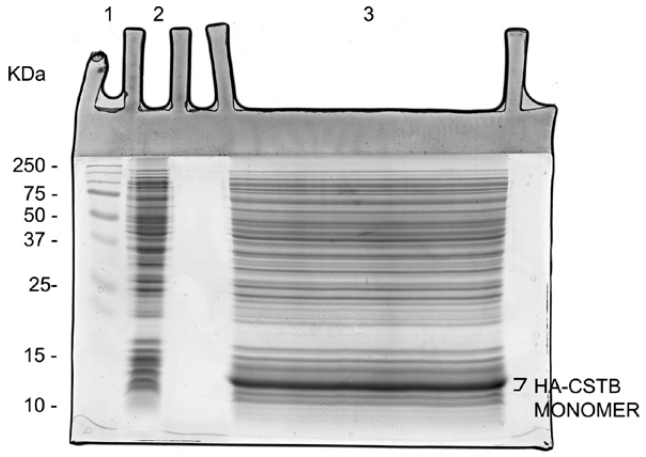

Preparative 15% SDS-PAGE stained with Coomassie Blue R250: 4 µl Protein MW marker (Lane 1), 40µg protein extract from E. coli transformed with pET16b-HA (lane2), 300µg protein extract from E. coli transformed with pET16b-HA-CSTB wt (lane3). The monomer band to be excised is indicated.

11.2. ELECTROELUTION

HA-CSTB monomers were recovered from the polyacrylamide gel using the Model 422 electro-eluter (Bio Rad) and 3.5 kDa cut-off membrane caps (BioRAD). Electroelution was carried out in 1X protein running buffer, applying constant 8 mA for 5hr. Monomer from 0.6 mg protein extract was collected in 500 µl of 1X protein running buffer.

12. POLYMERIZATION ASSAY

0.5 µl of electroeluted HA-CSTB monomer (see sec 11), wt and mutant, was incubated 10 min at RT with the indicated concentration of protein extract from E. coli transformed with pET16b-HA, lyzed in buffer 1 (see section 3.3.1.), and with equivalent concentration of column fractions as indicated. The reactions were stopped by addition of protein loading buffer with or without 50 mM DTT, as indicated.

13. SEPARATION OF E. COLI PROTEINS BY COLUMN FRACTIONATION

13.1. SEC WITH TRICORN SUPERDEX®200 PC 10/300

Approximately 2 mg protein extract from E. coli transformed with pET16b-HA, lyzed in buffer 1 (see section 3.3.1.) were loaded on Tricorn Superdex®200 PC 10/300 (Amersham) equilibrated with 50 mM Tris pH 7.5 and run at a flow rate of 0.5 ml/min. 500 µl fractions were collected. Calibration curve and graphic of the fraction OD against volume of elution are shown below.

Tricorn Superdex®200 PC 10/300 Calibration curve

	ml	ml	
Bovine serum albumine		15.13	67000
Ovalbumin		15.91	43000
Chimotrypsinogen		16.87	25000
Ribonuclease A		17.93	13700

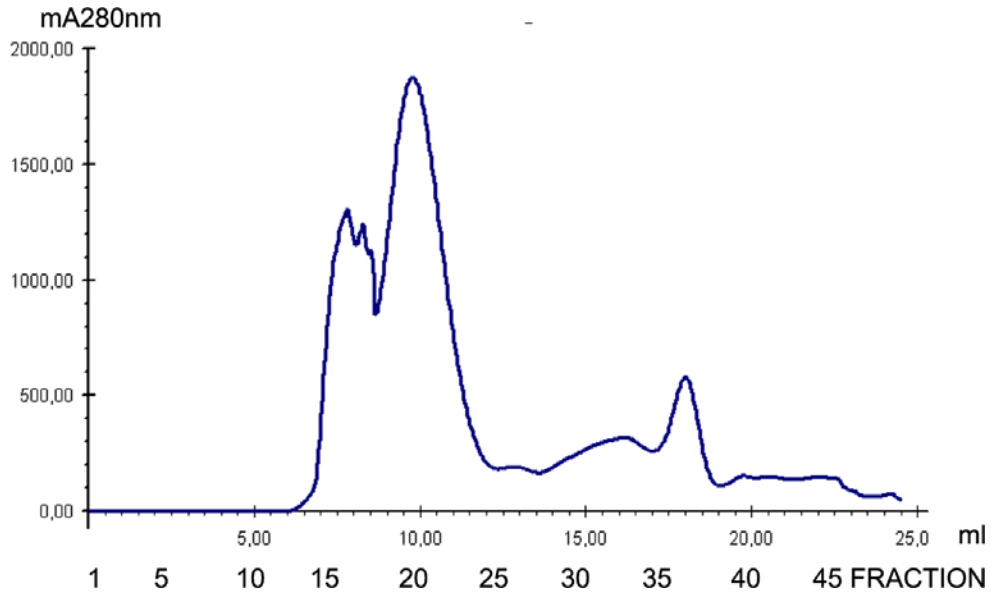

13.2. ION EXCHANGE CHROMATOGRAPHY (IEC) WITH TRICORN MONO Q 5/50 GL

Fractions 24-31 from SEC with Tricorn Superdex®200 PC 10/300 were pooled and loaded on a Tricorn Mono G 5/50 GL anion exchange column (Amersham). The elution was on a 0−1M NaCl in 16-column volumes gradient, in 20mM TRIS pH 7.9. 350 µl fractions were collected. Graphics of the fraction OD against volume of elution and of the elution gradient are shown below.

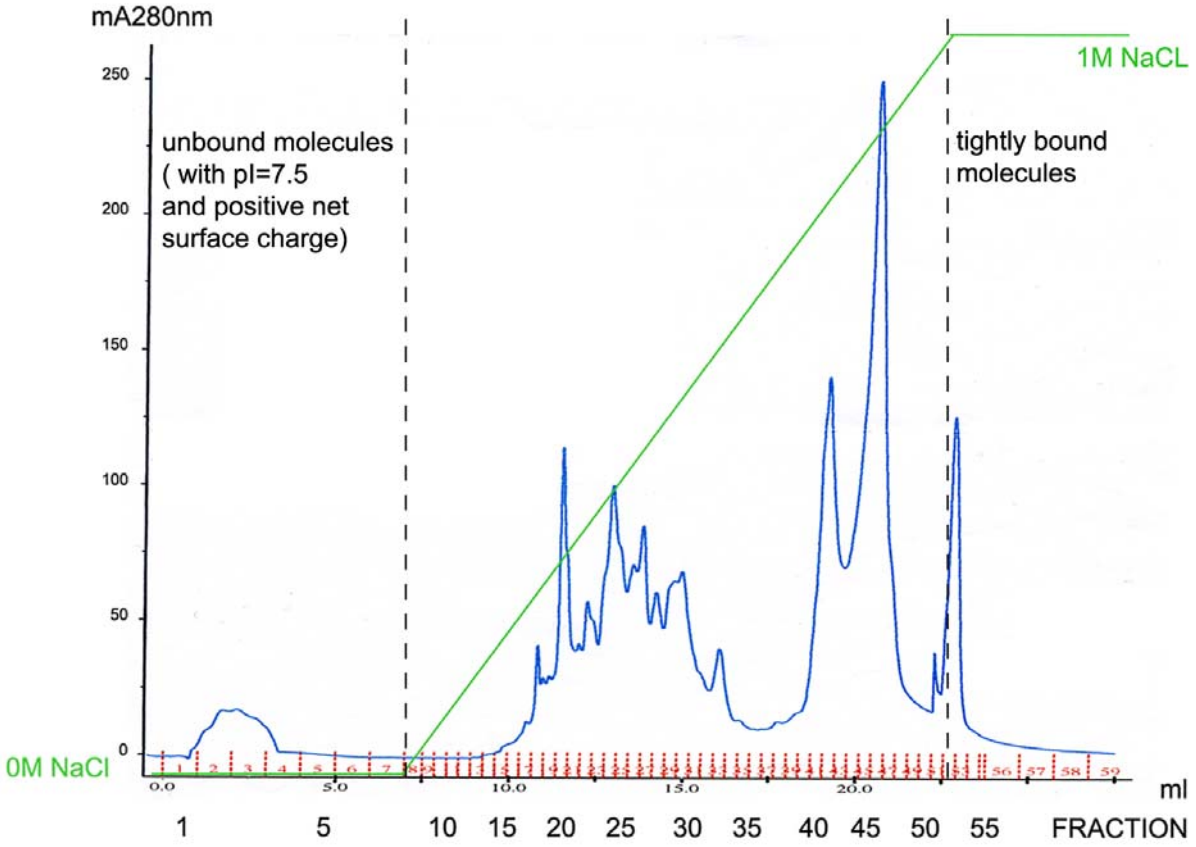

UV absorbance and ionic strength gradient traces of IEC with Tricorn Mono Q 5/50 GL of the pool of fractions 24-31 from SEC with Tricorn Superdex®200 PC 10/300.

13.3. SEC WITH TRICORN SUPERDEX®75 PC 3.2/30

Fractions 24, 26, 27, 28, 29 and 30 from the mono Q column were separately concentrated with 3 kDa cut-off centricon YM-3 (GE Healthcare Europe) and loaded on a Tricorn Superdex®75 PC 3.2/30 (Amersham) equilibrated with 50 mM Tris pH 7.5 and run at a flow rate of 50 µl/min. 100 µl fractions were collected. Calibration curve was as in section 10.1.The graphics of the fraction OD against volume of elution are shown below.

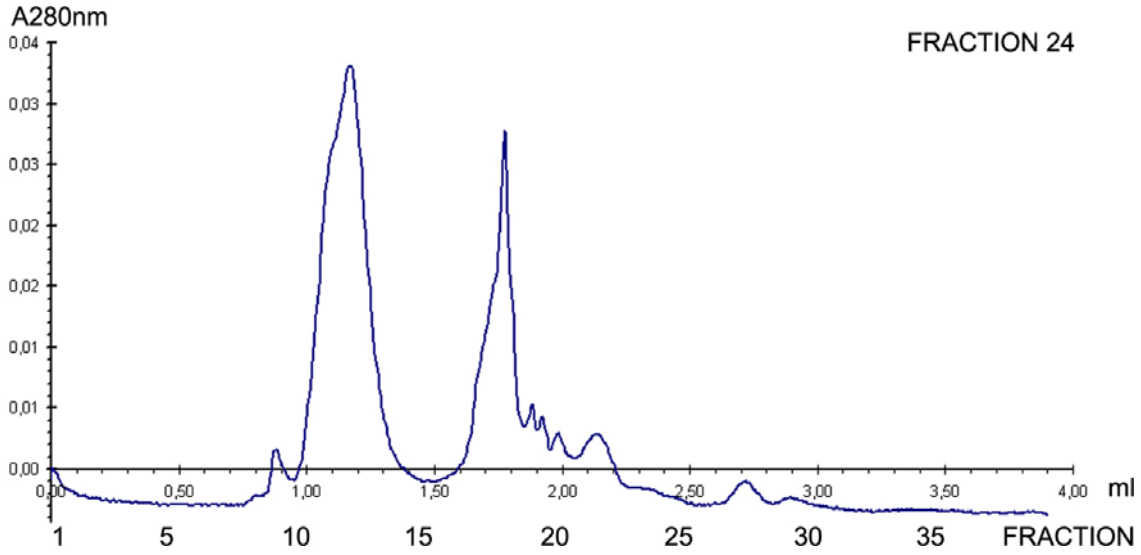
A280nm
FRACTION 24
0,04
0,03
0,03
0,02
0,02
0,01
0,01
0,00
0,00 0,50 1,00 1,50 2,00 2,50 3,00 3,50 4,00 ml
1 5 10 15 20 25 30 35 FRACTION

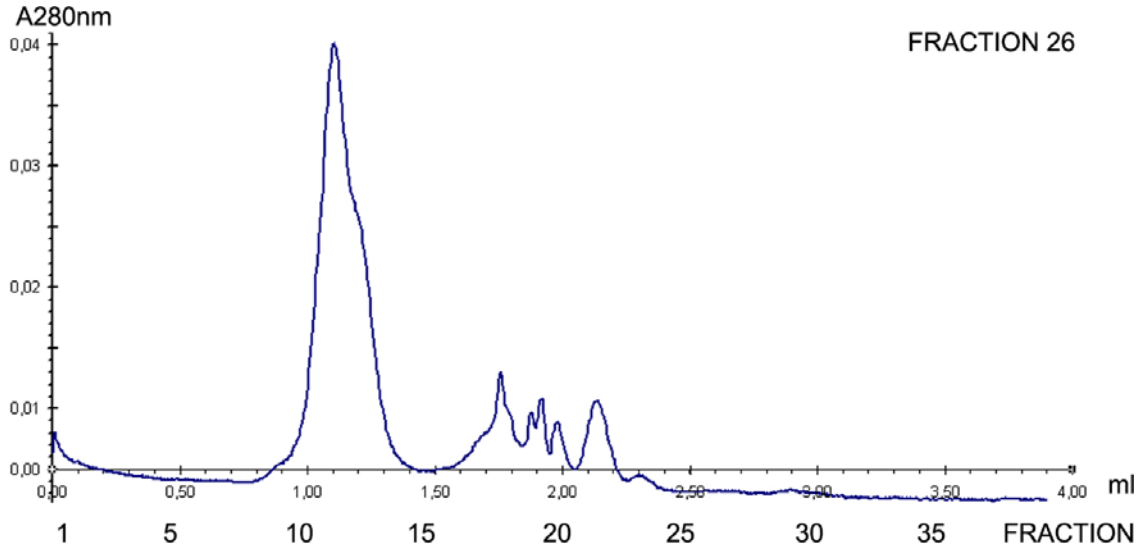
A280nm
FRACTION 26
0,04
0,03
0,02
0,01
0,00
0,00 0,50 1,00 1,50 2,00 2,50 3,00 3,50 4,00 ml
1 5 10 15 20 25 30 35 FRACTION

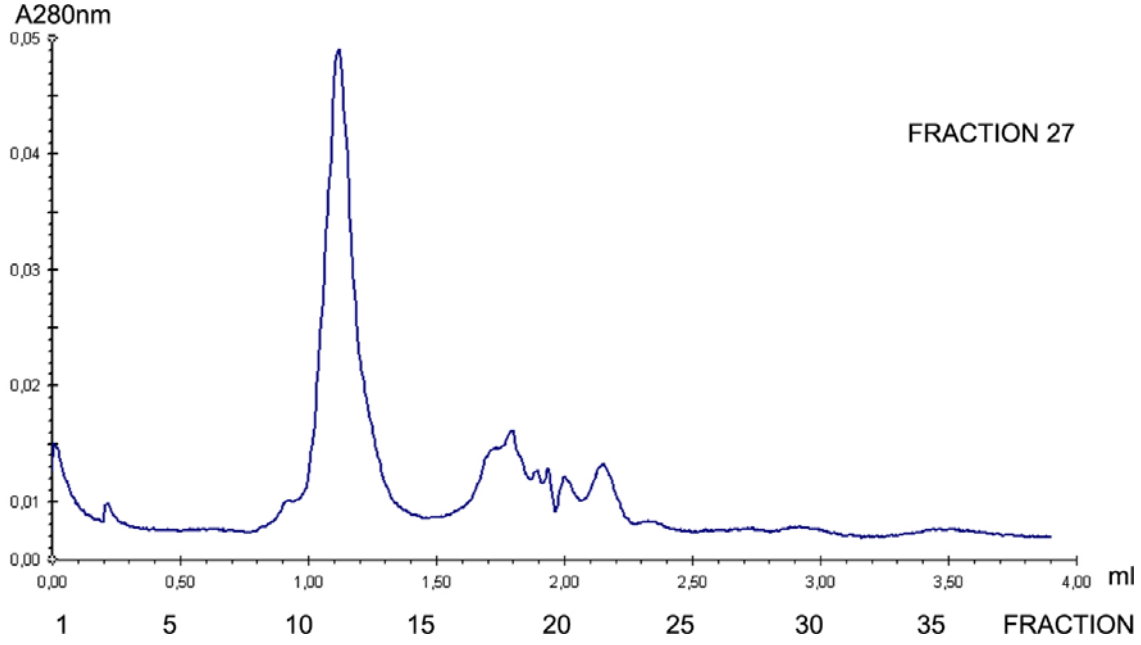
A280nm
FRACTION 27
0,05
0,04
0,03
0,02
0,01
0,00
0,00 0,50 1,00 1,50 2,00 2,50 3,00 3,50 4,00 ml
1 5 10 15 20 25 30 35 FRACTION

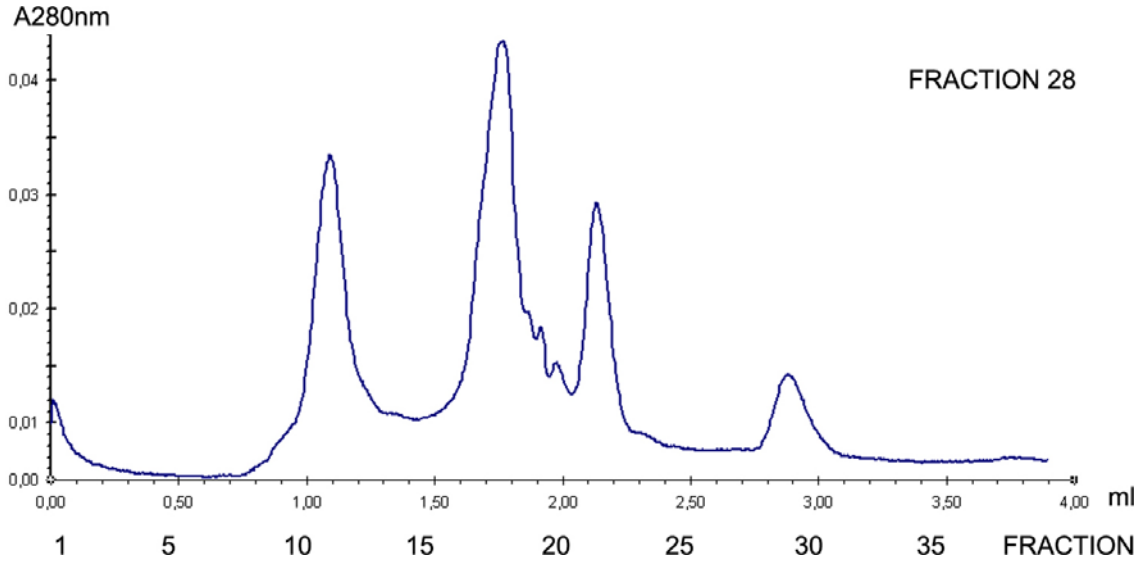
A280nm
FRACTION 28
0,04
0,03
0,02
0,01
0,00
0,00 0,50 1,00 1,50 2,00 2,50 3,00 3,50 4,00 ml
1 5 10 15 20 25 30 35 FRACTION

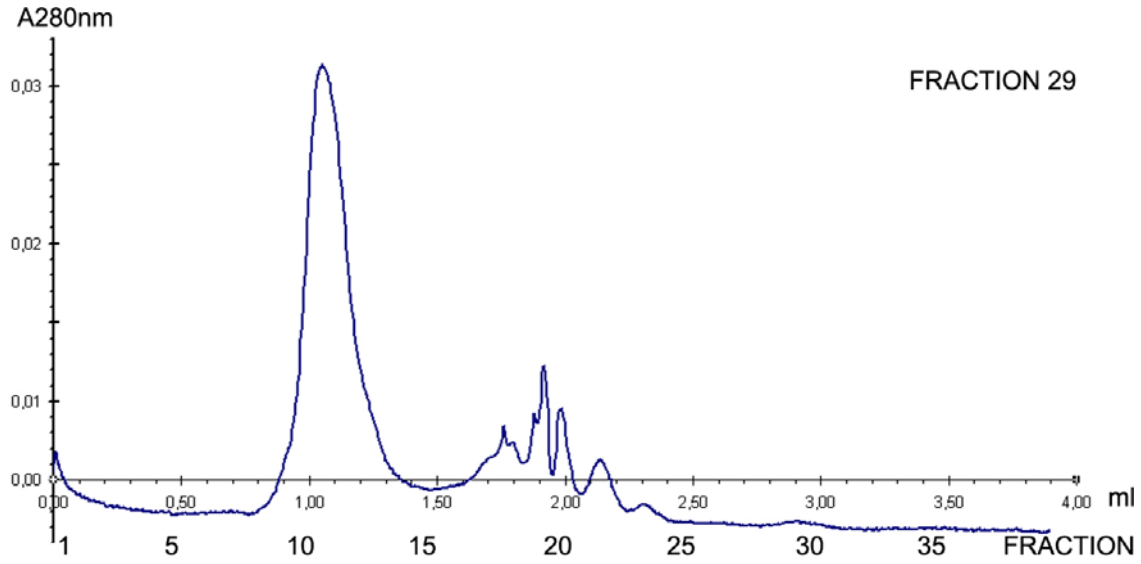
A280nm
FRACTION 29
0,03
0,02
0,01
0,00
0,00 0,50 1,00 1,50 2,00 2,50 3,00 3,50 4,00 ml
1 5 10 15 20 25 30 35 FRACTION

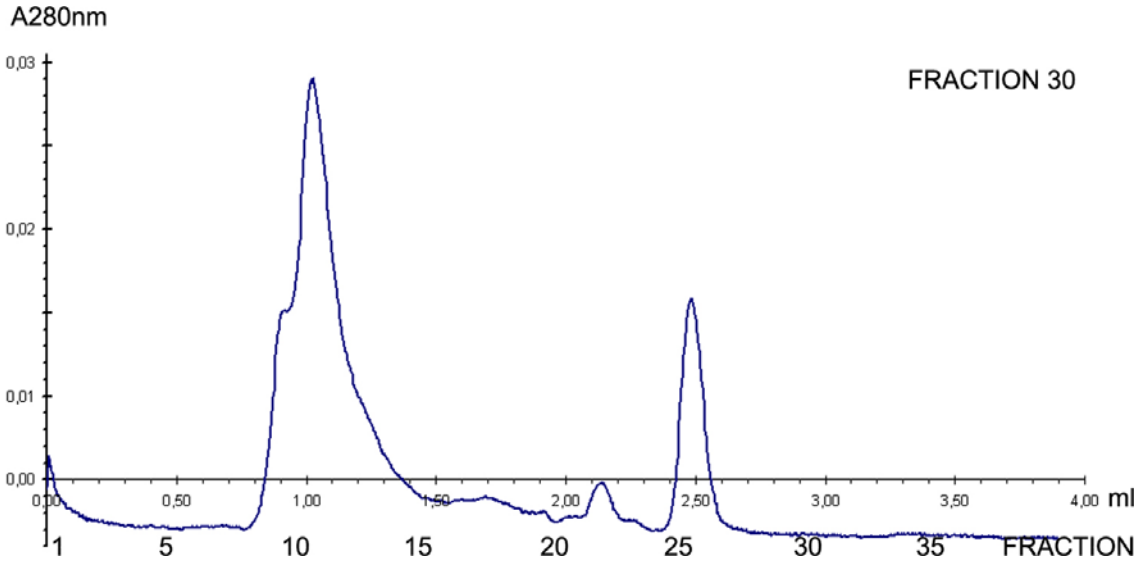
A280nm
FRACTION 30
0,03
0,02
0,01
0,00
0,00 0,50 1,00 1,50 2,00 2,50 3,00 3,50 4,00 ml
1 5 10 15 20 25 30 35 FRACTION

14. ANALYSIS OF CSTB EXPRESSION IN SKNBE CELLS

SKNBE cells were transfected with eukaryotic expression vectors containing the wt and mutated CSTB sequences. Confocal Microscopy analysys performed in collaboration with Massimo Riccio at Modena and Reggio Emilia University.

14.1. IMMUNOFLUORESCENCE ANALYSIS

SKNBE cells, plated on mycroscopy cover glass and transfected as described in section 3.2.1. were immunofluorescence labeled as follows.

- Wash the cells with 1XPBS, 2X20 sec, RT
- Fix 20 min at 4°C in 1XPBS containing 4% paraformaldehyde
- Wash the cells with 1XPBS, 3X20 sec, 4°C
- Permeabilize5 min at RT in PBS containing 0.1% Triton X100
- Wash the cells with 1XPBS, 3X20 sec, RT
- Block aspecific sites with 3% BSA 1XPBS, 1 hr, RT
- Incubate with the primary abs diluted in 3% BSA 1XPBS, 1 hr, RT
- Wash with 3% BSA 1XPBS, 5X5min, RT
- Incubate with the secondary abs diluted in 3% BSA 1XPBS, 1 hr, RT
- Wash with 3% BSA 1XPBS, 6X5min, RT
- Add a drop of DABKO (Sigma)
- Store in the dark at 4°C.

	PRIMARY ABS	
		Dilution
CSTB	Rabbit anti-cystatin b (Biogenesis)	1:10
HA	mouse anti HA (F-7) (Santa Cruz Biotechnology)	1:50

SECONDARY ABS	
	Dilution
Cy™5-conjugated donkey anti-rabbit abs $F(ab')_2$ fragment (Jackson).	ALL
FITC-conjugated sheep anti-mouse abs $F(ab')_2$ fragment (Sigma)	1:20

14.2. CONFOCAL MICROSCOPY AND CO-LOCALIZATION ANALYSIS

The confocal imaging was performed on a Radiance 2000 confocal laser scanning microscope (BioRAD) having a red diod and an argon-krypton laser. For the individuation of the two signals, FITC and Cy5, samples were sequentially excited with the 488 nm line of a krypton laser and the 637 nm line of the red diod laser. The emission signals were separated by a dichroic mirror and detected by two photomultiplier tubes.

The colocalization analysis was carried out by the LaserPix software (BioRAD) as described by [235].

	excitation λ	emission λ
FITC	488 nm (blu)	525 nm (green)
Cy5	637 nm (red)	660 nm (rar red)

The *in vivo* GFP signal in SKNBE cells was obtained by exciting the sample with the 488 nm line of the krypton laser attenuated at 10%. The emission signal was detected through a long pass filter (LP; 520) placed before the photomultiplier tube.

14.3. CELL COUNTS

SKNBE cells were transfected with pEGFP-C1 constructs of wt and mutant CSTB. The transfected cells were counted at 24, 48, 72 96, 120, 144 and 168 Hr of incubation. The percentage of transfected cells was calculated for each experimental point using triplicate samples. The number of GFP^+ cells containing intracellular aggregates was also calculated. The mean of these values was normalized and expressed as percentage of aggregate containing cells over the number of transfected cells. The statistical significance of the differences between the experimental points was evaluated by Student's *t*-test.

15. SOLUTIONS

15.1. SOLUTIONS FOR DNA AGAROSE GEL

DNA MW MARKERS

pBR322 DNA-Msp I Digest (New England BioLabs inc.), ϕX174 RF DNA/Hae III Fragments (Invitrogen), Lambda DAN/Eco RI + Hind III Marker (Promega)

TAE 50X

242 g Tris
57,1 ml Acetic Acid (glacial)
100 ml EDTA pH 8.0
Add H_2O to 1 L
Autoclave 20 min at 120°C

DNA LOADING BUFFER 10X

0,4% Bromophenol blue (AppliChem) or Xylene cyanole FF sodium salt (AppliChem)
50% Glycerol in H_2O

15.2. SOLUTIONS FOR BACTERIA CELL COLTURE

LB (LURIA BROTH)

10 g bacto tryptone (DIFCO)
5 g yeast extract (DIFCO)
10 g NaCl (Fluka)
Add H_2O to 1 L
Adjust to pH 7.2
Autoclave 20 min at 120°C

TERRIFIC BROTH

12 g bacto tryptone (DIFCO)
24 g yeast extract (DIFCO)
4 ml 100% Glycerol (Fluka)
100 ml 170 mM KH2PO4 720 mM K2HPO4 Solution
Add H_2O to 1 L

Adjust to pH 7.2
Autoclave 20 min at 120°C

KH2PO4 720 mM K2HPO4 SOLUTION

23.1 g KH2PO4
125.4 g K2HPO4
Add H_2O to 1 L
Autoclave 20 min at 120°C

2xYT

16 g bacto tryptone (DIFCO)
10 g yeast extract (DIFCO)
5 g NaCl (Fluka)
Add H_2O to 1 L
Adjust to pH 7
Autoclave 20 min at 120°C

AMPICILLIN 1000X

1 g ampicillin sodium salt (Fluka)
5 ml H2O
5 ml EtOH

KANAMYCIN 1000X
0.2 g KANAMYCIN sulfate (Sigma-Aldrich)
10 ml H2O

SOB

20 g bacto tryptone (DIFCO)
5 g yeast extract (DIFCO)
5 g NaCl (Fluka)
10 ml 250mM KCl
Add H_2O to 1 L
Adjust to pH 7
Autoclave 20 min at 120°C

SOC

200 μl 1 M glucose (sterile)

50 µl 2M $MgCl_2$ (sterile)
9,75 ml SOB

15.3. SOLUTIONS FOR IP EXPERIMENTS

PBS 1X

8g NaCl
0,2g KCl
1,44g Na_2HPO_4
0,24g KH_2PO_4
Add H_2O to 1 L
Adjust to pH 7.4
Autoclave 20 min at 120°C

IP BUFFER

150 mM NaCl
20 mM Hepes-KOH pH 8
0.5 %Nonidet P 40
2 mM DTT
0.4 mM EDTA pH 8

15.4. SOLUTIONS FOR SDS-PAGE

PROTEIN MW MARKER

Precision Plus Protein Standards ass Blue (BioRAD)

STACKING GEL

(3 ml)

H_2O	2.1 ml
30% Acrylamide mix [a]	0.5 ml
1.0 M Tris (pH 6.8)	380 µl
10% SDS	30 µl
10% APS	30 µl
TEMED	3 µl

SEPARATING GEL

	6% SEPARATING GEL (10 ml)	12% SEPARATING GEL (10 ml)	15% SEPARATING GEL (10 ml)
H_2O	5.3 ml	3.3 ml	2.3 ml
30% Acrylamide mix[a]	2.0 ml	4.0 ml	5.0 ml
1.5 M Tris (pH 8.8)	2.5 ml	2.5 ml	2.5 ml
10% SDS[b]	100 µl	100 µl	100 µl
10% APS[C]	100 µl	100 µl	100 µl
TEMED"	8 µl	4 µl	4 µl

[a]Commonly 29% acrylamide and 1% N,IV'-methylene-bis-acrylamide;

PROTEIN RUNNING BUFFER 1X

25 mM Tris
190mM Glycine
0.1% SDS

PROTEIN LOADING BUFFER 1X

(WITHOUT REDUCING AGENTS)

TRIS pH 6.8 12mM
Glycerol 5%
SDS 1%
Bromophenol Blue 0.02%

TRANSFER BUFFER WITH SDS

50 mM Tris, 380 mM Glycine, 0,1%SDS, 20% Methanol

TRANSFER BUFFER WITHOUT SDS

25mM Tris, 190mM Glycine, Methanol 20%

PONCEAU S SOLUTION 1X

0.2 g Ponceau S
3 g trichloroacetic acid
H2O2 to 100 ml

15.5. SOLUTIONS FOR 2D-PAGE

2X 2D-GEL BUFFER

14 M Urea
4 M Thiourea
8 %CHAPS
10 mM DTT
milli-Q-H2O to final volume

IPG REHYDRATION SOLUTION

8M Urea
2%CHAPS
10 mM DTT
milli-Q-H2O to final volume

Store at –20°C.

EQUILIBRATION BUFFER

50 mM Tris-HCI-0.5 M pH 6.8
6 M Urea
30 % (v/v)Glycerol
2%SDS
milli-Q-H20 to final volume

REDUCTION SOLUTION

10 ml Equilibration buffer
0.2 g DTT

ALKYLATION SOLUTION

10 ml Equilibration buffer
0. 25 g Iodoacetamide
10 μl Bromophenol Blue 0.1 %

AGAROSE SOLUTION

0.6 g agarose
1.5 ml TRIS Ph 6.8, 1M
50 μl Bromophenol Blue 0.1 %

120 µl SDS 10%
10.4 ml H2O

15.6. SOLUTIONS FOR SILVER STAIN

THIOSULFATE SOLUTION

0.2 g Na2S2O3
1L H2O

SILVER SOLUTION

0.4 g AgNO3
200 ml H2O

Store in the dark and at 4°C, before use add 100 µl 37% Formaldehyde.

DEVELOPING SOLUTION

12 g Na2CO3
4 ml Thiosulphate solution
H2O to final volume 200 ml

Store in the dark and at 4°C, before use add 100 µl 37% Formaldehyde.

STOP SOLUTION

18.6 g EDTA
Add H_2O to final volume 1L.
Adjust to pH 7 with NaOH

15.7. SOLUTIONS FOR COOMASSIE BLUE R250 STAINING

COOMASSIE BLUE R250 SOLUTION

0.4% Coomassie Brilliant Blue R250 (Fluka)
20% MetOH
80% H2O milli-Q

DESTAINIG SOLUTION

20% MetOH, 80% H2O milli-Q

APPENDIX A: HUMAN CYSTATIN B GENE

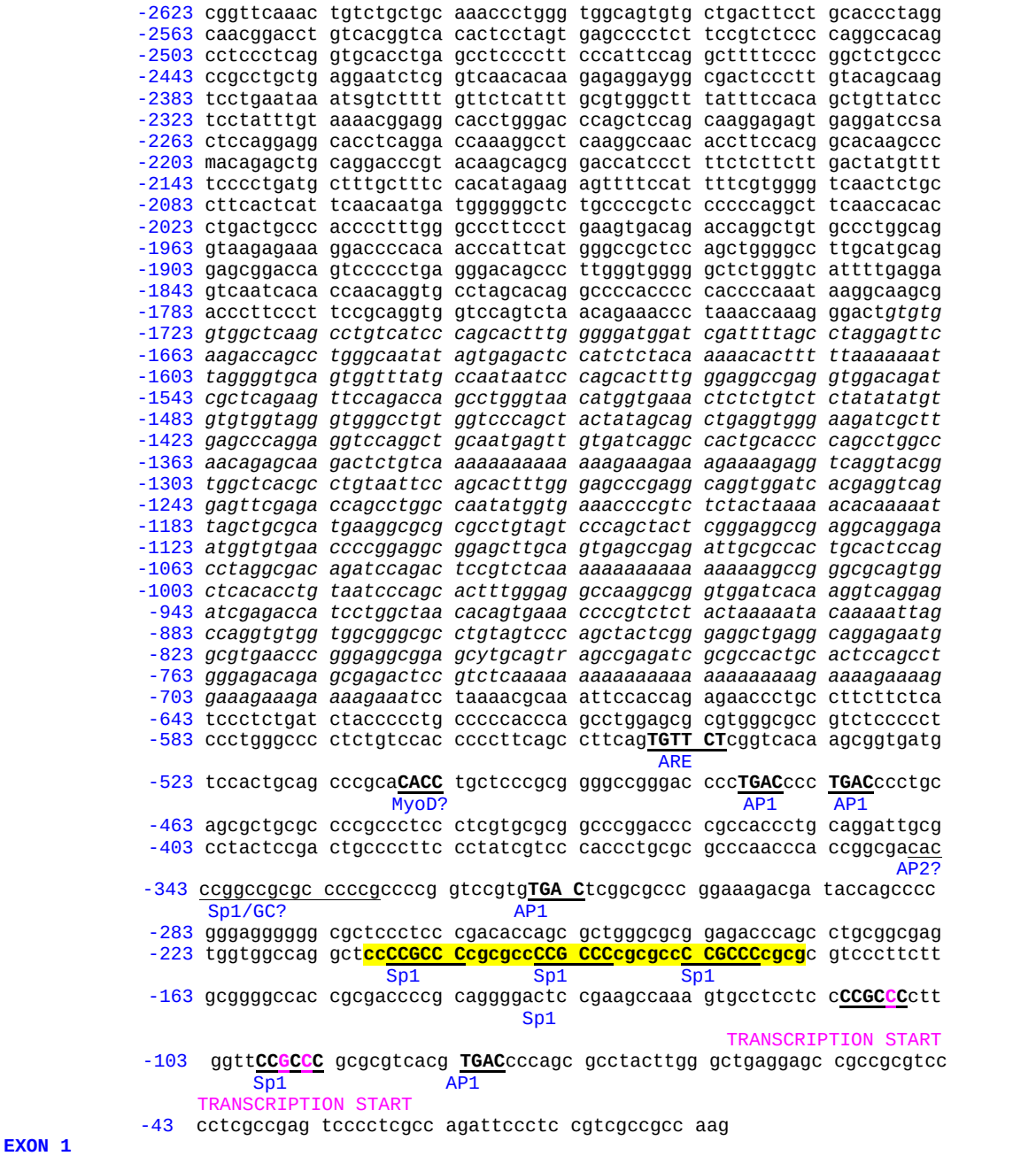

```
          678   taaaaactta agtgtatctg cataaaaggt ccacaggttt ctttacatgc ttccgattct
          738   agcactgttt caaactgtaa gtctaaataa aaagttaaaa cacagaaaaa caagataaaa
          798   accgggctgg gttgcagatg gcaaccttcc ctgtgtctcg gtttcctcgt ctgtaaaatg
          858   gacgtcctgt tgctctgcgc ctgccagaag attctggagg ggctgaaatg agcaggtcat
          918   ctgtgcaaga agccccctcc ggtggagcac aggccaggcc cgcctcgctg tcatggttgg
          978   tgaccgacgg gatgccccaa gcaagaacag gtccaggcga tgctgaggcc tgtgkttttt
         1038   ttktttgttt ttgagackca gtctcactct tgcccagggt ggagtgcagt ggcacaatct
         1098   cggcccactg caacctccgc ttcccaggtt caagggattc tcctgcctta gcctcccgag
         1158   tagctgggat tgcaggtgct cgccaccacg cccagctaat ttttgtattt ttagtagaaa
         1218   cggggttttg ccatttggct aggctggtct caaactcctg acctcaagtg atccgcccac
         1278   ctcagcctcc caaagttctg ggattacatc cttgagccac cgtacccagc tggaactgtt
         1338   tttttctact ttattattag gctgacagtt taaatgtccc ttcagttgta agagacaatt
         1398   gtgtgaagag ccagtgtcag aatcgtgtgt gtgctcacat gcgtgcaagt tactctagca
         1458   ggagggaatc caagaagcca ctgagacatc ctcattctgt cccttctgtc taG

EXON 2   1511   gtg agg tcc cag ctt gaa gag aaa gaa aac aag aag ttc cct gtg ttt aag
                  V23  R  S   Q  L   E   E  K E/y? N   K  K   F  P   V  F   K
                 gcc gtg tca ttc aag agc cag gtg gtc gcg gGg aca aac tac ttc atc aaG
                  A   V  S   F  K   S  Q46 V   V  A  G50  T   N  Y   F  I  K56

          1613   gtaga gtgtgggcct caggagggcc
          1638   tgccccgaac gggtgctggt aggaaaccgc ctgtgcaggc ccgggctgtg tggtcttagg
          1698   tgctggggcg ccctgtggct gccccctgag ataagcatcc tactgtgtgt gtccatcggc
          1758   ctttcaggag gactagggct tctggggagc taagaacccc aaggaaacaa gtgtgggatg
          1818   tgaggcatcc cctgcacatg caggagaaga caagattgtc ttcagctggc tgctaatgac
          1878   ctggaggggc gcagcaaggt gacttgggat cagaggcttc gctcactccg ctctcttccc Ag

EXON 3
1940 gtg cac gtc ggc gac gag gac ttc gta cac ctg Cga gtg ttc cAa TCt ctc cct cat gaa aac aag
     V57  H   V  G   D  E   D  F   V  H   L  R68  V  F  Q  S72  L P74 H75 E76  N   K
          ccc ttg acc tta tct aac tac cag acc aac aaa gcc aag cat gat gag ctg acc tat ttc tga
           P   L  T   L  S   N  Y   Q  T   N   K   A  K   H  D  E   L   T  Y  F98  *

          2069   tcctgactt tggacaaggc ccttcagcca gaagactgac aaagtcatcc
          2118   tccgtctacc agagcgtgca cttgtgatcc taaaataagc ttcatctccg ggctgtgccc
          2178   cttggggtgg aaggggcagg attctgcagc tgcttttgca tttctcttcc taaatttcat
          2238   tgtgttgatt tctttccttc ccaataggtg atcttaatta ctttcagaat attttcaaaa
                                  3' UTR    3'Downstream
          2298   tagatatatt tttaaaatcc ttacagattg cctcctttgt tttagacttt tttcttgctg
          2358   ctaaccaccc cgggcaggtc cttcccctcc aggcaggagg gcggagagag tc
```

In italic : region rich in alu sequences (-686/-1728).
In pink: transcription start and stop
Highlighted in yellow: dodecamer repeats and nt mutated in EPM1 patients.
Secondary Structure of the protein: loop in blu, α-helix in green, β-sheet in orange.
Question mark next to a transcription factor site: the binding is predicted but not verified *in vitro*.
(GenBank AB083085)

REFERENCES

1 Pennacchio LA, Bouley DM, Higgins KM, Scott MP, Noebels JL, Myers RM. (1998) Progressive ataxia, myoclonic epilepsy and cerebellar apoptosis in cystatin B-deficient mice. *Nat. Genet.* **20**: 251.

2. Staniforth RA, Giannini S, Higgins LD, Conroy MJ, Hounslow AM, Jerala R, Craven CJ, Waltho JP. (2001) Three-dimensional domain swapping in the folded and molten-globule states of cystatins, an amyloid-forming structural superfamily. *EMBO J*. **20**: 4774-4781.

3. Di Giaimo R et al. (2002) New insights into the molecular basis of Progressive Myoclonus Epilepsy (EPM1): a multiprotein complex with cystatin B. *Hum. Mol. Gen*. **11**: 2941.

4. Barret AJ, Kirschke H. (1981) Cystatin, the egg white inhibitor of cysteine proteinases. *Methods Enzymol.* **80**: 771.

5. Jarvinen M, Rinne A. (1982) Human spleen cysteine proteinase inhibitor. Purification, fractionation into isoelectric variants and some properties of the variants. *Biochim. Biophys. Acta.* **708**: 210.

6. Ritonja A, Popovic T, Turk V, Wiedenmann K, Machleidt W. (1985) Amino acid sequence of human liver cathepsin B. *FEBS Lett.* **181**: 169.

7. Jerala R, Trstenjak M, Lenarcic B, Turk V. (1988) Cloning a synthetic gene for human stefin B and its expression in E. coli. *FEBS. Lett.* **239**: 41.

8. Turk V, Bode W. (1991) The cystatins: Proteins inhibitors of cysteine proteinases. *FEBS Lett.* **285**: 213.

9. Pennacchio LA, Lehesjoki AE, Stone NE, Willour VL, Virtaneva K, Miao J, D'Amato E, Ramirez L, Faham M, Koskiniemi M, Warrington JA, Norio R, de la Chapelle A, Cox DR, Myers RM. (1996) Mutations in the gene encoding cystatin B in progressive myoclonus epilepsy (EPM1). *Science*. **271**: 1731-34.

10. Pennacchio LA, Myers RM. (1996) Isolation and characterization of the mouse cystatin B gene. *Genome Res*. **6**:1103-9.

11. Smid L, Strojan P, Budihna M, Skrk J, Vrhovec I, Zargi M, Kos J. (1997) Prognostic value of cathepsins B, D and steffins A and B in laryngeal carcinoma. *Eur Arch Otorhinolaryngol*. **254** Suppl 1: S 150-3.

12. Lalioti MD, Mirotsou M, Buresi C, Peitsch MC, Rossier C, Ouazzani R, Baldy-Moulinier M, Bottani A, Malafosse A, Antonarakis SE. (1997) Identification of mutations in cystatin B, the gene responsible for the Unverricht-Lundborg type of progressive myoclonus epilepsy (EPM1). *Am. J. Hum. Genet*. **60**: 342-351.

13. Moulard B, Genton P, Grid D, Jeanpierre M, Ouazzani R, Mrabet A, Morris M, LeGuern E, Dravet C, Mauguiere F, Utermann B, Baldy-Moulinier M, Belaidi H, Bertran F, Biraben A, Ali Cherif A, Chkili T, Crespel A, Darcel F, Dulac O, Geny C, Humbert-Claude V, Kassiotis P, Buresi C, Malafosse A. (2002) Haplotype study of West European and North African Unverricht-Lundborg chromosomes: evidence for a few founder mutations. *Hum Genet*. **111**: 255-62.

14. Lalioti MD, Scott HS, Buresi C, Rossier C, Bottani A, Morris MA, Malafosse A, Antonarakis SE. (1997) Dodecamer repest expansion in cystatin B gene in progressive myoclonus epilepsy. *Nature*. **386**: 847-851.

15. Alakurtti K, Virtaneva K, Joensuu T, Palvimo JJ, Lehesjoki AE. (2000) Characterization of the cystatin B gene promoter harboring the dodecamer repeat expanded in progressive myoclonus epilepsy, EPM1. *Gene*. **242**: 65-73.

16. Barret AJ, Fritz H, Grubb A, Isemura S, Järvinen M, Katunuma N, Machleidt W, Müller-Esterl W, Sasaki M, Turk V. (1986) Nomenclature and classification of the proteins homologous with the cysteine-proteinase inhibitor chicken cystatin. *Biochem J.* **236**: 312.

17. Stubbs M, Laber B, Bode W, Huber R, Jerala R, Lenarcic B, Turk V. (1990) The refined 2.4A X-ray crystal structure of recombinant human stefin B in complex with the cysteine proteinase papain: A novel type of proteinase inhibitor interaction. *EMBO J.* **9**: 1939.

18. Abrahamson M, Ritonja A,Brown MA, Grubb A, Machleidt W, Barrett AJ. (1987) *J. Biol. Chem.* **262**: 9688-9694.

19. Wakamatsu N, Kominami E, Takio K, Katunuma N. (1984) *J Biol Chem*. **259**: 13832-38.

20. Lenarčič B, Ritonja A, Šali A, Kotnik M, Turk V, Machleidt W. in: Cysteine Proteinases and their Inhibitors (Turk V eds.) 1986, 473-487, Walter de Gruyter, Berlin.

21. Katunuma N in: Intracellular Proteolysis Mechanisms and Regulations (Katunuma N and Kominami E eds.) 1989, 3-23, Japan Sci. Soc. Press, Tokyo.

22. Pol E, Bjork I. (2003) Contributions of individual residues in the N-terminal region of cystatin B (stefin B) to inhibition of cysteine proteinases. *Biochim Biophys Acta*. **1645**: 105-12.

23. Nikawa T, Towatari T, Ike Y, Katunuma N. (1989) Studies on the reactive site of the cystatin superfamily using recombinant cystatin A mutants. Evidence that the QVVAG region is not essential for cysteine proteinase inhibitory activities. *FEBS Lett.* **255**: 309-314.

24. Jerala R, Trstenjak-Prebanda M, Kroon-Zitko L, Lenarcic B, Turk V. (1990) Mutations in the QVVAG region of the cysteine proteinase inhibitor stefin B. *Biol Chem Hoppe Seyler*. **371** Suppl: 157-60.
25. Ritonja A, Machleidt W, Barret AJ. (1985) Amino acid sequence of the intracellular cysteine proteinase inhibitor cystatin B from human liver. *Biochem. Biophys. Res. Commun*. **131**: 1187-1192.
26. Pol E, Bjork. (1999) Importance of the second binding loop and the C-terminal end of cystatin B (stefin B) for inhibition of cysteine proteinases. *Biochemistry*. **38**: 10519-26.
27. Bespalova IN, Pranzatelli M, Burmeister M. (1997) G to C transversion at a splice acceptor site causes exon skipping in the cystatin B gene. *Mutat Res*. **382**: 67-74.
28. Fernandez MA, Abrahamson M. (2006) Structural and Protease Inhibitory Features of Cystatins. Chapter II, in "Human Stefins and Cystatins", E. Zerovnik and N. Kopitar Jerala, eds, "Molecular Anatomy and Physiology of Proteins" Series, V.N.Uversky Series ed, NOVA Science Publishers, New York, 2006.
29. Zerovnik E, Jerala R, Kroon-Žitko L, Turk V, Lohner K. (1997) Characterization of the equilibrium intermediatesin acid denaturation of human stefin B. *Eur J Biochem*. **245**: 364-72.
30. Zerovnik E, Jerala R, Virden R, Kroon Zitko L, Turk V, Waltho JP. (1998) On the mechanism of human stefin B folding: II. Folding from GuHCl unfolded, TFE denatured, acid denatured, and acid intermediate states. *Proteins*. **32**: 304-13.
31. Žerovnik E, Lenarčič B, Jerala R, Turk V. (1991) Folding studies of the cysteine protease inhibitor-human stefin A. *Biochim Biophys Acta*. **1078**: 313.
32. Žerovnik E, Jerala R, Kroon-Žitko L, Pain RH, Turk V. (1992a) Intermediates in denaturation of a small globular protein, recombinant human stefin B. *J. Biol. Chem.* **267**: 9041.
33. Žerovnik E, Lohner K, Jerala R, Laggner P, Turk V. (1992b) Calorimetric measurements of thermal denaturation of stefins A and B; comparison to predicted thermodynamics of stefin B unfolding. *Eur. J. Biochem.* **210**: 217.
34. Riccio M, Di Giaimo R, Pianetti S, Calmieri PP, Melli M, Santi S. (2001) Nuclear localization of cystatin B, the cathepsin inhibitor implicated in myoclonous epilepsy (EPM1*). Exper. Cell Res.* **262**: 84-94.
35. Calkins CC, Sameni M, Koblinski J, Sloane BF, Moin K. (1998) Differential localization of cysteine protease inhibitors and a target cysteine protease, cathepsin B, by immuno-confocal microscopy. *J Histochem Cytochem.* **46**: 745-51.
36. Di Giaimo R, Cipollini E, Riccio M, Santi S, Hoque M, Dembic M, Palmieri P, Carone S, Melli M. (2006) Alternative Functions for Cystatin B implicated by its interaction with Proteins other than Proteases. p. 43-60, in "Human Stefins and Cystatins", E. Zerovnik and N. Kopitar Jerala, eds, "Molecular Anatomy and Physiology of Proteins" Series, V. N. Uversky Series ed, NOVA Science Publishers, New York, 2006.
37. Alakurtti K, Weber E, Rinne R, Theil G, de Haan GJ, Lindhout D, Salmikangas P, Saukko P, Lahtinen U, Lehesjoki AE (2005) Loss of lysosomal association of cystatin B proteins representing progressive myoclonus epilepsy, EPM1, mutations. *Eur J Hum Genet.* **13**: 208.
38. Abrahamson M, Barrett AJ, Salvesen G, Grubb A. (1986) Isolation of six cystatine proteinase inhibitors from human urine. *J Biol Chem*. **261**: 11282-89.
39. Watanabe M, Watanabe T, Ishii Y, Matsuba H, Kimura S, Fujita T, Kominami E, Katunuma N, Uchiyama Y. (1988) Immunocytochemical localization of cathepsins B, H and their endogenous inhibitor, cystatin β in islet endocrine cells of the rat pancreas. *J Histochem Cytochem*. **36**: 783.
40. Riccio M, Santi S, Dembic M, Di Giaimo R, Cipollini E, Costantino-Ceccarini, E, Ambrosetti DC, Maraldi NM, Melli M. (2005) Cell-specific expression of the epm1 (cystatin B) gene in developing rat cerebellum. *Neurobiol. of Dis.* **20**: 104-114.
41. Lalioti MD, Scott HS, Antonarakis SE (1999) Altered spacing of promoter elements due to the dodecamer repeat expansion contributes to reduced expression of the cystatin B gene in EPM1. *Hum Mol Genet.* **8**: 1786.
42. Shannon P, Pennacchio LA, Houseweart MK, Minassian BA, Myers RM. (2002) Neuropathological changes in a mouse model of progressive myoclonus epilepsy: cystatin B deficiency and Unverricht-Lundborg disease. *J Neuropathol Exp Neurol.* **61**: 1085-91.
43. Koskiniemi M. (1979) Progressive myoclonus epilepsy; genetic and nosological aspects with special reference to 107 Finnish patients. *Clin Genet*. **15**: 382-98.
44. Eldridge R, Ljvanainen M, Stern R, Koerber T, Wilder BJ. (1983) "Baltic" myoclonus epilepsy: hereditary disorder of childhood made worse by phenytoin. *Lancet*. **2**: 838-42.
45. Koskiniemi M, Donner M, Majuri H, Haltia M, Norio R. (1974) Progressive myoclonus epilepsy: a clinical and histopathological study. *Acta Neurol. Scand.* **50**: 307-332.
46. Berkovic SF, Andermann F, Carpenter S, Walfe L. (1985) Progressive myoclonus epilepsies: specific causes and diagnosis. *N. Engl J. Med*. **315**: 296-305.
47. Delgado-Escueta AV,Ganesh S, Yamakawa K. (2001) Advances in the Genetics of Progressive Myoclonus Epilepsy. *American Journal of Medical Genetics* (Semin. Med. Genet.). **106**: 129-138.
48. Koskiniemi M. (1990) *Paediatric Epilepsy*. Sillanpää M, Johannessen SI, Blennow G, Dam D. eds; 30-144.

49. Rinne R, Saukko P, Jarvinen M, Lehesjoki AE. (2002) Reduced cystatin B activity correlates with enhanced cathepsin activity in progressive myoclonus epilepsy. *Ann Med*. **34**: 380-5.
50. Koskiniemi M, Fahn S, Marsden CP, Van Woert M, Baltic myoclonus eds. Advances in neurology, myoclonus. New York, Raven Press, (1986); 43, 57-64.
51. Lehesjoki AE, Koskiniemi M. (1999) Progressive myoclonus epilepsy of Unverricht-Lundborg type. *Epilepsia*. **40** Suppl 3: 23-8.
52. Mascalchi M, Michelucci R, Cosottini M, Tessa C, Lolli F, Riguzzi P, Lehesjoki AE, Tosetti M, Villari N, Tassinari CA. (2002) Brainstem involvement in Unverricht-Lundborg disease (EPM1): An MRI and H MRS study. *Neurology*. **58** : 1686-89.
53. Habib M, Roger J, Khalil R et al. (1985) Epilepsie myoclonique progressive dégénérative, Lésions olivo-cérébelleuses systématisées. *Rev Neurol*. **141** : 274-88.
54. Lafreniere RG, Rochefort DL, Chretien N, Rommens JM, Cochius JI, Kalviainen R, Nousiainen U, Patry G, Farrell K, Soderfeldt B, Federico A, Hale BR, Cossio OH, Sorensen T, Pouliot MA, Kmiec T, Uldall P, Janszky J, Pranzatelli MR, Andermann F, Andermann E, Rouleau GA. (1997) Unstable insertion in the 5' flanking region of the cystatin B gene is the most common mutation in progressive myoclonus epilepsy type 1, EPM1. *Nat. Genet.* **15**: 298-302.
55. Bespalova IN, Adkins S, Pranzatelli M, Burmeister M. (1997) Cystatin B mutation and diagnostic PCR assay in an Unverricht-Lundborg progressive myoclonus epilepsy patient. *Am J Med Genet*. **74**: 467-71.
56. Lalioti MD, Scott HS, Genton P, Grid D, Ouazzani R, M'Rabet A, Ibrahim S, Gouider R, Dravet C, Chkili T, Bottani A, Buresi C, Malafosse A, Antonarakis SE. (1998) A PCR amplification method reveals instability of the dodecamer repeat in progressive myoclonus epilepsy (EPM1) and no correlation between the size of the repeat and age at onset. *Am. J. Hum. Genet*. **62**: 842-847.
57. Lalioti MD, Scott HS, Antonarakis SE. (1999) Altered spacing of promoter elements due to the dodecamer repeat expansion contributes to reduced expression of the cystatin B gene in EPM1. *Hum. Mol. Genet.* **8**: 1791-1798.
58. Kagitani-Shimono K, Imai K, Okamoto N, Ono J, Okada S. (2002) Unverricht-Lundborg disease with cystatin B gene abnormalities. *Pediatr Neurol.* **26**: 55-60.
59. Virtaneva K, D'Amato E, Miao J, Koskiniemi M, Norio R, Avanzini G, Franceschetti S, Michelucci R, Tassinari CA, Omer S, Pennacchio LA, Myers RM, Dieguez-Lucena JL, Krahe R, de la Chapelle A, Lehesjoki AE. (1997) Unstable minisatellite expansion causing recessively inherited myoclonus epilepsy, EPM1. *Nat. Genet.* **15**: 393-396.
60. Virtaneva K, Paulin L, Krahe R, de la Chapelle A, Lehesjoki AE. (1998) The minisatellite expansion mutation in EPM1: resolution of an initial discrepancy. Mutatations in brief no. 186. Online. *Hum. Mutat.* **12**: 218.
61. Alakurtti K, Weber E, Rinne R, Theil G, de Haan GJ, Lindhout D, Salmikangas P, Saukko P, Lahtinen U, Lehesjoki AE (2005) Loss of lysosomal association of cystatin B proteins representing progressive myoclonus epilepsy, EPM1, mutations. *Eur J Hum Genet.* **13**: 208.
62. Joensuu T, Kuronen M, Alakurtti K, Tegelberg S, Hakala P, Aalto A, Huopaniemi L, Aula N, Michellucci R, Eriksson K, Lehesjoki AE. (2006) Cystatin B: mutation detection, alternative splicing and expression in progressive mioclonus epilepsy of Unverricht-Lundborg type (EPM1) patients. *Eur J Hum Genet*.
63. Lehesjoki A, Koskiniemi M. (1999) Progressive myoclonus epilepsy of Unverricht-Lundborg type. *Epilepsia.* **40**: 23.
64. Berkovic SF, Mazarib A, Walid S, Neufeld MY, Manelis J, Nevo Y, Korczyn AD, Yin J, Xiong L, Pandolfo M, Mulley JC, Wallace RH. (2005) A new clinical and molecular form of Unverricht–Lundborg disease localized by homozygosity mapping. *Brain*, **128**: 652.
65. Coppola G, Criscuolo C, De Michele G, Striano S, Barbieri F, Striano P, Perretti A, Santoro L, Brescia Morra V, Sacca F, Scarano V, D'Adamo AP, Banfi S, Gasparini P, Santorelli FM, Lehesjoki AE, Filla. (2005) Autosomal recessive progressive myoclonus epilepsy with ataxia and mental retardation. *J Neurol*. **252**(8): 897−900.
66. Pennacchio LA, Bouley DM, Higgins KM, Scott MP, Noebels JL, Myers RM. (1998) Progressive ataxia, myoclonic epilepsy and cerebellar apoptosis in cystatin B-deficient mice. *Nat Genet*. **20**: 251-8.
67. Lieuallen K, Pennacchio LA, Park M, Myers RM, Lennon GG. (2001) Cystatin B-deficient mice have increased expression of apoptosis and glial activation genes. *Hum Mol Genet.* **10**: 1867.
68. Houseweart MK, Vilaythong A, Yin XM, Turk B, Noebels JL, Myers RM. (2003) Apoptosis caused by cathepsins does not require Bid signaling in an in vivo model of progressive myoclonus epilepsy (EPM1). *Cell Death Differ*. **10** (12): 1329−35.
69. Houseweart MK, Pennacchio LA, Vilaythong A, Peters C, Noebels JL, Myers RM. (2003) *J Neurobiol*. **563**: 15−27.
70. Kopitar-Jerala N, Schweiger A, Myers RM, Turk V, Turk B (2005) Sensitization of stefin B-deficient thymocytes towards staurosporin-induced apoptosis is independent of cysteine cathepsins. *FEBS Lett.* **579**: 2149.

71. Shiraishi T, Mori M, Tanaka S, Sugimachi K, Akiyoshi T. (1998) Identification of cystatin B in human esophageal carcinoma, using differential displays in which the gene expression is related to lymph-node metastasis. *Int J Cancer*. **79**: 175-8.
72. Kos J, Krasovec M, Cimerman N, Nielsen HJ, Christensen IJ, Brunner N. (2000) Cysteine proteinase inhibitors stefin A, stefin B, and cystatin C in sera from patients with colorectal cancer: relation to prognosis. *Clin Cancer Res*. **6**: 505-11.
73. Strojan P, Budihna M, Smid L, Svetic B, Vrhovec I, Kos J, Skrk J. (2000) Prognostic significance of cysteine proteinases cathepsins B and L and their endogenous inhibitors stefins A and B in patients with squamous cell carcinoma of the head and neck. *Clin Cancer Res*. **6**: 1052-62.
74. Zajc I, Sever N, Bervar A, Lah TT. (2002) Expression of cysteine peptidase cathepsin L and its inhibitors stefins A and B in relation to tumorigenicity of breast cancer cell lines. *Cancer Lett*. **187**: 185-90.
75. Levicar N, Kos J, Blejec A, Golouh R, Vrhovec I, Frkovic-Grazio S, Lah TT. (2002) Comparison of potential biological markers cathepsin B, cathepsin L, stefin A and stefin B with urokinase and plasminogen activator inhibitor-1 and clinicopathological data of breast carcinoma patients. *Cancer Detect Prev*. **26**: 42-9.
76. Zhang R, Tremblay TL, McDermid A, Thibault P, Stanimirovic D. (2003) Identification of differentially expressed proteins in human glioblastoma cell lines and tumors. *Glia*. **42**: 194-208.
77. Trinkaus M, Vranic A, Dolenc VV, Lah TT. (2005) Cathepsins B and L and their inhibitors stefin B and cystatin C as markers for malignant progression of benign meningiomas. *Int J Biol Markers*. **20**: 50.
78. Budihna M, Strojan P, Smid L, Skrk J, Vrhovec I, Zupevc A, Rudolf Z, Zargi M, Krasovec M, Svetic B, Kopitar-Jerala N, Kos J. (1996) Prognostic value of cathepsins B, H, L, D and their endogenous inhibitors stefins A and B in head and neck carcinoma. *Biol Chem Hoppe Seyler*. **377**: 385-90.
79. Ebert E, Werle B, Julke B, Kopitar-Jerala N, Kos J, Lah T, Abrahamson M, Spiess E, Ebert W. (1997) Expression of cysteine protease inhibitors stefin A, stefin B, and cystatin C in human lung tumor tissue. *Adv Exp Med Biol*. **421**: 259-65.
80. Lefebvre C, Cocquerelle C, Vandenbulcke F, Hot D, Huot L, Lemoine L, Salzet M. (2004) Transcriptomic analysis in the leech *Theromyzon tessulatum*: involvement of cystatin B in innate immunity. *Biochem. J*. **380**: 617.
81. Suzuki T, Hashimoto S, Toyoda N, Nagai S, Yamazaki N, Dong HY, Sakai J, Yamashita T, Nukiwa T, Matsushima K. (2000) Comprehensive gene expression profile of LPS-stimulated human monocytes by SAGE. *Blood*. **96**: 2584.
82. Helms LR, Wetzel R. (1996) Specificity of abnormal assembly in immunoglobulin light chain deposition disease and amyloidosis. *J Mol Biol.* **257**: 77.
83. Wells CA, Ravasi T, Sultana R, Yagi K, Carninci P, Bono H, Faulkner G, Okazaki Y, Quackenbush J, Hume DA, Lyons PA. (2003) Continued discovery of transcriptional units expressed in cells of the mouse mononuclear phagocyte lineage. **13**: 1360.
84. Vos JB, van Sterkenburg MA, Rabe KF, Schalkwijk J, Hiemstra PS, Datson NA. (2005) Transcriptional response of bronchial epithelial cells to Pseudomonas aeruginosa: identification of early mediators of host defense. *Physiol Genomics.* **21**: 324.
85. Hopsu-Havu VK, Joronen IA, Jarvinen M, Rinne A, Aalto M. (1984) Cysteine protease inhibitors produced by mononuclear phagocytes. *Cell Tissue Res*. **236**: 161.
86. Verdot L, Lalmanach G, Vercruysse V, Hartmanni S, Luciusi R, Hoebeke J, Gauthier F, Vray B**. (**1996) Cystatins Up-regulate Nitric Oxide Release from Interferon-g activated Mouse Peritoneal Macrophages. *J. Biol. Chem.* **271**: 28077.
87. Olafsson I, Thorsteinsson L, Jensson O. (1996) The molecular pathology of hereditary cystatin C amyloid angiopathy causing brain hemorrhage. *Brain Pathol.* **6**: 121.
88. Levy E, Lopez-Otin C, Ghiso J, Geltner D, Frangione B. (1989) Stroke in Icelandic patients with hereditary amyloid angiopathy is related to a mutation in the cystatin C gene, an inhibitor of cysteine proteases. *J Exp Med.* **169**: 1771.
89. Abrahamson M, Grubb A. (1994) Increased body temperature accelerates aggregation of the Leu-68-->Gln mutant cystatin C, the amyloid-forming protein in hereditary cystatin C amyloid angiopathy. *Proc Natl Acad Sci U S A*. **86**: 1416.
90. Ekiel I, Abrahamson M. (1996) Folding-related dimerization of human cystatin C. *J Biol Chem.* **271**: 1314.
91. Jerala R, Zerovnik E. (1999) Accessing the global minimum conformation of stefin A dimer by annealing under partially denaturing conditions. *J Mol Biol.* **286**: 1079.
92. Benussi L, Ghidoni R, Steinhoff T, Alberici A, Villa A, Mazzoli F, Nicosia F, Barbiero L, Broglio L, Feudatari E, Signorini S, Finckh U, Nitsch RM, Binetti G. (2003) Alzheimer disease-associated cystatin C variant undergoes impaired secretion. *Neurobiol Dis.* **13**: 15.
93. Carrette O, Demalte I, Scherl A, Yalkinoglu O, Corthals G, Burkhard P, Hochstrasser DF, Sanchez JC. (2003) A panel of cerebrospinal fluid potential biomarkers for the diagnosis of Alzheimer's disease. *Proteomics.* **3**: 1486.

94. Bernstein HG, Kirschke H, Wiederanders B, Pollak KH, Zipress A, Rinne A. (1996) The possible place of cathepsins and cystatins in the puzzle of Alzheimer disease: a review. *Mol Chem Neuropathol.* **27**: 225.
95. Deng A, Irizarry MC, Nitsch RM, Growdon JH, Rebeck GW. (2001) Elevation of Cystatin C in Susceptible Neurons in Alzheimer's Disease. *Am. J. Pathol.* **159**: 1061.
96. Finckh U, von der Kammer H, et al. and Nitsch RM. (2000) Genetic association of a cystatin C gene polymorphism with late-onset Alzheimer disease. *Arch Neurol*. **57**: 1579.
97. Beyer K, Lao JI, Gomez M, Riutort N, Latorre P, Mate JL, Ariza A. (2001). Alzheimer's disease and cystatin C gene polymorphism: an association study. *Neurosci. Lett*. **315**: 17.
98. Ii K, Ito H, Kominami E, Hirano A. (1993) Abnormal distribution of cathepsin proteinases and endogenous inhibitors (cystatins) in the hippocampus of patients with Alzheimer's disease, parkinsonism-dementia complex on Guam, and senile dementia and in the aged. *Virchows Arch A Pathol Anat Histopathol.* **423**: 185.
99. Stubbs M T, Laber B, Bode W, Huber R, Jerala R, Lenarčič B, Turk V. (1990) The refined 2.4 A X-ray crystal structure of recombinant human stefin B in complex with the cysteine protease papain: a novel type of protease inhibitor interaction. *EMBO J.* **9**: 1939.
100. Martin JR, Craven CJ, Jerala R, Kroon-Žitko L, Žerovnik E, Turk V, Waltho JP. (1995). The three-dimensional solution structure of human stefin A. *J. Mol. Biol*. **246**: 331.
101. Jerala R, Žerovnik E. (1999) Accessing the global minimum conformation of stefin A dimer by annealing under partially denaturing conditions. *J. Mol. Biol*. **291**: 1079-1089.
102. Janowski R, Kozak M, Jankowska E, Grzonka Z, Grubb A, Abrahamson M, Jaskolski M. (2001) Human cystatin C, an amyloidogenic protein, dimerizes through three-dimensional domain swapping. *Nat Struct Biol.* **8**: 316-320
103. Abrahamson M, Grubb A. (1994) Increased body temperature accelerates aggregation of the LEU68→GLN mutant cystatin C, the amyloid-forming protein in hereditary cystatin C amyloid Angiopathy. *Proc. Natl. Acad. Sci. USA*. **91**: 1416-1420.
104. Calero M, Pawlick M, Soto C, Castaño EM, Sigurdsson EM, Kumar A, Gallo G, Frangione B, Levy E. (2001) Distinct properties of wild-type and the amyloidogenic human cystatin C variant of hereditary cerebral hemorrhage with amyloidosis, Icelandic type. *J. Neurochem*. **77**: 628.
105. Žerovnik E, Pompe-Novak M, Škarabot M, Ravnikar M, Muševič I, Turk V. (2002) Human stefin B readily forms amyloid fibrils in vitro. *Biochim. Biophys. Acta.* **1594**: 1.
106. Žerovnik E, Zavašnik-Bergant V, Kopitar-Jerala N, Pompe-Novak M, Škarabot M, Goldie K, Ravnikar M, Muševič I, Turk V. (2002) Amyloid fibril formation by human stefin B in vitro: immunogold labelling and comparison to stefin A. *Biol. Chem.* **383**: 859.
107. Žerovnik E, Stoka V, Tušek-Žnidarič M, Pompe-Novak M, Giannini S, Staniforth RA. (2006) On the Mechanism of Amyloid Fibrillation; Stefin B as a Good Model Protein. Chapter VI, in "Human Stefins and Cystatins", E. Žerovnik and N. Kopitar Jerala, eds, "Molecular Anatomy and Physiology of Proteins" Series, V. N. Uversky Series ed, NOVA Science Publishers, New York.
108. Kad NM, Myers SL, Smith DP, Smith DA, Radford SE, Thomson NH. (2003) Hierarchical assembly of β_2-microglobulin amyloid *in vitro* revealed by atomic force microscopy. *J. Mol. Biol*. **330**: 785.
109. Tjernberg LO, Pramanik A, Bjorling S, Thyberg P, Thyberg J, Nordstedt C, Berndt KD, Terenius L, Rigler R. (1999) Amyloid beta-peptide polymerization studied using fluorescence correlation spectroscopy. *Chem. Biol.* **6**: 53.
110. Kad NM, Thomson NH, Smith DP, Smith DA, Radford SE. (2001) β_2-microglobulin and its deamidated variant, N17D, form amyloid fibrils with a range of morphologies in vitro. *J. Mol. Biol*. **313**: 559.
111. Buxbaum J. (1992) Mechanisms of disease: monoclonal immunoglobulin deposition. Amyloidosis, light chain deposition disease, and light and heavy chain deposition disease. *Hematol Oncol Clin North Am.* **6**: 323.
112. Khurana R, Gillespie JR, Talapatra A, Minert LJ, Ionescu-Zanetti C, Millett I, Fink AL. (2001) Partially folded intermediates as critical precursors of light chain amyloid fibrils and amorphous aggregates. *Biochemistry.* **40**: 3525.
113. Seilheimer B, Bohrmann B, Bondolfi L, Muller F, Stuber D, Dobeli H. (1997) The toxicity of the Alzheimer's beta-amyloid peptide correlates with a distinct fiber morphology. *J Struct Biol.* **119**: 59.
114. Zurdo J, Guijarro JI, Jimenez JL, Saibil HR, Dobson CM. (2001) Dependence on solution conditions of aggregation and amyloid formation by an SH3 domain. *J Mol Biol.* **311**: 325.
115. Hilbich C, Kisters-Woike B, Reed J, Masters CL, Beyreuther K. (1991) Aggregation and secondary structure of synthetic amyloid beta A4 peptides of Alzheimer's disease. *J Mol Biol.* **218**: 149.
116. Giannini S, Sanders A, Jaskolski M, Grubb A, Staniforth RA. (2006) Cystatins: 3D Domain-Swapping and Amyloid Angiopathy. A General Mechanism for the Formation of Amyloid Fibrils? Chapter V, in "Human Stefins and Cystatins", E.Zerovnik and N. Kopitar Jerala, eds, "Molecular Anatomy and Physiology of Proteins" Series, V. N. Uversky Series ed, NOVA Science Publishers, New York.

117. Ekiel I, Abrahamson M, Fulton DB, Lindahl P, Storer AC, Levadoux W, Lafrance M, Labelle S, Pomerleau Y, Groleau D, LeSauteur L, Gehring K. (1997) NMR structural studies of human cystatin C dimers and monomers. *J Mol Biol.* **271**: 266.
118. Schlunegger MP, Bennett MJ, Eisenberg D. (1997) Oligomer formation by 3D domain swapping: a model for protein assembly and misassembly. *Adv Protein Chem.* **50**: 61.
119. Zegers I, Deswarte J, Wyns L. (1999) Trimeric domain-swapped barnase. *Proc Natl Acad Sci U S A*. **96**: 818.
120. Janowski R et al. (2005) 3D Domain-swapped human cystatin C with amyloid-like intermolecular β-sheets. *Proteins: Structure, Function, and Bioinformatics.* **61**: 570-578.
121. Ekiel I, Abrahamson M. (1996) Folding-related dimerization of human cystatin C. *J. Biol. Chem.* **271** : 1314-1321.
122. Sanders A et al. (2004) Cystatin forms a Tetramer through Structural Rearrangement of Domain-swapped Dimers prior to Amyloidogenesis. *J. Mol. Biol.* ***33*6**: 165-178.
123. Janowski R et al. (2004) Domain swapping in N-truncated human cystatin C. *J. Mol. Biol.* **341**: 151-160.
124. Jerala R, Žerovnik E. (1999) Accessing the global minimum conformation of stefin A dimer by annealing under partially denaturing conditions. *J. Mol. Biol.* **291**: 1079-1089.
125. Žerovnik E, Jerala R, Kroon-Žitko L, Turk V, Lohner K. (1997) Characterization of the equilibrium intermediates in acid denaturation of human stefin B. *Eur. J. Biochem.* **245**: 364-372.
126. Kokalj SJ, Guncar G, Štern I, Morgan G, Rabzelj S, Kenig M, Staniforth RA, Waltho JP, Žerovnik E, Turk D. (2006) Essential Role of Proline Isomerization in Stefin B Tetramer Formation. *J. Mol. Biol*. doi:10.1016/j.jmb.2006.12.025
127. Nardelli E, Buonanno F, Onnis L, Rizzuto N. (1975) Progressive myoclonic epilepsy: anatomo-clinical study of a sporadic case with a marked cerebellar symptomatology. *Riv. Patol. Nerv. Ment.* **96**: 221.
128. Ron D, Chen CH, Caldwell J, Jamieson L, Orr E, Mochly-Rosen D. (1994) Cloning of an intracellular receptor for protein kinase C: a homolog of the beta subunit of G proteins. *Proc. Nat. Acad. Sci.* **91**: 839-843.
129. Buensuceso CS, Woodside D, Huff JL, Plopper GE, O'Toole TE. (2001) The WD protein Rack1 mediates protein kinase C and integrin-dependent cell migration. *J Cell Sci*. **114**: 1691-8.
130. Chang BY, Conroy KB, Machleder EM, Cartwright CA. (1998) RACK1, a receptor for activated C kinase and a homolog of the beta subunit of G proteins, inhibits activity of src tyrosine kinases and growth of NIH 3T3 cells. *Mol Cell Biol*. **18**: 3245-56.
131. Chang BY, Chiang M, Cartwright CA. (2001) The interaction of Src and RACK1 is enhanced by activation of protein kinase C and tyrosine phosphorylation of RACK1. *J Biol Chem*. **276**: 20346-56.
132. Chang BY, Harte RA, Cartwright CA. (2002) RACK1: a novel substrate for the Src protein-tyrosine kinase. *Oncogene*. **21**: 7619-29.
133. Mourton T, Hellberg CB, Burden-Gulley SM, Hinman J, Rhee A, Brady-Kalnay SM. (2001) The PTPmu protein-tyrosine phosphatase binds and recruits the scaffolding protein RACK1 to cell-cell contacts. *J Biol Chem*. **276**: 14896-901.
134. Kiely PA, Sant A, O'Connor R. (2002) RACK1 is an insulin-like growth factor 1 (IGF-1) receptor-interacting protein that can regulate IGF-1-mediated Akt activation and protection from cell death. *J Biol Chem*. **277**: 22581-9.
135. Hermanto U, Zong CS, Li W, Wang LH. (2002) RACK1, an insulin-like growth factor I (IGF-I) receptor-interacting protein, modulates IGF-I-dependent integrin signaling and promotes cell spreading and contact with extracellular matrix. *Mol Cell Biol*. **22**: 2345-65.
136. Liliental J, Chang DD. (1998) Rack1, a receptor for activated protein kinase C, interacts with integrin beta subunit. *J Biol Chem*. **273**: 2379-83.
137. Liliental, J., and Chang, D.D. 1998, RACK1, a receptor for activated protein kinase C, interacts with integrin -b-subunit. *J. Biol. Chem., 273*, 2379.
138. Pascale A, Fortino I, Govoni S, Trabucchi M, Wetsel WC, Battaini F. (1996) Functional impairment in protein kinase C by RACK1 (Receptor for Activated C Kinase 1) deficiency in aged rat brain cortex. *J. Neurochem.* **67**: 2471.
139. Battaini F, Pascale A, Paoletti R, Govoni S. (1997) The role of anchoring protein RACK1 in PKC activation in the ageing rat brain. *TINS*. **20**: 410.
140. Berns H, Humar R, Hengerer B, Kiefer FN, Battegay EJ. (2000) RACK1 is up-regulated in angiogenesis and human carcinomas. *FASEB J*. **14**: 2549-58.
141. Rosdahl JA, Mourton TL, Brady-Kalnay SM. (2002) Protein kinase C delta (PKCdelta) is required for protein tyrosine phosphatase mu (PTPmu)-dependent neurite outgrowth. *Mol Cell Neurosci*. **19**: 292-306.
142. Yaka R, He DY, Phamluong K, Ron D. (2003) Pituitary Adenylate Cyclase-activating Polypeptide (PACAP(1-38)) Enhances N-Methyl-D-aspartate Receptor Function and Brain-derived Neurotrophic Factor Expression via RACK1. *J Biol Chem*. **278**: 9630-8.
143. Angelides KJ, Smith KE, Takeda M. (1989) Assembly and exchange of intermediate filament proteins of neurons: neurofilaments are dynamic structures. *J Cell Biol*. **108** (4): 1495-506.

144. Gee Y, Liem R. (1999) Analysis of the roles of the head domains of type IV rat neuronal intermediate filament proteins in filament assembly using domain- swapped chimeric proteins. *J Cell Science*. **112**: 2233-40.
145. Robertson J, Kriz J, Nguyen MD, Julien JP. (2002) Pathways to motor neuron degeneration in transgenic mouse models**.** *Biochimie*. **84**: 1151-60.
146. Dong DL, Xu ZS, Chevrier MR, Cotter RJ, Cleveland DW, Hart GW. (1993) Glycosylation of mammalian neurofilaments. Localization of multiple O-linked N-acetylglucosamine moieties on neurofilament polypeptides L and M. *J Biol Chem.* **268**: 16679-87.
147. Tsuneishi S. (1992) Regulation of neurite outgrowth through protein kinase C and protease nexin-1 in neuroblastoma cell Kobe. *J Med Sci.* **38**: 147-59.
148. Terry-Lorenzo RT, Inoue M, Connor JH, Haystead TA, Armbruster BN, Gupta RP, Oliver CJ, Shenolikar S. (2000) Neurofilament-L is a protein phosphatase-1-binding protein associated with neuronal plasma membrane and post-synaptic density. *J Biol Chem*. **275**: 2439-46.
149. Ehlers MD, Fung ET, O'Brien RJ, Huganir RL. (1998) Splice variant-specific interaction of the NMDA receptor subunit NR1 with neuronal intermediate filaments. *J Neurosci.* **18**: 720-30.
150. De Jonghe P, Mersivanova I, Nelis E, Del Favero J, Martin JJ, Van Broeckhoven C, Evgrafov O, Timmerman V. (2001) Further evidence that neurofilament light chain gene mutations can cause Charcot-Marie-Tooth disease type 2E. *Ann Neurol.* **49**: 245-9.
151. Gemignani F, Marbini A. (2001) Charcot-Marie-Tooth disease (CMT): distinctive phenotypic and genotypic features in CMT type 2. *J Neurol Sci.* **184**: 1-9.
152. De Sandre-Giovannoli A, Chaouch M, Kozlov S, Vallat JM, Tazir M, Kassouri N, Szepetowski P, Hammadouche T, Vandenberghe A, Stewart CL, Grid D, Levy N. (2002) Homozygous defects in LMNA, encoding lamin A/C nuclear-envelope proteins, cause autosomal recessive axonal neuropathy in human (Charcot-Marie-Tooth disorder type 2) and mouse. *Am J Hum Genet*. **70**: 726-36.
153. Yoshihara T, Yamamoto M, Hattori N, Misu K, Mori K, Koike H, Sobue G. (2002) Identification of novel sequence variants in the neurofilament-light gene in a Japanese population: analysis of Charcot-Marie-Tooth disease patients and normal individuals. *J Peripher Nerv Syst.* **7**: 221-4.
154. Georgiou DM, Zidar J, Korosec M, Middleton LT, Kyriakides T, Christodoulou K. (2002) A novel NF-L mutation Pro22Ser is associated with CMT2 in a large Slovenian family. *Neurogenetics*. **4**: 93-6.
155. Kuchel GA, Poon T, Irshad K, Richard C, Julien JP, Cowen T. (1997) Decreased neurofilament gene expression is an index of selective axonal hypotrophy in ageing. *Neuroreport*. **8**: 799-805.
156. Krekoski CA, Parhad IM, Fung TS, Clark AW. (1996) Aging is associated with divergent effects on Nf-L and GFAP transcription in rat brain. *Neurobiol Aging*. **17**: 833-41.
157. Nakamura Y, Hasimoto R, Kashiwagi Y, Miyamae Y, Shinosaki K, Nishikawa T, Hattori H, Kudo T, Takeda M. (1997) Abnormal distribution of neurofilament L in neurons with Alzheimer's disease. *Neurosci Lett.* **225**: 201-4.
158. Wang J, Tung YC, Wang Y, Li XT, Iqbal K, Grundke-Iqbal I. (2001) Hyperphosphorylation and accumulation of neurofilament proteins in Alzheimer disease brain and in okadaic acid-treated SY5Y cells. *FEBS Lett*. **507**: 81-7.
159. Hashimoto R, Nakamura Y, Tsujio I, Tanimukai H, Kudo T, Takeda M. (1999) Quantitative analysis of neurofilament proteins in Alzheimer brain by enzyme linked immunosorbent assay system. *Psychiatry Clin Neurosci.* **53** : 587-91.
160. Schmidt ML, Murray J, Lee VM, Hill WD, Wertkin A, Trojanowski JQ. (1991) Epitope map of neurofilament protein domains in cortical and peripheral nervous system Lewy bodies. *Am J Pathol*. **139**: 53-65.
161. Hill WD, Lee VM, Hurtig HI, Murray JM, Trojanowski JQ. (1991) Epitopes located in spatially separate domains of each neurofilament subunit are present in Parkinson's disease Lewy bodies. *J Comp Neurol*. **309** : 150-60.
162. Bergeron C, Beric-Maskarel K, Muntasser S, Weyer L, Somerville MJ, Percy ME. (1994) Neurofilament light and polyadenylated mRNA levels are decreased in amyotrophic lateral sclerosis motor neurons. *J Neuropathol Exp Neurol*. **53** : 221-30.
163. Julien JP, Beaulieu JM. (2000) Cytoskeletal abnormalities in amyotrophic lateral sclerosis: beneficial or detrimental effects? *J Neurol Sci.* **180**: 7-14.
164. Ralston G, Cronin T, Branton D. (1996) Self-association of spectrin's repeating segments. *Biochemistry*. **35**: 5257-63.
165. Begg GE, Harper SL, Morris MB, Speicher DW. (2000) Initiation of spectrin dimerization involves complementary electrostatic interactions between paired triple-helical bundles. *J Biol Chem*. **275**: 3279-87.
166. Speicher DW, Marchesi VT. (1984) Erythrocyte spectrin is comprised of many homologous triple helical segments. *Nature*. **311**: 177-80.
167. Lee A, Morrows JS, Fowler VM. (2001) Caspase remodeling of the spectrin membrane skeleton during lens development and aging. *J Biol Chem*. **276**: 20735-42.

168. Nicolas G, Fournier CM, Galand C, Malbert-Colas L, Bournier O, Kroviarski Y, Bourgeois M, Camonis JH, Dhermy D, Grandchamp B, Lecomte MC. (2002) Tyrosine phosphorylation regulates alpha II spectrin cleavage by calpain. *Mol Cell Biol*. **22**: 3527-36.
169. Speicher DW, Morrow, JS, Knowles WJ, Marchesi VT. (1980) *Pro*c. *Nat*l. *Aca*d. *Sc*i. U.S.A. **77**: 5673-5677.
170. Yan Y, Winograd E, Viel A, Cronin T, Harrison SC, Branton D. (1993) *Science.* **262** : 2027-2030.
171. Malchiodi-Abedi F, Ceccarini M, Winkelmann JC, Morrow JS, Petrucci TC. (1993) The 270 kDa splice variant of erythrocyte β-spectrin (βIΣ2) segregates in vivo and in vitro to specific domains of cerebellar neurons. *J Cell Science*. **106**: 67-78.
172. Lambert S, Bennett V. (1993) *Eur J Biochem*. **211**: 1-6.
173. Ursitti JA, Martin L, Resneck WG, Chaney T, Zielke C, Alger BE, Bloch R. (2001) Spectrins in developing rat hippocampal cells. *Dev Brain Res*. **129**: 81-93.
174. Bennet V. (1992) Ankyrins. Adaptors between diverse plasma membrane proteins and the cytoplasm. *J Biol Chem*. **267**: 8703-06.
175. Lombardo CR, Weed SA, Kennedy SP, Forget SP, Morrow JS. (1994) β11-spectrin (fodrin) and β1Σ2-spectrin (muscle) contain NH_2 - and COOH - terminal membrane association domains (MAD1 and MAD2). *J Biol Chem*. **269**: 29212-19.
176. Steiner JP, Bennet V. (1988) Ankyrin-independent membrane protein-binding sites for brain and erythrocyte spectrin. *J Biol Chem*. **263**: 14417-25.
177. De Matteis MA, Morrow JS. (1998) The role of ankyrin and spectrin in membrane transport and domain formation. *Curr Opin Cell Biol*. **10**: 542-49.
178. Stankewich MC, Tse WT, Peters LL, Ch'ng Y, John KM, Stabach PR, Devarajan P, Morrow JS, Lux SE. (1998) A widely expressed betaIII spectrin associated with Golgi and cytoplasmic vesicles. *Proc Natl Acad Sci USA*. **95**: 14158-14163.
179. McMahon LW, Walsh CE, Lambert MW. (1999) Human alpha spectrin II and the Fanconi anemia proteins FANCA and FANCC interact to form a nuclear complex. *J Biol Chem*. **274**: 32904-08.
180. Tse WT, Tang J, Jin O, Korsgren C, John KM, Kung AL, Gwynn B, Peters LL, Lux SE. (2001) A new spectrin, beta-IV, has a major truncated isoform that associates with promyelocytic leukemia protein nuclear bodies and the nuclear matrix. *J Biol Chem.* **276**: 23974-23985.
181. Beck KA, Buchanan JA, Nelson WJ. (1997) Golgi membrane skeleton: identification, localization and oligomerization of a 195 kDa ankyrin isoform associated with the Golgi complex. *J Cell Sci*. **110**: 1239-1249.
182. Bloch RJ, Morrow JS. (1989) An anusual beta-spectrin associated with clustered acetylcholinc receptors. *J Cell Biol*. **108**: 481-493.
183. Moorthy S, Chen L, Bennet V. (2000) Caenorhabditis elegans beta-G spectrin is dispensable for establishment of epithelial polarity, but essential for muscular and neuronal function. *J Cell Biol*. **149**: 915-930.
184. Hammarlund M, Davis WS, Jorgensen EM. (2000) Mutations beta-spectrin disrupt axon outgrowth and sarcomere structure. *J Cell Miol*. **149**: 931-942.
185. Berghs S, Aggujaro D, Dirkx R, Maksimova E, Stabach P, Hermel JM, Zhang JP, Philbrick W, Slepnev V, Ort T, Solimena M. (2000) Beta IV spectrin, a new spectrin localized at axon initial segments and nodes of ranvier in the central and peripheral nervous system. *J Cell Biol*. **151**: 985-1002.
186. Frappier T, Stetzkowski-Marden F, Pradel LA. (1986) Interaction domains of neurofilament light chain and brain spectrin. *Biochem. J*. **275**: 521.
187. Macioce P, Gandolfi N, Leung CL, Chin SS, Malchiodi-Albedi F, Ceccarini M, Petrucci TC, Liem RK. (1999) Characterization of NF-L and beta II Sigma1-spectrin interaction in liver cells. *Exp. Cell Res.* **250**: 142.
188. Frappier T, Regnouf F, Pradel LA. (1987) Binding of brain spectrin to the 70-kDa neurofilament subunit protein. *Eur J Biochem*. **169**: 651-7.
189. Rodriguez MM, Ron D, Touhara K, Chen CH, Mochly-Rosen D. (1999) RACK1, a protein kinase C anchoring protein, coordinates the binding of activated protein kinase C and select pleckstrin homology domains in vitro. *Biochemistry*. **38**: 13787-94.
190. Hayes MV, Sessions RB, Brady RL, Clarke AR. (1999) Engineered assembly of intertwined oligomers of an immunoglobulin chain. *J. Mol. Biol*. **285**: 1857–1867.
191. Crestfield AM, Stein WH, Moore S. (1962) *Arch. Biochem. Biophys.* Suppl. 1: 217–222.
192. Liu Y, Hart PJ, Schlunegger MP, Eisenberg DS. (1998) *Proc. Natl. Acad. Sci. USA,* **95**: 3437–3442.
193. Fruchter RC, Crestfield AM. (1965) *J. Biol. Chem*. **240**: 3868–3874.
194. Libonati M, Bertoldi M, Sorrentino S. (1996) The activity on double-stranded RNA of aggregates of ribonuclease A higher than dimers increases as a function of the size of the aggregates. *Biochem. J*. **318**: 287–290.
195. Liu Y, Gotte G, Libonati M, Eisenberg D. (2001) A domain-swapped RNase A dimer with implications for amyloid formation. *Nature Structural Biology*. **8** (3): 211.
196. Nenci A, Gotte G, Bertoldi M, Libonati M. (2001) Structural properties of trimers and tetramers of ribonuclease A. *Protein Sci.* **10**: 2017-2027.

197. Liu Y, Gotte G, Libonati M, Eisenberg D. (2002) Structures of the two 3D domain-swapped RNase A trimers. *Protein Sci.* **11**: 371-380.
198. Steiner JP, Walke HT Jr, Bennet V. (1989) Calcium/calmodulin inhibits direct binding of spectrin to synaptosomal membranes. *J. Biol. Chem*. **264**: 2783-2791.
199. USA FDA Center For Biologics Evaluation And Research, Meeting of May 16 2001 Dr. Van der Eb's Part Page 77-85.
200. Kim SO, Merchant K, Nudelman R, Beyer WF Jr, Keng T, DeAngelo J, Hausladen A, Stamler JS. (2002) OxyR: a molecular code for redox-related signaling. *Cell*. **109**: 383-96.
201. Ghezzi P, Bonetto V. (2003) Redox proteomics: Identification of oxidatively modified proteins. *Proteomics*. **3**: 1145-1153.
202. Rawlings ND, Barrett AJ. (1990) Evolution of proteins of the cystatin superfamily. *J Mol Evol*. **30**: 60-71.
203. Levy E, Jaskolski M, Grubb A. (2006) The role of cystatin C in cerebral amyloid angiopathy and stroke: cell biology and animal models. *Brain Pathol.* **16**: 60-70.
204. Muchowski PJ, Wacker JL. (2005) Modulation of neurodegeneration by molecular chaperones. *Nat. Rev. Neurosci.* **6**: 11-22.
205. Rajan RS, Illing ME, Bence NF, Kopito RR. (2001) Specificity in intracellular protein aggregation and inclusion body formation. *Proc Natl Acad Sci U S A*. **98**: 13060-5.
206. Lee JO, Rieu P, Arnaout MA, Liddington R. (1995) *Cell.* **80**: 1467-1477.
207. Tomsig JL, Snyder SL, Creutz CE. (2003) Identification of Targets for Calcium Signaling through the Copine Family of Proteins. *The Journal of Biological Chemistry*. **278** (12): 10048-54.
208. Nakayama T, Yaoi T, Kuwajima G. (1999) Localization and Subcellular Distribution of N-Copine in Mouse Brain. *Journal of Neurochemistry*. **72**: 372-379.
209. Gerke V, Creutz CE, Moss SE. (2005) Annexins: Linking Ca2+ Signalling To Membrane Dynamics. *Nature Reviews in Molecular Cell Biology*. **6**: 449-461.
210. Gerke V, Moss SE. (2002) Annexins: from structure to function. *Phys. Rev*. **82**: 331–371.
211. Merrifield CJ et al. (1999) Endocytic vesicles move at the tips of actin tails in cultured mast cells. *Nature Cell Biol.* **1**: 72–74.
212. Merrifield CJ et al. (2001) Annexin 2 has an essential role in actin-based macropinocytic rocketing. *Curr. Biol.* **11**: 1136–1141.
213. Guo et al. (2003) Identification of an N-domain histidine essential for chaperone function in calreticulin. *J biol Chem*. **278**: 50645-53.
214. Helenius A, Aebi M. (2004) Roles of N-linked glycans in the endoplasmic reticulum. *Annu. Rev. biochem*. **73**: 1019-49.
215. Mizutani A. et al. (1992) CAP-50, a newly identified annexin, localizes in nuclei of cultured fibroblast 3Y1 cells. *J. Biol. Chem.* **267**: 13498–13504.
216. Tomas A, Moss SE. (2003) Calcium-and cell cycledependent association of annexin 11 with the nuclear envelope. *J. Biol. Chem.* **278**: 20210–20216.
217. Tomas A, Futter C, Moss SE. (2004) Annexin 11 is required for midbody formation and completion of the terminal phase of cytokinesis. *J. Cell Biol.* **165**: 813–822.
218. Manning M, Colòn W. (2004) Structural basis of protein kinetic stability: resistance to sodium dodecyl sulfate suggests a central role for rigidity and a bias toward beta-sheet structure. *Biochemistry*. **43**: 11248-54.
219. Walsh DM, Klyubin I, Fadeeva JV, Cullen WK, Anwyl R, Wolfe MS, Rowan MJ, Selkoe DJ. (2002) Naturally secreted oligomers of amyloid beta protein potently inhibit hippocampal long-term potentiation in vivo. *Nature*. **416**: 535-9.
220. Walsh DM, Townsend M, Podlisny MB, Shankar GM, Fadeeva JV, Agnaf OE, Hartley DM, Selkoe DJ. (2005) Certain inhibitors of synthetic amyloid beta-peptide (Abeta) fibrillogenesis block oligomerization of natural Abeta and thereby rescue long-term potentiation. *J Neurosci.* **25**: 2455-62.
221. Lesne S, Koh MT, Kotilinek L, Kayed R, Glabe CG, Yang A, Gallagher M, Ashe KH. (2006) A specific amyloid-beta protein assembly in the brain impairs memory. *Nature*. **440**: 352-57.
222. Oesch B, Jensen M, Nilsson P, Fogh J. (1994) Properties of the scrapie prion protein: quantitative analysis of protease resistance. *Biochemistry*. **33**: 5926-31.
223. Zerovnik E, Turk V, Waltho JP. (2002b) Amyloid fibril formation by human stefin B: influence of the initial pH-induced intermediate state. *Biochem Soc Trans*. **30**: 543-7.
224. Knaus KJ, Morillas M, Swietnicki W, Malone M, Surewicz WK, Yee VC. (2001) Crystal structure of the human prion protein reveals a mechanism for oligomerization. *Nat Struct Biol*. **8**: 770-4.
225. Spiess C, Meyer AS, Reissmann S, Frydman J. (2004). TRENDS in *Cell Biology*. **14**: 598-604.
226. Lindquist S. (1997) Mad cows meet psi-chotic yeast: the expansion of the prion hypothesis. *Cell*. **89**: 495-8.
227. Tuite MF, Cox BS. (2003) Propagation of yeast prions. *Nat Rev Mol Cell Biol.* **4**: 878-90.
228. Dobson CM. (2003) Protein folding and misfolding. *Nature*. **426**: 884-90.

229. Harris DA, True HL. (2006) New insights into prion structure and toxicity. *Neuron*. **50**: 353-7.
230. Collins SR, Douglass A, Vale RD, Weissman JS. (2004) Mechanism of prion propagation: amyloid growth occurs by monomer addition. *PLoS Biol.* **2**: 1582-1590.
231. Berson JF, Theos AC, Harper DC, Tenza D, Raposo G, Marks MS. (2003) Proprotein convertase cleavage liberates a fibrillogenic fragment of a resident glycoprotein to initiate melanosome biogenesis. *J Cell Biol*. **161**: 521-33.
232. Chapman MR, Robinson LS, Pinkner JS, Roth R, Heuser J, Hammar M, Normark S, Hultgren SJ. (2002) Role of Escherichia coli curli operons in directing amyloid fiber formation. *Science*. **295**: 851-5.
233. Kelly JW, Balch WE. (2003) Amyloid as a natural product. *J Cell Biol*. **12**: 461-462.
234. Ceru S, Rabzelj S, Kopitar-Jerala N, Turk V, Zerovnik E. (2005) Protein aggregation as a possible cause for pathology in a subset of familial Unverricht-Lundborg disease. *Med Hypotheses*. **64**: 955.
235. Riccio M, Dembic M, Cinti C, Santi S (2004) Multifluorescence labeling and colocalization analysis. *Methods Mol Biol*. **285**: 171-177.